MODELLING SPATIAL DYNAMICS OF LANDSLIDES: INTEGRATION OF GIS-BASED CELLULAR AUTOMATA AND MULTICRITERIA EVALUATION METHODS

by

Terence Lai
B.Sc., Simon Fraser University, 2009

THESIS SUBMITTED IN PARTIAL FULFILLMENT OF
THE REQUIREMENTS FOR THE DEGREE OF

MASTER OF SCIENCE

In the
Department of Geography
Faculty of Environment

SIMON FRASER UNIVERSITY
Summer 2011

APPROVAL

Name: **Terence Lai**

Degree: **Master of Science**

Title of Thesis: **Modelling Spatial Dynamics of Landslides: Integration of GIS-Based Cellular Automata and Multicriteria Evaluation Methods**

Examining Committee:

Chair: **Dr. Eugene McCann**
Associate Professor
Department of Geography, SFU

____

Dr. Suzana Dragicevic, Professor
Senior Supervisor
Department of Geography, SFU

____

Dr. Shivanand Balram, Lecturer
Committee Member
Department of Geography, SFU

____

Dr. Margaret Schmidt, Associate Professor
Committee Member
Department of Geography, SFU

____

Dr. Jinfei Wang, Professor
External Examiner
Department of Geography, UWO

Date Defended/Approved: August 25, 2011

ABSTRACT

Landslides occur when the slopes become unstable due to natural causes as well as by disturbances from human activities. Landslides have adverse socio-economic consequences and negatively impact natural resources, public safety, and property. Urban planners require tools to make informed decisions that will mitigate landslide hazards. The objective of this research is the development of a GIS-based methodology coupled with cellular automata (CA) theory and multicriteria evaluation (MCE) methods for modelling landslide flow. Landslides are viewed as geographic phenomena that exhibit complex system behaviour that can be effectively modelled in both space and time. The integration of GIS, logistic regression, MCE and CA was used to model the dynamics of landslide flow. The methodology was tested on historical landslide data for Metro Vancouver, Canada. The results showed a strong degree of correlation. This research makes a unique contribution to knowledge by introducing non-linear dynamics into GIS-CA landslide models, further improving our ability to understand processes and predictions for applications in urban planning and disaster management.

Keywords: Cellular Automata, Complexity, Multicriteria Evaluation, Geographic Information Science, Landslide Modelling

DEDICATION

To my mother and her sacrifice that allows me to walk this path.

ACKNOWLEDGEMENTS

I would like to acknowledge the Natural Sciences and Engineering Research Council (NSERC) of Canada for full support of this study under the Discovery Grant Program awarded to Dr. Suzana Dragicevic. I am also appreciative to the GIS Department of the District of North Vancouver for providing the geospatial data used in this research.

I want to thank my supervisor, Dr. Suzana Dragicevic, for her valuable ideas, expertise and patient guidance throughout the course of my research. I appreciate the many hours she spent revising and re-revising the chapters of this thesis. I would also like to thank my supervisory committee members, Dr. Shivanand Balram and Dr. Margaret Schmidt, for their constructive feedback and comments. And of course, thank you to my friends in the Spatial Analysis and Modeling Lab and Department of Geography for your support and companionship.

Last but not least, I am thankful to my mother, brothers, and best friends for their love and support. Their words of encouragement go a long way.

TABLE OF CONTENTS

LIST OF FIGURES

LIST OF TABLES

CHAPTER 1 INTRODUCTION

1.1 Introduction

Landslides are a natural occurrence and the term describes a wide variety of processes that result in the downward and outward movement of slope-forming materials including rock, soil, artificial fill, or a combination of these (Varnes 1978). Landslides are primarily associated with mountainous regions, but they also occur in areas of low relief. There are many types of landslides with different flow materials, such as rock avalanches, rockfalls, shallow landslides, and channelized debris flows. Urban landslides typically occur along escarpments where residential development encroaches on steeper slopes, leading to increased risks of fatality and property damage (Eisbacher and Clague 1981). These slides are often caused by the presence of hillside lots that require leveling of the escarpment slope for house construction. As population growth continues and pressure to build on sloped areas increases, it is necessary to understand landslide processes to remediate human and property loss. In order to address this need, the most practical way of studying a natural phenomenon not easily reproducible in a lab setting is through simulation modelling using single or multiple techniques. In this thesis, multiple techniques will be used to improve confidence in the output results.

In areas where landslides are a constant hazard, the most common tool that urban planners possess is a susceptibility map that predicts the probability of failure. This method typically integrates an evaluation technique and a geographic information system (GIS). One such evaluation technique often used in combination with a GIS is logistic regression, in which the dichotomous variable is viewed as the presence or absence of a landslide event occurring. Logistic regression forms a multivariate regression relation between a dependent variable and several independent variables by analyzing the link between the distribution of historical landslides and a set of landslide-conditioning parameters. This technique for producing susceptibility maps using logistic regression was applied with much success in landslide prone areas of Canada (Chen and Wang 2007), Korea (Lee and Min 2001), Hong Kong (Dai and Lee 2002), Japan (Ayalew and Yamagishi 2005), Turkey (Duman et al. 2006; Kincal et al. 2009; Yilmaz 2009), and the Himalayas (Chauhan et al. 2010). The general form of logistic regression involves using a logit model to fit the dependent variable (Menard 2001). A benefit of logistic regression is that the type of parameters accepted can be either continuous or discrete variables, or a combination of both types (Bai et al. 2010). Another popular approach is the integration of a multicriteria evaluation (MCE) technique and a GIS (Jankowski 1995). For example, the integration between GIS and an analytic network process has been tested in Nepal (Neaupane and Piantartakulchai 2006) and integration between GIS and an analytic hierarchy process (AHP) has been extensively examined in Cuba (Castellanos Abella and Van Westen 2007), Japan (Ayalew et al. 2004) and Turkey (Akgun and Bulut 2007; Yalcin 2008). This approach uses GIS as a framework for the application of MCE techniques because MCE techniques on their own are only mathematical formulae without data handling capabilities that GIS possesses (Carver 1991). The most widely used technique for MCE models to calculate factor weights involves using AHP, developed by Saaty (1980), which is a technique able to handle both qualitative and quantitative parameters. AHP constructs a pair-wise comparison matrix where the decision maker compares the importance of factors relative to each other and the weight for each factor is calculated based on these relative rankings. Since this process involves a level of subjectivity on which parameters trigger landslides, the decision maker should have expert knowledge in order to properly build the comparison matrix (Ayalew et al. 2005). Calculation of factor weights then results in a landslide susceptibility map; however, the disadvantage of this MCE technique and logistic regression is that the susceptibility maps are static in nature and apply to the particular spatial data at the time of data collection. In other words, the result lacks a temporal component and is most often disregarded (Komac 2006).

Considering the dynamic nature of landslides, where the continuous flow of debris down a slope depends on many factors changing over time, implementing a cellular automata (CA) modelling approach in a GIS framework can provide both spatial and temporal components (White and Engelen 1993). CA has been favored in the past as an alternative to solving extremely laborious differential flow equations that require substantial simplifications to be made (Toffoli 1984). CA, however, uses simple rules that represent local interactions between cells and neighbours as they occur in the real world, and therefore avoids solving complex differential equations of physics-based models. The added advantage of a rule-based system, in comparison to approaches based on differential equations, is the consequent computational efficiency (White and Engelen 1997). A CA is based on a grid of cells of identical shape, where each cell is surrounded by neighbour cells and is described by one of a predefined set of cell states (Couclelis 1985; Clarke et al. 1997). Each cell's state is updated in discrete time steps according to a set of transition rules that define how each cell evolves given the attributes of its surrounding neighbours. Through the application of simple rules that describe processes on a local level, global patterns emerge (Wolfram 1984; Batty and Xie 1994). In other words, transition rules are derived by properly separating the phenomena's processes such that combined results realistically represent the behavior of the phenomena.

A traditional CA is described by White and Engelen (2000) in five components: 1) grid space, 2) cell states, 3) neighbourhood, 4) transition rules, and 5) time steps. The *grid space* is typically comprised of a homogeneous two dimensional square lattice. This space represents the environment in which the CA is operating on. Each cell is defined discretely by a set of *cell states* appropriate to the phenomena modeled. Models can represent a binary set of states such as the *presence* or *absence* of fire. Other models use multiple states such as various land use types (i.e. *residential*, *commercial*, *industrial*, *streets*, *green space*). The *neighbourhood* defines the geographical extent of influence for each cell. The two commonly used neighbourhoods are the von Neumann neighbourhood (four cells adjacent to the sides of the central cell) and the Moore neighbourhood (all eight cells surrounding the central cell). *Transition rules* examine the cells in the neighbourhood to determine if and how the central cell changes states. The set of these rules represent the logic of the process being modeled. The temporal component of the model progresses in discrete steps of time as cells update their states after transition rules are applied. Each application is known as a *time step* and may represent any increment in time as the phenomenon is modeled (i.e. minutes, days, seasons, years).

In the past, CA theory was implemented in geographical applications such as urban growth (Couclelis 1985; White and Engelen 1993; Batty and Xie 1994). The application of GIS-based CA models for simulating landslides has only recently been explored. A CA model implementing rules for scour, deposit, path selection, and the spread for each moving cell was tested on a study area in Vancouver Island, BC (Guthrie et al. 2008). Several debris flows in Italy were simulated by various versions of a CA model based on the equivalent fluid approach, known as SCIDDICA (Smart Computational Innovative method for the Detection of Debris/mud flow path with Interactive Cellular Automata) (Di Gregorio et al. 1999; Avolio et al. 2000; D'Ambrosio et al. 2003; Iovine et al. 2003). SCIDDICA does not implement a traditional CA, but attempts to fully incorporate physical laws, which requires a large dataset of global parameters.

1.2 Research Problem

Complexity describes many non-linear geographic, biological, environmental, human processes consisting of seemingly complex local constituents interacting as a whole and usually leading to emerging global patterns. Complex systems theory is concerned with simplifying system characteristics by relying on simple mathematical equations and a number of assumptions of how complex systems operate (Manson 2001). The formulation of equations represents the relationships between individual components, which ultimately affect changes in emerging patterns.

Cellular automata is one particular spatially explicit model used to understand complex systems and it was proposed as an efficient model to represent landslides (Toffoli 1984). The traditional CA approach is ideal for GIS-based modelling of landslide flow over time, as opposed to the static outputs of current landslide susceptibility studies. Cells are represented by *landslide* and *non-landslide* states as the initial failure flows from one cell to another based on the information gathered from a specified neighbourhood of cells. Furthermore, each time step of the CA represents a single advancement of flow according to the spatial resolution of the raster grid. While the components of CA appear suitable for modelling landslides, three main problems exist. The first is to understand landslide behaviour and to predict where landslides occur at different spatial scales. The second involves the need to incorporate a temporal component to the modelling. The third is to overcome limited data availability.

In this thesis, the first problem dealing with the determination of landslide susceptibility is addressed using MCE. Methods used to predict landslides are a fundamental tool for government departments in order to produce maps that become the basic information for landscape management. The definition of landslide susceptibility is the characterization of the spatial distribution and classification of terrain units according to their predisposition to result in landslides (Fell et al. 2008). The constant force causing landslides to occur is gravity and this is complicated by the many relationships that exist between a slope and its surrounding environment. Topographic, climatic, and anthropogenic factors contribute to the susceptibility of landslide occurrence however, there is inconsistency among the factors chosen in the MCE approach for calculating susceptibility. In addition to this problem, the scale and spatial resolution of the susceptibility mapping is influenced by available data, but the effect of these on the output result is often not analysed. Therefore, significant uncertainty is present when attempting to assign susceptibility to a raster-based geospatial data representation of a landscape at the scale of a region, municipality, or even local area.

The second problem related to the temporal component is addressed by extending the knowledge of the spatial distribution of the landslide probability to the actual flow of the landslide front. The advantage of modelling the dynamic flow of landslides is knowing the impact of such an event. For example, a landslide susceptibility map only provides a probability of an event occurring, but a model of landslide flow can indicate the downslope risk areas and their extents. The fundamental change from a static MCE map output to one that incorporates a temporal component requires an additional method integrated with susceptibility mapping because GIS alone is insufficient (Park and Wagner 1997). GIS contains the data storage capability and analytical tools for spatial modelling, but the addition of CA provides the ability to represent time explicitly. An integrated spatio-temporal model has coupled GIS, MCE, and CA approaches for modelling urban land use dynamics (Wu and Webster 1998), but has received limited attention in landslide research.

The third problem dealing with limited data availability is addressed by deriving additional information from available satellite imagery or aerial photography. The limitation of available data is an important factor affecting the applicability of any model, as there is a trade-off between costs for procuring data and its expected benefits. Therefore, it is imperative to develop a landslide model that takes into account the limited nature of available data, while achieving a high degree of effectiveness.

The following research questions were formalized to address the stated research problems:

1. Can a GIS-based CA model be used to simulate landslide flow?
2. Can a GIS-based MCE model predict landslide susceptibility at different scales?

3. Can a GIS-based CA model be enhanced to simulate landslide flow through integration of MCE?

4. Can the modelled approaches achieve achieve high effectiveness with limited data availability?

1.3 Research Objectives

In order to respond to the questions addressing specific research problems, four objectives were established in an attempt to reach a solution. The goals of this thesis is to understand the underlying processes of predicting shallow landslide susceptibility at different spatial scales, incorporating a temporal component, and tackling limited data availability by the development of a GIS-based methodology coupled with CA theory for modelling a complex dynamic process such as landslide flow. To achieve these goals, four objectives were addressed:

1. Develop an integrated GIS-based CA model incorporating inputs from the logistic regression techniques to simulate shallow landslide flow.

2. Develop multicriteria evaluation techniques to determine multiscale landslide susceptibility in order to assess landslide prediction in different scales and resolutions.

3. Develop a novel GIS-based approach integrating CA and MCE techniques to improve predictions of shallow landslide flow at fine scales.

4. Apply the proposed modelling approaches on historical landslide cases in order to test the performance and applicability to the decision-making of urban planning and disaster management.

1.4 Study Site and Data

In this research, three separate study sites were used and each site was examined at a different scale. The first study site located in Metro Vancouver, British Columbia, Canada was chosen to examine the proposed landslide susceptibility model at a regional scale. During the time period between 1905 and 2007, 171 separate landslide events have been recorded and mapped (BGC Engineering 2011). Metro Vancouver consists of 21 municipalities occupying an area of 2 877 km^2 and is home to approximately 2 249 725 residents (BC Stats 2007). The DEM was provided by the National Topographic Data Base (NTDB) at a scale of 1:50,000 and the spatial resolution of the DEM is 50 m.

In addition to the Metro Vancouver regional study, the effect of varying scale is examined by determining landslide susceptibility at a municipal level using the second study site. The District of North Vancouver (DNV), which is located just north of the City of Vancouver and occupied by 86 954 residents (BC Stats 2007), was chosen for its mountainous terrain and the proximity of residential areas to steep slopes. The DNV GIS department provided a 10 m spatial resolution DEM.

Within the DNV study site, a third study site was selected to assess landslide susceptibility and also to test the landslide model at a local scale. In particular, six historical shallow landslides that have occurred since the 1970s along the Berkley Escarpment were examined. The Escarpment runs along a ridge east of the lower Seymour River area and the study site is 2.7 km^2 in area. Data for the Berkley Escarpment were derived from a topographic base map (scale 1:2,000) consisting of 2 m elevation contour intervals commissioned by the DNV on March 6, 2006. Digitization, conversion, and interpolation of the contour intervals produced a high detailed DEM at a spatial resolution of 1 m.

1.5 Thesis Overview

The thesis is composed of 5 chapters. Chapter 1 starts with the Introduction, where the literature review, research problems, questions, and objectives are provided. The three subsequent chapters addresses the objectives through the development of modelling approaches that integrate GIS, logistic regression, multicriteria evaluation, and cellular automata.

Chapter 2 presents a CA modelling approach for landslide flow and provides simulations of landslide flow behaviour based on information from a logistic regression analysis. This model presents a prototype in which an integrated CA approach can effectively simulate landslides and forms the basis for the following chapters.

Chapter 3 describes the development of the MCE approach at multiple scales and spatial resolutions for determining landslide susceptibility. Landslide susceptibility zonation is produced at regional, municipal, and local scales. This chapter explains the development of the MCE-derived input used in Chapter 4 in order to enhance the CA modelling approach.

Chapter 4 is based on the development of the MCE for determining landslide susceptibility, which is used as an input for CA modelling. The main objective was to explore a method for deriving information from the landslide susceptibility map to enhance the performance of the model.

Chapter 5 concludes the thesis by providing an overall summary of the research results. This chapter discusses the potential and limitations of the methods used, and provides suggestions for further research.

1.6 References

Akgun, A. and F. Bulut (2007). "GIS-based landslide susceptibility for Arsin-Yomra (Trabzon, North Turkey) region." Environmental Geology **51**(8): 1377-1387.

Avolio, M. V., S. Di Gregorio, et al. (2000). "Simulation of the 1992 Tessina landslide by a cellular automata model and future hazard scenarios." International Journal of Applied Earth Observation and Geoinformation **2**(1): 41-50.

Ayalew, L. and H. Yamagishi (2005). "The application of GIS-based logistic regression for landslide susceptibility mapping in the Kakuda-Yahiko Mountains, Central Japan." Geomorphology **65**(1-2): 15-31.

Ayalew, L., H. Yamagishi, et al. (2005). "Landslides in Sado Island of Japan: Part II. GIS-based susceptibility mapping with comparisons of results from two methods and verifications." Engineering Geology **81**(4): 432-445.

Ayalew, L., H. Yamagishi, et al. (2004). "Landslide susceptibility mapping using GIS-based weighted linear combination, the case in Tsugawa area of Agano River, Niigata Prefecture, Japan." Landslides **1**(1): 73-81.

Bai, S. B., J. Wang, et al. (2010). "GIS-based logistic regression for landslide susceptibility mapping of the Zhongxian segment in the Three Gorges area, China." Geomorphology **115**(1-2): 23-31.

Batty, M. and Y. Xie (1994). "From cells to cities." Environment and Planning B-Planning & Design **21**: 531-538.

BC Stats. (2007). "Municipal Population Estimates." Retrieved June 18, 2011, from http://www.bcstats.gov.bc.ca/data/pop/pop/mun/Mun2007txt.pdf.

BGC Engineering (2011). Metro Vancouver Landslide Inventory [shapefile].

Carver, S. J. (1991). "Integrating multi-criteria evaluation with geographical information systems." International Journal of Geographical Information Systems **5**(3): 321-339.

Castellanos Abella, E. A. and C. J. Van Westen (2007). "Generation of a landslide risk index map for Cuba using spatial multi-criteria evaluation." Landslides **4**(4): 311-325.

Chauhan, S., S. Mukta, et al. (2010). "Landslide susceptibility zonation of the Chamoli region, Garhwal Himalayas, using logistic regression model." Landslides **7**(4): 411-423.

Chen, Z. and J. Wang (2007). "Landslide hazard mapping using logistic regression model in Mackenzie Valley, Canada." Natural Hazards **42**(1): 75-89.

Clarke, K. C., S. Hoppen, et al. (1997). "A self-modifying cellular automaton model of historical urbanization in the San Francisco Bay area." Environment and Planning B-Planning & Design **24**(2): 247-261.

Couclelis, H. (1985). "Cellular worlds: a framework for modeling micro-macro dynamics." Environment and Planning A **17**(5): 585-596.

D'Ambrosio, D., S. Di Gregorio, et al. (2003). "First simulations of the Sarno debris flows through Cellular Automata modelling." Geomorphology **54**(1-2): 91-117.

Dai, F. C. and C. F. Lee (2002). "Landslide characteristics and, slope instability modeling using GIS, Lantau Island, Hong Kong." Geomorphology **42**(3-4): 213-228.

Di Gregorio, S., R. Rongo, et al. (1999). "Mount ontake landslide simulation by the cellular automata model SCIDDICA-3." Physics and Chemistry of the Earth Part a-Solid Earth and Geodesy **24**(2): 131-137.

Duman, T. Y., T. Can, et al. (2006). "Application of logistic regression for landslide susceptibility zoning of Cekmece Area, Istanbul, Turkey." Environmental Geology **51**(2): 241-256.

Eisbacher, G. H. and J. J. Clague (1981). "Urban landslides in the vicinity of Vancouver, British Columbia, with special reference to the December 1979 rainstorm." Canadian Geotechnical Journal **18**(2): 205-216.

Fell, R., J. Corominas, et al. (2008). "Guidelines for landslide susceptibility, hazard and risk zoning for land-use planning." Engineering Geology **102**(3-4): 99-111.

Guthrie, R. H., P. J. Deadman, et al. (2008). "Exploring the magnitude-frequency distribution: a cellular automata model for landslides." Landslides **5**(1): 151-159.

Iovine, G., S. Di Gregorio, et al. (2003). "Debris-flow susceptibility assessment through cellular automata modeling: an example from 15–16 December 1999 disaster at Cervinara and San Martino Valle Caudina (Campania, southern Italy)." Natural Hazards and Earth System Sciences **3**: 457-468.

Jankowski, P. (1995). "Integrating geographical information systems and multiple criteria decision-making methods." International Journal of Geographical Information Systems **9**(3): 251-273.

Kincal, C., A. Akgun, et al. (2009). "Landslide susceptibility assessment in the Izmir (West Anatolia, Turkey) city center and its near vicinity by the logistic regression method." Environmental Earth Sciences **59**(4): 745-756.

Komac, M. (2006). "A landslide susceptibility model using the Analytical Hierarchy Process method and multivariate statistics in penialpine Slovenia." Geomorphology **74**(1-4): 17-28.

Lee, S. and K. Min (2001). "Statistical analysis of landslide susceptibility at Yongin, Korea." Environmental Geology **40**(9): 1095-1113.

Manson, S. M. (2001). "Simplifying complexity: a review of complexity theory." Geoforum **32**(3): 405-414.

Menard, S. (2001). Applied logistic regression analysis. Thousand Oaks, CA, Sage University Paper Series on Quantitative Applications in Social Sciences.

Neaupane, K. M. and M. Piantartakulchai (2006). "Analytic network process model for landslide hazard zonation." Engineering Geology **85**(3-4): 281-294.

Park, S. and D. F. Wagner (1997). "Incorporating Cellular Automata simulators as analytical engines in GIS." Transactions in GIS **2**(3): 213-231.

Saaty, T. L. (1980). The analytical hierarchy process: Planning, priority setting, resource allocation. New York, McGraw-Hill.

Toffoli, T. (1984). "Cellular Automata as an alternative to (rather than an approximation of) differential equations in modeling physics." Physica D: Nonlinear Phenomena **10**(1-2): 117-127.

Varnes, D. (1978). Slope movement types and processes. Landslides, analysis and control. R. Schuster and R. Krizek, National Research Council, National Academy Press**:** 11-13.

White, R. and G. Engelen (1993). "Cellular automata and fractal urban form: a cellular modelling approach to the evolution of urban land-use patterns." Environment and Planning A **25**(8): 1175-1199.

White, R. and G. Engelen (1997). "Cellular automata as the basis of integrated dynamic regional modelling." Environment and Planning B-Planning & Design **24**(2): 235-246.

White, R. and G. Engelen (2000). "High-resolution integrated modelling of the spatial dynamics of urban and regional systems." Computers, Environment and Urban Systems **24**(5): 383-400.

Wolfram, S. (1984). "Cellular automata as models of complexity." Nature **311**(5985): 419-424.

Wu, F. L. and C. J. Webster (1998). "Simulation of land development through the integration of cellular automata and multicriteria evaluation." Environment and Planning B-Planning & Design **25**(1): 103-126.

Yalcin, A. (2008). "GIS-based landslide susceptibility mapping using analytical hierarchy process and bivariate statistics in Ardesen (Turkey): Comparisons of results and confirmations." Catena **72**(1): 1-12.

Yilmaz, I. (2009). "Landslide susceptibility mapping using frequency ratio, logistic regression, artificial neural networks and their comparison: A case study from Kat landslides (Tokat-Turkey)." Computers & Geosciences **35**(6): 1125-1138.

CHAPTER 2 DEVELOPMENT OF AN URBAN LANDSLIDE CELLULAR AUTOMATA MODEL: A CASE STUDY OF NORTH VANCOUVER, CANADA[1]

2.1 Abstract

Many GIS-based landslide models require detailed datasets that are ideally collected from field measurements, which can incur high costs for carrying out surveys. Even when the data is on hand, implementing physics-based slope stability techniques can be difficult. Common research practice uses differential equations to characterize the dynamic flow of a landslide, but it is often laborious without making substantial simplifications. A possible solution is to implement a cellular automata modelling approach, which represents both spatial and temporal components, to simulate the dynamics of the landslide propagation process. In this study, a simplified cellular automata model is developed for the effective prediction of shallow landslide flow, where the data requirement is a high resolution digital elevation model (DEM). Parameters, such as slope and slope curvature features, are derived from the DEM and coupled with logistic regression. The developed model is implemented on the Patrick and Dawson-Chu Slide in North Vancouver, Canada. The results from this study site were favorable and sensitivity analysis was performed on the initiation sites.

[1] A version of this chapter has been published. "Lai, T., Dragicevic, S., 2011. Development of an urban landslide cellular automata model: A case study of North Vancouver, Canada. *Journal of Earth Science Informatics*. 4(2): 69-80."

2.2 Introduction

Landslides are the downward and outward movement of natural rocks, artificial fill, or combinations of these materials that shape mountainous areas and redistribute sediment in gentler terrain (Sidle and Ochiai 2006). Urban landslides typically occur along escarpments where residential development encroaches on steeper slopes, leading to increased risks of fatality and property damage (Alexander 1989). These shallow landslides are often caused by the presence of hillside lots that involve the stripping of natural vegetation and leveling of the escarpment slope for house construction (Evans 1982). Changes in land use, slope management, and intensified residential development have placed more people at risk, therefore it is necessary to understand and predict landslide processes to remediate human and property loss (Eisbacher and Clague 1981). The most practical way of studying a complex spatial phenomenon that is not easily reproducible in a lab setting is through a single simulation model or combination of techniques (Santini et al. 2009).

Research methods in landslide science are numerous and can be categorized in terms of quantifying the risk or probability of an event occurring (i.e. hazard zonation) or predicting landslide flow. Application of multi-criteria evaluation techniques, which is dependent on the knowledge of the expert on triggering factors, generates landslide susceptibility maps (Neaupane and Piantartakulchai 2006; Akgun and Bulut 2007; Yalcin and Bulut 2007; Castellanos Abella and Van Westen 2008). Factor of safety investigates the spatial distribution of slope stability using limit equilibrium methods (Wu and Sidle 1995; Luzi and Pergalani 1996; Van Westen and Terlien 1996; Paulin and Bursik 2009). For landslide flow modelling, the majority of research carried out includes deterministic physical models largely centered around flow equations, however, these models require large amounts of detailed input data derived from laboratory tests and field measurements (Van Westen et al. 2006). Aside from Wu and Sidle (1995), model results lacked a temporal component and outputs typically were hazard zonation maps.

Considering the dynamic nature of landslides, where the continuous flow of debris down a slope depends on many factors changing over time, implementing a cellular automata (CA) modelling approach and a geographic information system (GIS) can address the dynamics and complexity of landslides. CA has been favored in the past as an alternative to solving extremely laborious differential flow equations that require substantial simplifications to be made (Toffoli 1984). CA uses simple rules that represent local interactions between cells and neighbours as they occur in the real world, and therefore is able to avoid solving complex differential equations of physics-based models. The added advantage of a rule-based system and spatio-temporal components, in comparison to approaches based on differential equations, is the consequent computational efficiency (White and Engelen 2000). A CA is based on a grid of cells of identical shape, where each cell is surrounded by neighbour cells and described by a set of transition rules that define how each cell evolves given the attributes of its surrounding neighbours. Through the application of simple rules that describe processes on a local level, global patterns emerge (Wolfram 1984). In other words, transition rules are derived by properly separating the phenomena’s processes such that combined results realistically represent the behavior of the phenomena.

In geography, CA models were widely applied for simulating urban growth and land use and land cover change (Couclelis 1985; Clarke et al. 1997; White and Engelen

1997; Yeh and Li 2001; Wu 2002; Barredo et al. 2003). In landslide modelling, several approaches used CA in order to overcome solving governing flow equations (e.g. Navier-Stokes equations for viscous fluids) without making substantial simplifications. Malamud and Turcotte (2000) presented a simple CA "sand pile" model to be applied to landslides from a statistical viewpoint. Segre and Deangeli (1995) presented a numerical model based on CA that was mainly descriptive in nature. Dattilo and Spezzano (2003) developed a tool that allowed interactive exploration of the simulation, while changing parameters on the fly.

The integration of CA and a geographic information system (GIS) is both beneficial and necessary because a GIS possesses the ability to support different types of data models by providing the environment to perform spatial analyses and modelling (Goodchild et al. 1992). For example, coupling CA and a raster GIS provides convenience of data compatibility, neighbourhood space, and predefined analytical tools for a CA to apply transition rules, which essentially are sequences of GIS operations applied repetitively to neighbourhood cells (Wagner 1997). However, GIS handles the temporal dimension inadequately and therefore lacks the ability to perform spatial dynamic modelling processes (Dragićević and Marceau 2000). Since GIS alone lacks a temporal component, the addition of CA provides the ability to represent time explicitly, while GIS analytical tools carry out spatial dynamic modelling (Park and Wagner 1997).

An example of a landslide model coupling GIS and CA is SCIDDICA (Smart Computational Innovative method for the Detection of Debris/mud flow path with Interactive Cellular Automata), which included multiple versions applied to specific landslide cases around the world (Di Gregorio et al. 1999; Avolio et al. 2000;

D'Ambrosio et al. 2003; Iovine et al. 2003). SCIDDICA is not a classical CA model as it still attempts to implement physical laws in a discrete a-centric context, where the conservation laws of physics are followed (D'Ambrosio et al. 2002). SCIDDICA included varying levels of complexity representing many geotechnical parameters of an actual landslide. Parameters such as thickness of the landslide, width of the flow front, water content, water loss and solidification of the landslide, slope and altitude, among others. These values were calculated based on a set of global parameters specific to the study site. Although SCIDDICA was applied successfully for specific landslide cases, further simplifications in the derivation of transition rules can potentially reduce data and computational resources. It was shown that both high accuracy and high efficiency was achieved in a model based on simple slope-based rules, therefore an abundance of complex rules do not guarantee enhanced results (Benda and Cundy 1990).

A second CA model developed for a study area in Vancouver Island, BC implemented rules for scour, deposit, path selection, and movement/spread for each moving landslide cell (Guthrie et al. 2008). Rules followed probability distributions were compiled through experience on Coastal British Columbia terrain and field work gathered. The CA model performed well in the areas of predicting realistic path selections and the size and shape of landslides. The weakness of the model, on the other hand, was its inability to model long channelized debris flows and landslides bifurcated more often compared to reality. Despite the complexity of a landslide, the model presented showed that simple empirically based rules derived from landslides across the world can be used in other regions, which may alleviate the need for a vast landslide inventory.

The availability of high resolution data, especially for detailed soil properties, is currently not as ubiquitous as elevation data, which means soil surveys must be carried out. However, data collection for soil sampling and measurement often consumes a significant portion of a project's budget (Domburg et al. 1997). On the other hand, high resolution elevation information in the form of a digital elevation model (DEM) is readily available at relatively low cost. Thus, combining the availability of a high resolution DEM with the simplicity and efficiency of a CA modelling approach can be proven advantageous over existing landslide CA models presented in the literature.

The main objective of this study is to develop a CA model for simulating urban landslide flow paths using a DEM, geographic information systems (GIS) and logistic regression. Moreover sensitivity analysis of the model is performed in order to test model parameters. This model is designed and implemented to effectively simulate the propagation of debris down slope based on CA transition rules derived from important triggering factors determined from logistic regression. This work provides a model and the tool for a low cost methodology to predict landslide deposition areas without acquiring detailed data for deterministic physical models.

2.3 Methods

The proposed urban landslide CA model consists of a logistic regression (LR) and a cellular automata theory that both accesses high resolution spatial and digital elevation data from a raster-based GIS (Figure 2-1). The inputs to the GIS are data layers related to landslide triggering factors and initial failure locations. The LR procedure determines the important factors and helps derive transition rules for the CA to simulate landslide run out from the initial failure polygon.

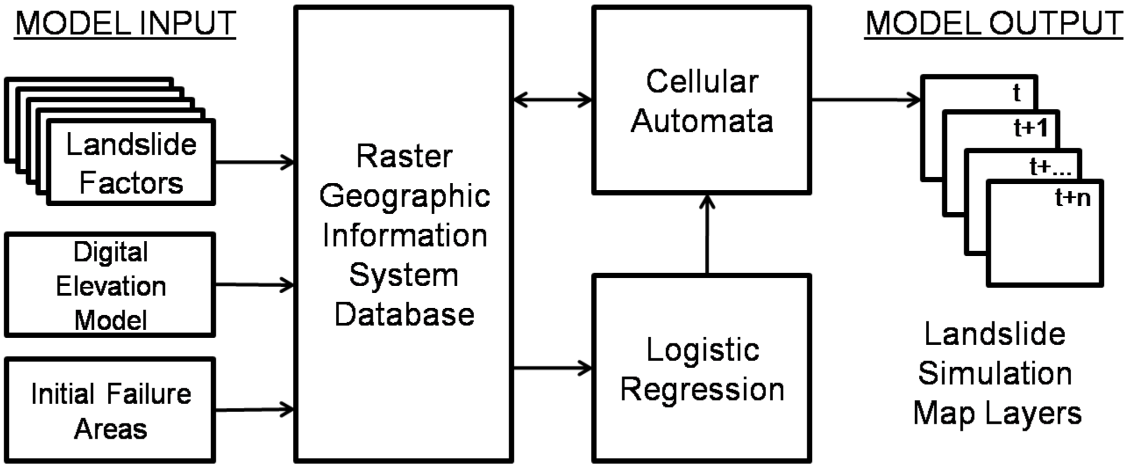

Figure 2-1. Design and interaction of components of the DEM-CA landslide model.

2.3.1 The Cellular Automata Landslide Model

The CA model is defined by following five components: the grid space, the neighbourhood of the CA, the finite set of states of each individual automaton, the transition rules, and the time step. The grid space is the defined region of the study site which limits where the phenomenon evolves. The spatial resolution of the raster grid determines the incremental distance the landslide travels when an empty cell is transitioned to a landslide cell. The neighbourhood of the CA in this model incorporates a 3 by 3 cell Moore neighbourhood, where each cell is surrounded by 8 cell neighbours. The finite set of states for each individual cell is defined as either a *landslide* or *no landslide*, which provides dichotomous states of simulation outputs.

The transition rules consist of the deterministic functions that govern and simulate the evolution of the phenomena. Rules can be drawn from a physical basis or empirical approach. The principal transition rule for landslide flow depends on the landslide front to search lower elevations and the steepest descent gradient to flow (Claessens et al.

2007). The rule is based on finding the greatest elevation difference between the center and neighbouring cells, which is similar to the aspect-ranking method employed by Guthrie et al. (2008). A constraint to landslide flow is the assumption that upslope movement does not occur. A landslide cell will not flow from a cell of lower elevation to a cell of higher elevation. Also, flow stoppage would occur when slope gradients became gentler than 5°, which is based on empirical studies (Benda and Cundy 1990). The CA accesses the elevation information from the DEM and calculates to which cell the landslide will propagate.

The final component to this CA model is the time step or iteration, which corresponds to a single application of the transition rules and updating of the new landslide area. The rules are applied synchronously, meaning every cell updates at the same time. Prior to a simulation, however, a polygon is introduced in the geospatial dataset to initialize the failure point of landslide movement. Following an entire model run, the rate of movement can be calculated using landslide extents and the number of time steps to provide a temporal correspondence (i.e. temporal resolution of landslide propagation).

2.3.2 Integrating Logistic Regression and Cellular Automata

Logistic regression (LR) is a type of predictive model that measures the probability of a dichotomous variable, such as 0 and 1or true and false, determined from the influence of one or more independent parameters (Menard 2001). In the case of applying LR to landslide prediction, the goal of LR would be to find the best fitting model to describe the relationship between the presence or absence of landslides (dependent variable) and slope and topographic feature parameters (independent variables). Generally, LR involves fitting the dependent variable using the equation following logistic transformation:

$$Y = \mathrm{Logit}\ (p) = \ln\left(\frac{p}{1\text{-}p}\right) = B_0 + B_1X_1 + B_2X_2 + \cdots + B_nX_n \qquad \text{Equation 2-1}$$

where p is the probability that the dependent variable (Y) is 1, $p/(1\text{-}p)$ is the odds or likelihood ratio, B_0 is the intercept, and B_1, B_2, … , B_n are regression coefficients, which measure the contribution of X_1 X_2, … , X_n (independent factors) to the variations in Y. The logistic transformation is applied to linearize the model and to ensure the predicted probability will be continuous within the range from 0-1 (Ayalew and Yamagishi 2005). If a regression coefficient is positive, its transformed value will be greater than one, meaning the event is more likely to occur. If a coefficient is negative, the log value will be less than one and the odds of the event occurring decreases. A coefficient of 0 has a log value of 1, therefore not changing the odds either way. Regression coefficients act as a guide to determine the relative importance of parameter classes for slope and topographic features.

Without digital GIS data representing soil parameters, such as soil depth and wetness, to determine how landslides propagate, geometrical parameters from the DEM can be directly extracted (Fabbri et al. 2003). For example, slope, aspect, hillshading, and topographic features are easily obtained from a DEM using predefined algorithms in a raster GIS. In this model, slope and topographic features were chosen as parameters to condition the transition rules in the CA. These DEM-derived parameters were selected because of their influence on soil water content, which is one of the primary triggers of slope failure during intense rainfall (Guinau et al. 2007). This also allows the indirect inclusion of soil parameters not available.

In order to determine which classes within slope and topographic features are important, parameters are fit according to Equation 2-1. The resulting coefficient weights represent the degrees of influence in predicting landslides. Weights from the logistic regression are used to adjust the values of the DEM, which affect the application of the transition rules in the CA. The parameters derived from the DEM either contribute or impede landslide entrainment and the degree of effect is adjusted in elevation according to the coefficient weight. Since the principal transition rule involves evaluating neighbours for the lowest elevations, the lowering and raising of elevations on the DEM controls how the flow occurs. Contributing parameters (i.e. positive weights) will alter the DEM by decreasing elevation where those features are found in order to increase the chance of flow into those areas. Conversely, parameters impeding flow (i.e. negative weights) will increase the elevation of the DEM in those areas to decrease the likelihood of flow.

2.4 Model Implementation

2.4.1 Study Area

The Berkley Escarpment in the District of North Vancouver (DNV), British Columbia is one particular area where urban landslides have been a common occurrence. According to engineering reports (Porter 2006), five landslides have initiated along the escarpment since 1972, while the latest failure occurred in 2005. The latest failure was brought on during a period of intense rainfall. These landslides caused property damage and in some cases human loss, which prompted the Provincial Government of British Columbia to order evacuations and to purchase at-risk homes.

The two cases of landslides used for this study are located in DNV, named Patrick Slide and Dawson-Chu Slide, occurred on December 17, 1979 following a period of heavy rain (Figure 2-2). The landslide fronts for Patrick Slide and Dawson-Chu Slide travelled approximately 180 m and 210 m, respectively. The distances for these slides were similar, but the areas affected differed. The Dawson-Chu Slide left behind a scar of 7410 m^2, compared to 3160 m^2 produced by the smaller Patrick Slide.

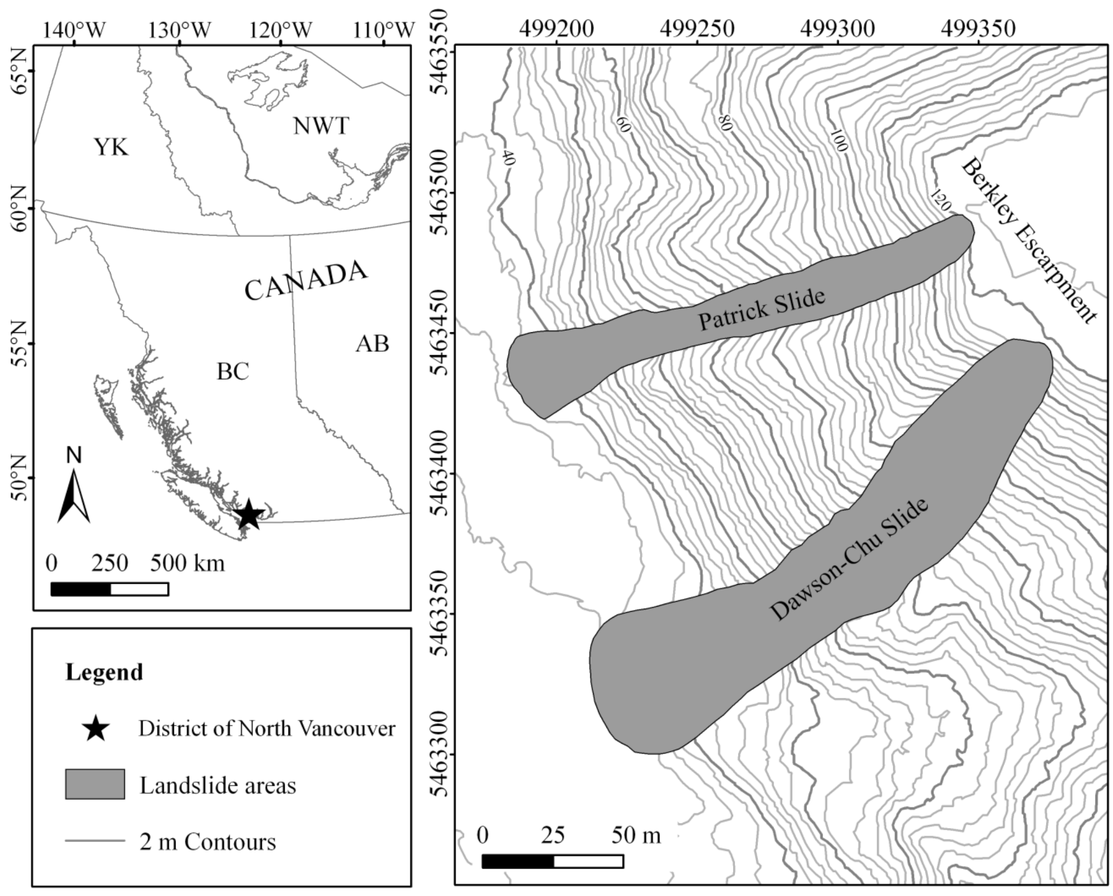

Figure 2-2. Location of two urban landslides on the Berkley Escarpment in District of North Vancouver, Canada.

2.4.2 Geospatial Data

A high resolution DEM was generated using 2 m LIDAR contour intervals made available through maps (1:2000) by the DNV in 2006. Digitization, conversion, and interpolation of the contour intervals, which resulted in a 1 m cell resolution DEM performed in Idrisi Taiga GIS software (Eastman 2009). The high resolution data provided the application of transition rules at a fine scale, which meant landslide flow moved at 1 m increments.

Using the derived high resolution DEM, slope and topographic features were extracted. Resulting slope gradients were continuous, therefore the values were discretized into 5° slope classes. The topographic feature classification resulted in the following features: convex hillside, concave hillside, inflection hillside, saddle hillside, ravine, and ridge.

The actual spatial extents of the Patrick Slide and Dawson-Chu Slide were also digitized from maps provided by the DNV. Since this CA model simulates the flow and not the initiation of landslides, the initial location of failure sites were approximated from the digitized landslide areas. A collection of cells, forming a polygon the initial width of the landslide, represented the initial failure mass. Since the objective was to examine landslide flow, rather than the initial failure process, a group of cells were used as a starting point instead of a single cell. The size of these initial sites should not be large enough to dictate the flow of the landslide, but provide an origin for the CA transition rules to simulate flow. The sizes of the polygons were estimated by the initial widths of the landslides The areas of the initial failure sites were 100 m^2 and 250 m^2, respectively for the Patrick Slide and Dawson-Chu Slide.

2.4.3 Specifying the CA Neighbourhood

A typical CA model employing a regular Moore neighbourhood would involve each cell taking into account interactions between 8 neighbours, however some neighbours can be omitted since their influence to the automaton is negligible based on position. For example, since the slopes in the study area face southwest, the neighbours of most influence are those at higher elevations in the northeast potentially with debris to fill the centre cell. Thus, downslope neighbours in cell locations [-1,0], [-1,-1], and [0,-1] have no significance and can be disregarded to form a modified Moore neighbourhood (Figure 2-3). Each automaton is then influenced only by interactions with its 5 northern and eastern neighbours. The omission of bottom-left neighbours allows the general direction of landslide flow to be assumed based on the direction of the slope aspect.

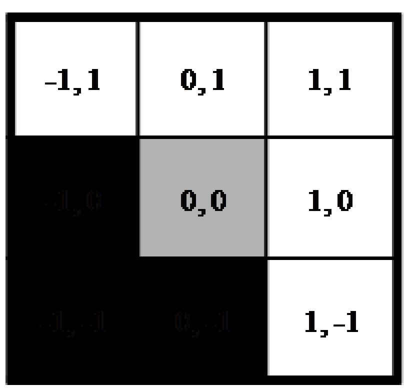

Figure 2-3. Modified Moore neighbourhood accounting for a southwest-facing aspect.

2.4.4 Logistic Regression and Transition Rules

The LR analysis was performed in Idrisi Taiga using slope classes and topographic features derived from the DEM as independent variables and the location of the past landslides as the dependent variable. The resulting regression coefficients are calculated for each individual variable (Table 2-1).

Table 2-1. Regression coefficients.

Independent variables	Coefficient
Slopes 0-5°	+0.002
Slopes 6-10°	+0.019
Slopes 11-15°	-0.063
Slopes 16-20°	+0.029
Slopes 21-25°	+0.081
Slopes 26-30°	+0.070
Slopes 31-35°	-0.071
Slopes 36-40°	+0.043
Slopes 41-45°	-0.023
Slopes 46-50°	+0.019
Concave Hillside	+0.204
Convex Hillside	-0.053
Inflection Hillside	-0.006
Saddle Hillside	+0.206
Ravine	-0.047
Ridge	+0.121
Intercept	-0.983

The regression coefficients determined statistically whether parameters contributed to the occurrence of landslides. Parameters with a positive coefficient indicated that the location of these parameters was related to the occurrence of landslides. Negative coefficients indicated that the location of these parameters had little to do with where landslides occurred. The magnitude of a coefficient explained the degree of influence towards whether a landslide occurred or not.

The result of the LR procedure was to modify the DEM such that it affects the flow of a landslide. For example, the most positively influential parameters given in Table 1 were concave and saddle hillsides. The hillside features overlaid on the DEM decreased elevation at those locations. Since the movement of flow is dictated by the CA seeking lower elevations, the attractiveness of flow to these areas is therefore enhanced. On the other hand, the most negative regression coefficient for topographic features was convex hillside, which meant deposition of debris avoided areas associated with convex features. These features increased the elevation on the DEM to reflect the aversion of flow to these areas. A flow chart of how CA utilized the changed elevations and transition rules is presented (Figure 2-4). Transition rules implemented for the landslide flow downhill, the prevention of upslope flow, and landslide stoppage, were combined with the adjustment of elevations to govern landslide flow.

2.4.5 Model Calibration and Sensitivity Analysis

The regression coefficients calculated from the LR procedure determined the influence of each parameter class for slope and topographic features. These in turn impacted how the DEM changed the attractiveness or avoidance of a cell, therefore the elevation change in the DEM for each parameter becomes very important. The magnitudes of regression coefficients of parameters determined the relative additions or subtractions of elevation to the DEM. The calibration procedure involves varying the magnitudes of changes to the DEM to create a temporary DEM layer, while maintaining the relative weights to find the right set of elevation changes that will produce accurate predictions.

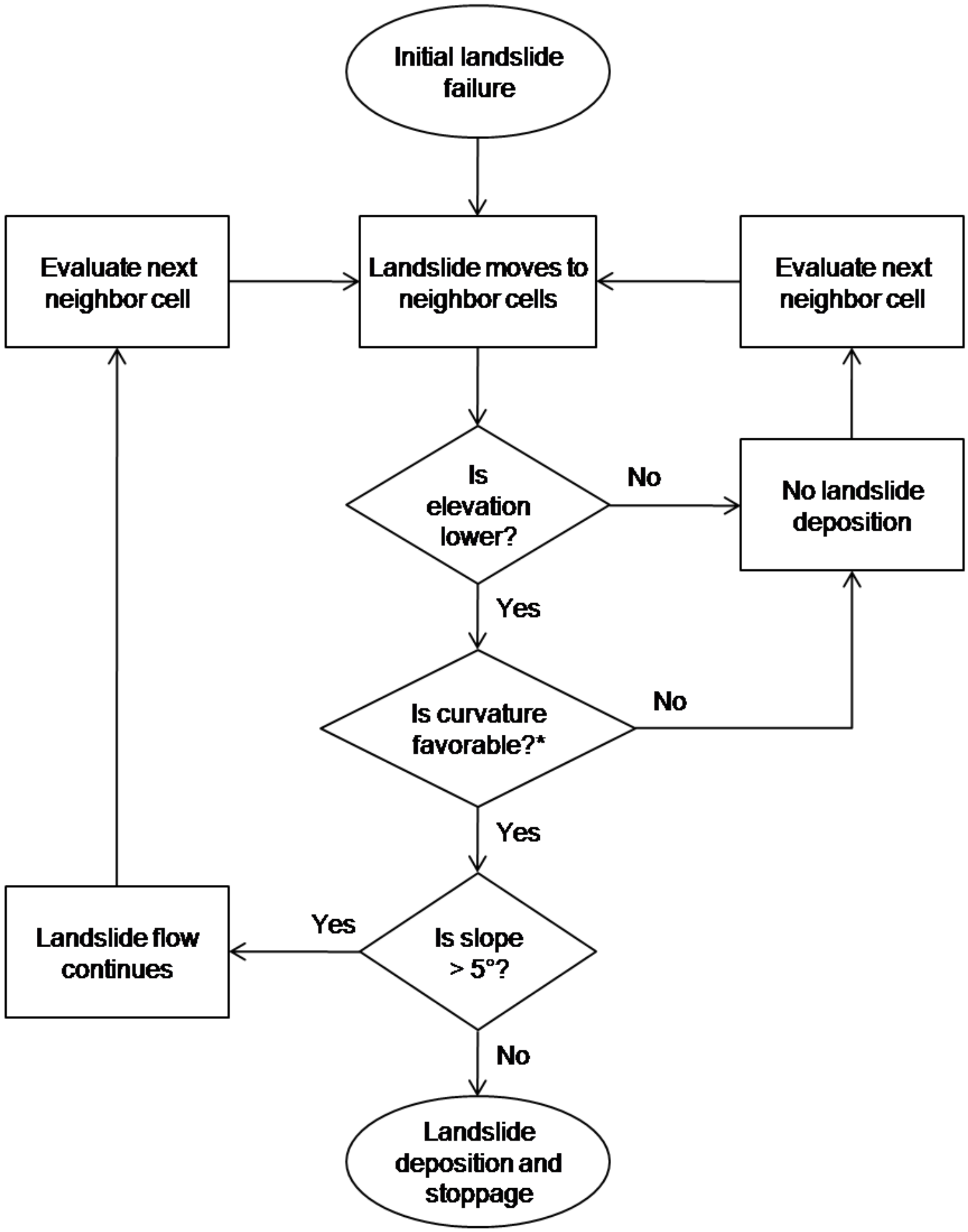

Figure 2-4. Flow diagram of the modelling process. (* Refers to the topographic features derived from the DEM and whether the curvature of the feature is prone to landsliding.)

Sensitivity analysis is performed to assess the relationship between model outputs based on model input variations and it is often considered mandatory in the model building process (Saltelli et al. 1999; Kocabas and Dragićević 2006). For spatial modelling, sensitivity analysis can be used to understand the behavior of a model and the coherence between a model and the real world (Crosetto et al. 2000). Given the uncertainty of the location of the initial failure areas, the starting locations of landslide failure are shifted along the top of the escarpment to determine the sensitivity of the model to initial conditions. This procedure investigates the model response and how the landslide will flow given different initial failure locations, which is a type of risk assessment for the particular region neighbouring the original landslide. This type of analysis can verify whether the factors chosen by LR properly represent the flow of a landslide. This is important because the regression coefficients directly influence the application of transition rules of the CA model.

2.5 Results

This section presents the landslide simulation outcomes based on the logistic regression procedure followed by the sensitivity analysis and the discussion on the computational efficacy of the developed model.

2.5.1 Logistic Regression Implementation

The DEM-based landslide CA model was applied to the Patrick Slide after calibration following the LR procedure. It is important to determine whether LR was applied appropriately and the overall statistics of the regression conducted in this study are summarized (Table 2-2). The model chi-square value calculates the difference between -2ln L (L=likelihood) for the best-fitting model and -2ln L_0 for the hypothesis that all coefficients except the intercept are 0. The result is a measure of the improvement in fit that the independent variables brought into the regression. For the CA model, the high value for model chi-square indicated that the occurrence of landslides was far less likely without landslide influencing parameters than the full regression model, where parameters were included. In other words, a large relative difference between -2ln L and -2ln L_0 suggests the significance of the input parameters. The pseudo R^2 value, which is calculated from 1-(ln L/ ln L_0), gives an indication of how well the logit model fits the data (Menard 2001). The pseudo R^2 value ranges from 0 to 1, where 0 shows no relationship and 1 indicates a perfect fit. Clark and Hosking (1986) demonstrated that a pseudo R^2 value exceeding 0.2 corresponds to a relatively good fit, which was the case in this study. An alternative approach called the relative operating characteristic (ROC) used spatial statistics, which is much easier to interpret and looks at how well the model actually predicts the dependent variable. ROC compares a Boolean map of the actual presence or absence of landslides with the probability map produced by the regression (Ayalew and Yamagishi 2005). The ROC value ranges from 0.5 to 1, where 1 indicates a perfect fit and 0.5 represents a random fit. A value of 0.8650 was obtained in this study, which indicates a strong association between independent variables and dependent variables.

Table 2-2. Summary statistics for logistic regression analysis.

Summary Statistics	Value
-2ln L (L=likelihood)	84626
-2ln L_0	63794
Model chi-square	20832
Pseudo R^2	0.2462
ROC	0.8650

2.5.2 Urban Landslide CA Model Simulations

Simulation results for the Patrick Slide site are presented as the landslide progresses down slope (Figure 2-5). The first tile on the top-left shows the seed polygon at the initial state and the following tiles show the front of the landslide advancing as the set of transition rules are applied iteratively. In order to quantify accuracy and determine model performance, a map overlay method followed by cross tabulation was used. Accurate predictions, over-predictions, and missed predictions were spatially calculated by overlaying the simulated results over the true landslide (Figure 2-6). First, the ratio of accurate landslide cell predictions to real landslide cells was 89%. Second, the ratio of under-predicted landslide cells to real landslide cells was 11%. Finally, the ratio of over-predicted landslide cells to real occurrences was 23%. The adequacy of these results compare favorably to ratios achieved by other work published (D'Ambrosio et al. 2002).

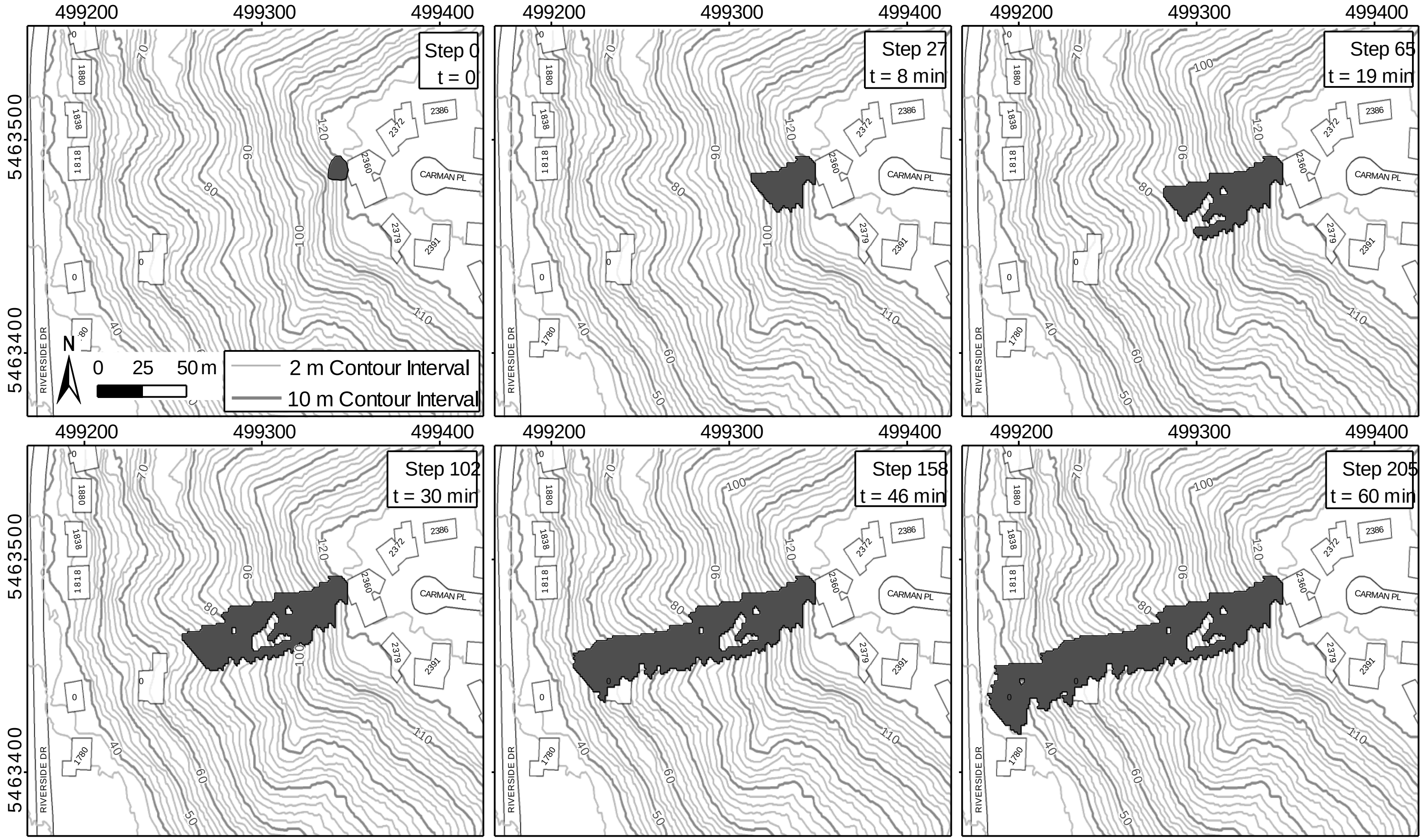

Figure 2-5. Snapshots of simulations between time steps 0 and 205 for Patrick Slide.

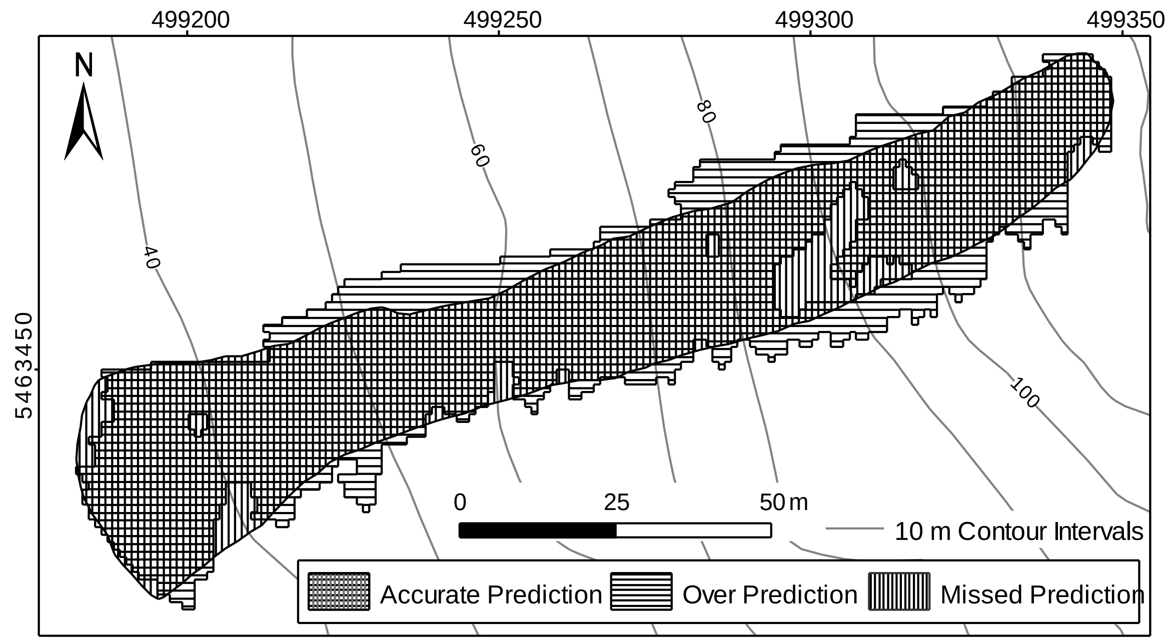

Figure 2-6. Map comparison of the predicted and actual Patrick Slide.

The CA model was also tested on the Dawson-Chu Slide and its progression is presented (Figure 2-7). The same map overlay measures of accuracies were calculated, but were not as favorable. The accurate landslide cell ratio, under-predicted landslide cell ratio, and over-predicted landslide cell ratio were 61%, 39%, and 5%, respectively. The obtained results may be a result of changes in elevation from 1979 to 2006, however data from 1979 was not available for verification. Although the results differ from the first site, the flow direction of the landslide was on the right path and curved southwest at the correct location (Figure 2-8).

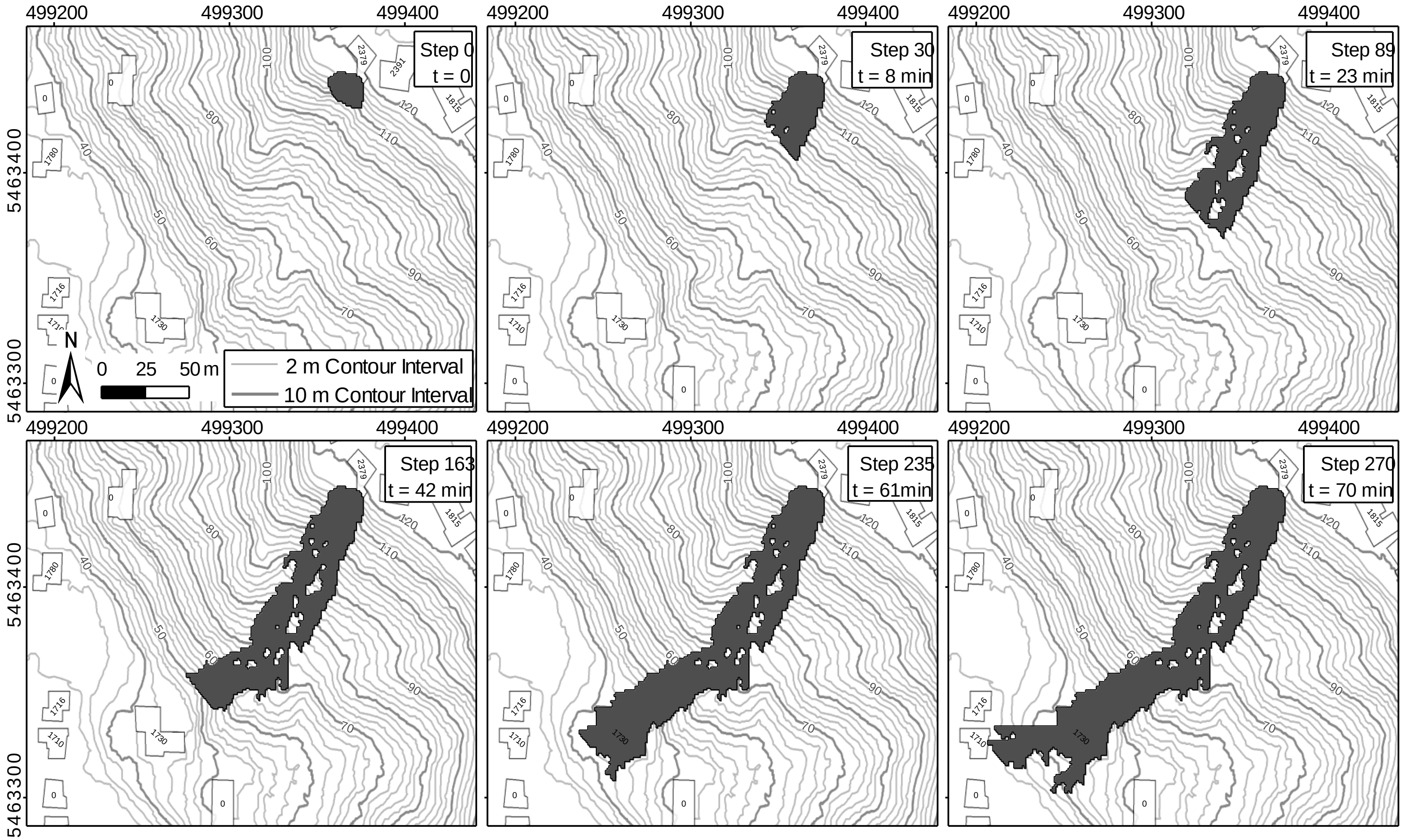

Figure 2-7. Snapshots of simulations between time steps 0 and 270 for Dawson-Chu Slide.

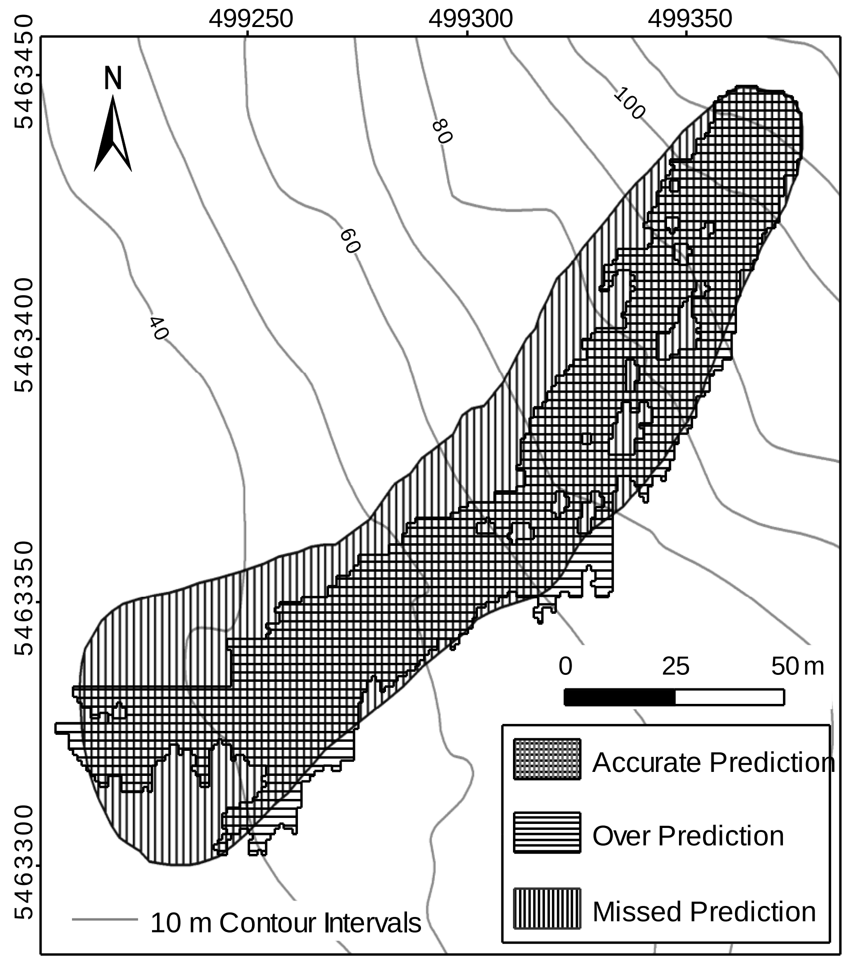

Figure 2-8. Map comparison of the predicted and actual Dawson-Chu Slide.

In terms of time, the Patrick Slide required 205 time steps to reach final deposition, while 270 were required for the Dawson-Chu Slide. The actual time from landslide initiation to deposition is unknown because there was no temporal account and record of the event, therefore an exact velocity cannot be obtained. In fact, recorded landslide start and end times or front velocity were characteristics rarely available in past cases because the precise timing of such an event was unpredictable (Legros 2002).

A solution to this unknown parameter was to estimate velocity based on seven classes of destructive significance of the landslide (Landslides 1995). Each classification of damage in terms of human and property loss corresponded to a range of maximum velocities. The report also provided a list of examples of landslide maximum velocities and resulting damage. One description matched the damages caused by the simulated landslides. The February 1990 Converney Landslide near Lausanne, Switzerland had a maximum velocity of 3 m/min and the damage caused was one demolished house and four other houses damaged, while no one was hurt. For the sake of calculating flow velocities, it can be assumed that the maximum velocities of the Patrick and Dawson-Chu Slides were equal to that of the Converney Landslide, based on similar damage impacts. The Patrick Slide had a flow length of 180 m, which translated to the event duration of 60 minutes. Thus it was estimated that the temporal scale of the CA model iteration for Patrick Slide corresponded to 17 seconds. Similarly, the Dawson-Chu Slide had an assumed maximum velocity of 3 m/min, which resulted in a 70 min long event for a 270 m landslide. Therefore, an iteration modelling the Dawson-Chu Slide represented 15 seconds.

2.5.3 Sensitivity Analysis

A sensitivity analysis was performed on the Patrick Slide in order to test sensitivity of simulation outcomes when landslide initiation location moved laterally. Simulations were run for each initiation or seed polygon shifted 11 m and 22 m both north and south along the top of escarpment. The overlap of multiple simulations is presented (Figure 2-9).

The northern most simulation began at a location where it was no longer within the confines of the original channel and therefore flowed in a different direction (Figure 2-10a). The straight line observed was due to the predefined notion of aspect-based movement, constricting the landslide from traveling north or northwest. The three other simulations (Figure 2-10b, 10c, 10d) began within the same channel as the original landslide and therefore propagated downslope over the same path of least resistance, despite initiating at varying locations. These results indicated not only that landslide movement flowed correctly downslope, but also followed the correct curvature within the channel and the intricacies of the DEM. Repeated simulations of landslide movement flow through common preferential routes, despite using different initial failure conditions, indicated that the model is robust when applied to this escarpment.

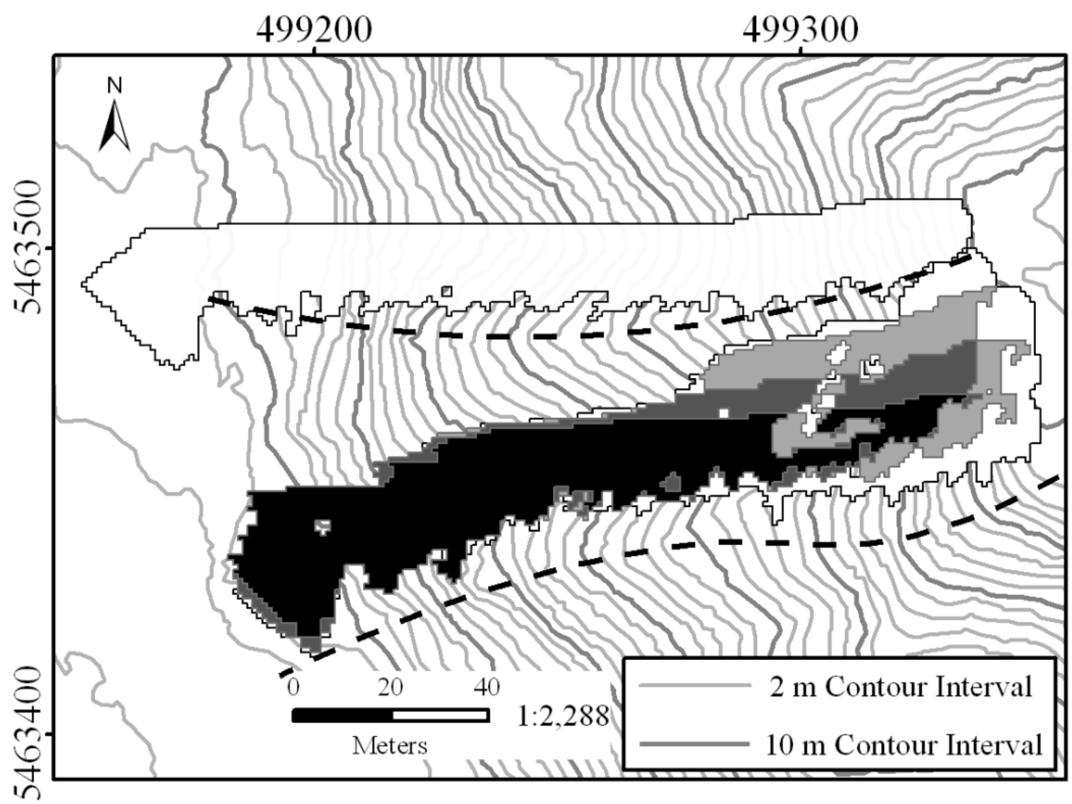

Figure 2-9. Sensitivity analysis on initial seed polygon. Darker colors indicate overlap between model runs. Dashed lines indicate the boundaries of the main channel.

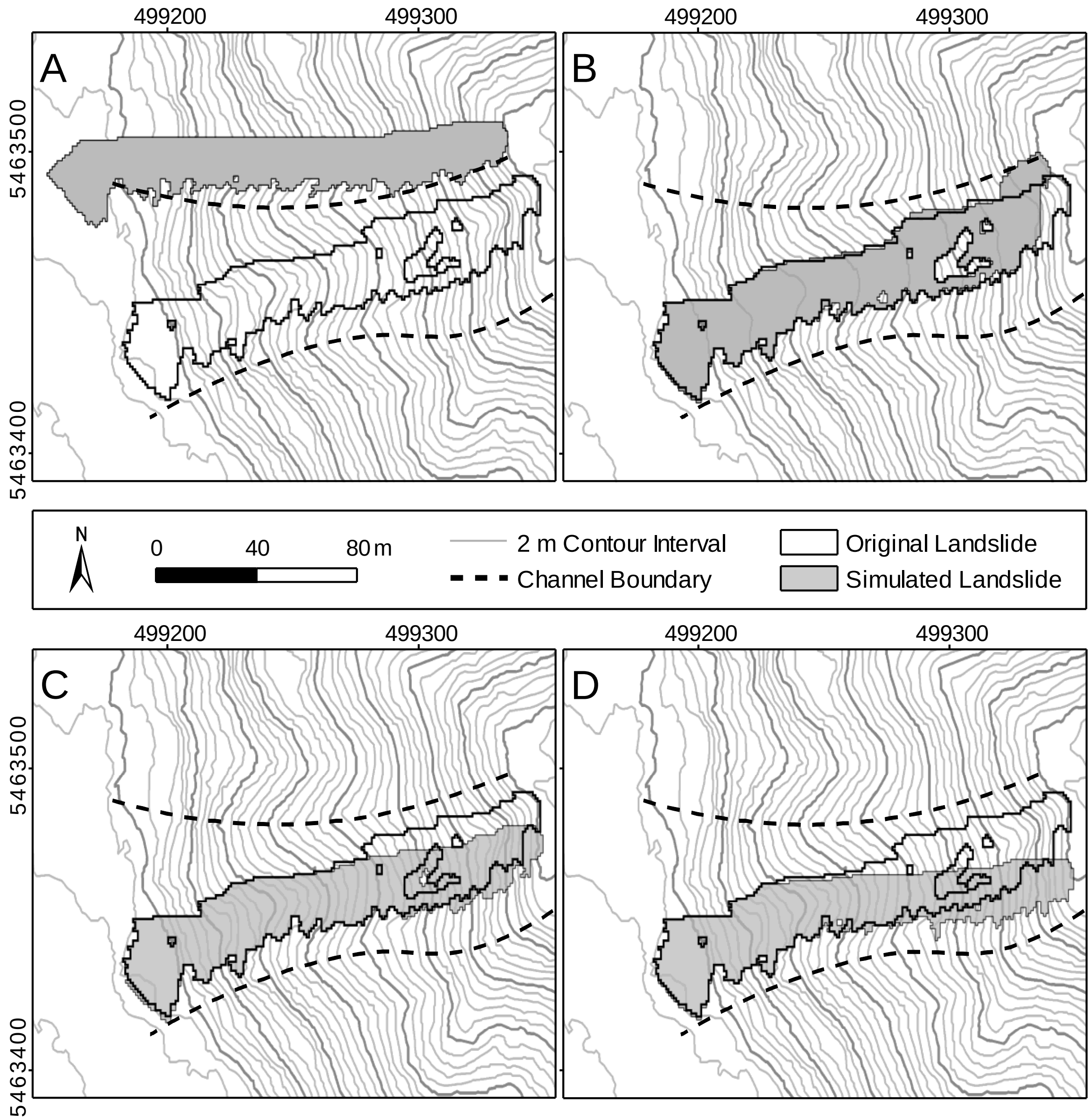

Figure 2-10. Testing the sensitivity of model simulations when initial failure location changes (a, b, c, d) on Patrick Slide.

2.5.4 Computational Efficiency

This CA model ran on a Pentium 3 Xeon processor (2.92 GHz) and required 15 minutes to generate 270 time steps, which was computationally efficient. For practical modelling, results should arrive in a timely manner and time spent on running the model becomes important, however the efficiency will depend on the computational power of the computer used. The reason for the high efficiency was due to the simplicity and straightforward calculations of the model parameters and transition rules. The purpose was to accurately model landslide flow using limited availability of data. The simulation outcomes indicated that the model of landslide simulation is adequate and feasible without demanding a vast amount of detailed information and computational efforts solving exhaustive physically-based differential equations.

2.6 Conclusion

The developed model for landslides used an integrated GIS and CA approach that required only a DEM dataset has proved to be sufficiently accurate and efficient. Simple transition rules were incorporated to route the landslide flow to concave and saddle areas where deposition would more likely occur and avoided convex up features because flows would not naturally occur in those areas. This proposed approach could be useful where landslides are a constant hazard and the availability of detailed data from field surveys are a constraint. High resolution elevation data is readily available and could provide a low-cost solution for determining landslide flow given known potential initiation zones.

Acknowledgements

The authors are thankful for full support of this study to the Natural Sciences and Engineering Research Council (NSERC) of Canada Discovery Grant awarded to the second author. Acquisition of elevation base maps, contour maps, and landslide extent maps used are provided by the District of North Vancouver GIS Department, British Columbia, Canada.

2.7 References

Akgun, A. and F. Bulut (2007). "GIS-based landslide susceptibility for Arsin-Yomra (Trabzon, North Turkey) region." Environmental Geology **51**(8): 1377-1387.

Alexander, D. (1989). "Urban landslides." Progress in Physical Geography **13**(2): 157-191.

Avolio, M. V., S. Di Gregorio, et al. (2000). "Simulation of the 1992 Tessina landslide by a cellular automata model and future hazard scenarios." International Journal of Applied Earth Observation and Geoinformation **2**(1): 41-50.

Ayalew, L. and H. Yamagishi (2005). "The application of GIS-based logistic regression for landslide susceptibility mapping in the Kakuda-Yahiko Mountains, Central Japan." Geomorphology **65**(1-2): 15-31.

Barredo, J. I., M. Kasanko, et al. (2003). "Modelling dynamic spatial processes: simulation of urban future scenarios through cellular automata." Landscape and Urban Planning **64**(3): 145-160.

Benda, L. E. and T. W. Cundy (1990). "Predicting deposition of debris flows in mountainous channels." Canadian Geotechnical Journal **27**: 409-417.

Castellanos Abella, E. A. and C. J. Van Westen (2008). "Qualitative landslide susceptibility assessment by multicriteria analysis: A case study from San Antonio del sur, Guantanamo, Cuba." Geomorphology **94**(3-4): 453-466.

Claessens, L., J. M. Schoorl, et al. (2007). "Modelling the location of shallow landslides and their effects on landscape dynamics in large watersheds: An application for Northern New Zealand." Geomorphology **87**(1-2): 16-27.

Clark, W. A. and P. L. Hosking (1986). Statistical methods for geographers. New York, John Wiley and Sons.

Clarke, K. C., S. Hoppen, et al. (1997). "A self-modifying cellular automaton model of historical urbanization in the San Francisco Bay area." Environment and Planning B-Planning & Design **24**(2): 247-261.

Couclelis, H. (1985). "Cellular worlds: a framework for modeling micro-macro dynamics." Environment and Planning A **17**(5): 585-596.

Crosetto, M., S. Tarantola, et al. (2000). "Sensitivity and uncertainty analysis in spatial modelling based on GIS." Agriculture Ecosystems & Environment **81**(1): 71-79.

D'Ambrosio, D., S. Di Gregorio, et al. (2002). "Simulating the Curti-Sarno debris flow through cellular automata: the model SCIDDICA (release S2)." Physics and Chemistry of the Earth **27**(36): 1577-1585.

D'Ambrosio, D., S. Di Gregorio, et al. (2003). "First simulations of the Sarno debris flows through Cellular Automata modelling." Geomorphology **54**(1-2): 91-117.

Dattilo, G. and G. Spezzano (2003). "Simulation of a cellular landslide model with CAMELOT on high performance computers." Parallel Computing **29**(10): 1403-1418.

Di Gregorio, S., R. Rongo, et al. (1999). "Mount ontake landslide simulation by the cellular automata model SCIDDICA-3." Physics and Chemistry of the Earth Part a-Solid Earth and Geodesy **24**(2): 131-137.

Domburg, P., J. J. de Gruijter, et al. (1997). "Designing efficient soil survey schemes with a knowledge-based system using dynamic programming." Geoderma **75**(3-4): 183-201.

Dragićević, S. and D. J. Marceau (2000). "A fuzzy set approach for modeling time in GIS." International Journal of Geographical Information Science **14**(3): 225-245.

Eastman, J. R. (2009). IDRISI Taiga. Worcester, MA, Clark University.

Eisbacher, G. H. and J. J. Clague (1981). "Urban landslides in the vicinity of Vancouver, British Columbia, with special reference to the December 1979 rainstorm." Canadian Geotechnical Journal **18**(2): 205-216.

Evans, S. G. (1982). "Landslides and surficial deposits in urban areas of British Columbia: A review." Canadian Geotechnical Journal **19**(3): 269-288.

Fabbri, A. G., C.-J. F. Chung, et al. (2003). "Is Prediction of Future Landslides Possible with a GIS?" Natural Hazards **30**(3): 487-503.

Goodchild, M., R. Haining, et al. (1992). "Integrating GIS and spatial data analysis: problems and possibilities." International Journal of Geographical Information Systems **6**(5): 407-423.

Guinau, M., I. Vilajosana, et al. (2007). "GIS-based debris flow source and runout susceptibility assessment from DEM data - a case study in NW Nicaragua." Natural Hazards and Earth System Sciences **7**(6): 703-716.

Guthrie, R. H., P. J. Deadman, et al. (2008). "Exploring the magnitude-frequency distribution: a cellular automata model for landslides." Landslides **5**(1): 151-159.

Iovine, G., S. Di Gregorio, et al. (2003). "Debris-flow susceptibility assessment through cellular automata modeling: an example from 15–16 December 1999 disaster at Cervinara and San Martino Valle Caudina (Campania, southern Italy)." Natural Hazards and Earth System Sciences **3**: 457-468.

Kocabas, V. and S. Dragićević (2006). "Assessing cellular automata model behaviour using a sensitivity analysis approach." Computers Environment and Urban Systems **30**(6): 921-953.

Landslides, I. W. I. U. o. G. S. W. G. o. (1995). "A suggested method for describing the rate of movement of a landslide." Bulletin of Engineering Geology and the Environment **52**(1): 75-78.

Legros, F. (2002). "The mobility of long-runout landslides." Engineering Geology **63**(3-4): 301-331.

Luzi, L. and F. Pergalani (1996). "Applications of statistical and GIS techniques to slope instability zonation (1:50.000 Fabriano geological map sheet)." Soil Dynamics and Earthquake Engineering **15**(2): 83-94.

Malamud, B. D. and D. L. Turcotte (2000). "Cellular-automata models applied to natural hazards." Computing in Science & Engineering **2**(3): 42-51.

Menard, S. (2001). Applied logistic regression analysis. Thousand Oaks, CA, Sage University Paper Series on Quantitative Applications in Social Sciences.

Neaupane, K. M. and M. Piantartakulchai (2006). "Analytic network process model for landslide hazard zonation." Engineering Geology **85**(3-4): 281-294.

Park, S. and D. F. Wagner (1997). "Incorporating Cellular Automata simulators as analytical engines in GIS." Transactions in GIS **2**(3): 213-231.

Paulin, G. L. and M. Bursik (2009). "Logisnet: A tool for multimethod, multiple soil layers slope stability analysis." Computers & Geosciences **35**(5): 1007-1016.

Porter, M. (2006). District of North Vancouver, Berkley Landslide Risk Management: Phase 2 Assessment of Risk Control Options, BGC Engineering**:** 1-33.

Saltelli, A., S. Tarantola, et al. (1999). "A quantitative model-independent method for global sensitivity analysis of model output." Technometrics **41**(1): 39-56.

Santini, M., S. Grimaldi, et al. (2009). "Pre-processing algorithms and landslide modelling on remotely sensed DEMs." Geomorphology **113**(1-2): 110-125.

Segre, E. and C. Deangeli (1995). "Cellular automaton for realistic modelling of landslides." Nonlinear Processes in Geophysics **9407**(2).

Sidle, R. C. and H. Ochiai (2006). Landslides: Processes, Prediction, and Land Use. Washington, DC, American Geophysical Union.

Toffoli, T. (1984). "Cellular Automata as an alternative to (rather than an approximation of) differential equations in modeling physics." Physica D: Nonlinear Phenomena **10**(1-2): 117-127.

Van Westen, C. J. and M. T. J. Terlien (1996). "An approach towards deterministic landslide hazard analysis in GIS. A case study from Manizales (Colombia)." Earth Surface Processes and Landforms **21**(9): 853-868.

Van Westen, C. J., T. W. J. Van Asch, et al. (2006). "Landslide hazard and risk zonation - why is it still so difficult?" Bulletin of Engineering Geology and the Environment **65**(2): 167-184.

Wagner, D. F. (1997). "Cellular automata and geographic information systems." Environment and Planning B-Planning & Design **24**(2): 219-234.

White, R. and G. Engelen (1997). "Cellular automata as the basis of integrated dynamic regional modelling." Environment and Planning B-Planning & Design **24**(2): 235-246.

White, R. and G. Engelen (2000). "High-resolution integrated modelling of the spatial dynamics of urban and regional systems." Computers, Environment and Urban Systems **24**(5): 383-400.

Wolfram, S. (1984). "Cellular automata as models of complexity." Nature **311**(5985): 419-424.

Wu, F. L. (2002). "Calibration of stochastic cellular automata: the application to rural-urban land conversions." International Journal of Geographical Information Science **16**(8): 795-818.

Wu, W. M. and R. C. Sidle (1995). "A distributed slope stability model for steep forested basins." Water Resources Research **31**(8): 2097-2110.

Yalcin, A. and F. Bulut (2007). "Landslide susceptibility mapping using GIS and digital photogrammetric techniques: a case study from Ardesen (NE-Turkey)." Natural Hazards **41**(1): 201-226.

Yeh, A. G. O. and X. Li (2001). "A constrained CA model for the simulation and planning of sustainable urban forms by using GIS." Environment and Planning B-Planning & Design **28**(5): 733-753.

CHAPTER 3 GIS-BASED FUZZY MULTICRITERIA EVALUATION AND MULTISCALE ANALYSIS TO CHARACTERIZE LANDSLIDE SUSCEPTIBILITY[2]

3.1 Abstract

Landslides have a severe impact on the socio-economic and natural environment as well as on the well-being of individuals and communities. In landslide susceptibility analysis, maps are generated to show various levels of threat to human populations. Conducting an effective landslide susceptibility analysis is crucial in minimizing the impact of landslides on human lives. However, important factors such as data availability, data quality and spatial data resolution influence the scale at which landslide susceptibility analysis is done. The challenges of working with limited data often lead researchers to conduct analyses at only a single spatial scale and resolution. In this study, multiscale analysis is integrated into a GIS-based fuzzy multicriteria evaluation (MCE) approach to determine landslide susceptibilities in the Metro Vancouver region, British Columbia, Canada. A set of landslide-conditioning parameters is chosen for each analysis scale based on the relevance and effect these parameters have on the scale of analysis. A digital elevation model is used to calculate relevant topographic variables such as slope gradient, aspect gradient, stream power index, and topographic wetness index at three geographic scales. The scales of analysis are: a regional scale at 50 m resolution; a municipal scale at 10 m resolution; and a local scale at 1 m resolution. GIS-based fuzzy

[2] A version of this chapter is under review for publication in the *Journal of Environmental Management* under the co-authorship of Suzana Dragicevic and Shivanand Balram.

MCE models are developed for each scale and the seed cell area index method is used to test the validity of the output landslide susceptibility maps against real landslide inventory data. The developed approach allows various end users such as urban planners and emergency managers to assess landslide susceptibility conditions at various scales thereby enabling more effective community planning, targeting of emergency services, and the allocation of limited resources.

3.2 Introduction

Landslides are described as the mass movements of slope-forming materials composed of rocks, soils, artificial fill, or combination of these materials (Sidle and Ochiai 2006). They occur swiftly and can have devastating consequences on the well-being of individuals and communities especially in areas where urban areas coincide with mountainous regions. The costs incurred are related to relocating communities, repairing building structures, resolving disrupted transportation networks, and restoring the quality of water in streams and rivers (Yalcin 2007).

The Joint Technical Committee on Landslides and Engineered Slopes characterizes landslide susceptibility zoning as the spatial distribution and classification of terrain units according to their predisposition to result in landslides (Fell et al. 2008). Assessments of landslide susceptibility are important to engineers and city planners since susceptibility maps are an additional tool used to support the selection of areas for development. In order to reduce the adverse effects of landslides, landslide susceptibility and hazard zoning techniques have been developed since the 1970s by manually delineating zones of susceptibility using aerial photographs (Brabb et al. 1972; Drennon and Schleining 1975). In the recent decades, there has been steady progress in preparing hazard zoning maps because of the rapid development of Geographical Information Systems (GIS) that has greatly advanced the susceptibility mapping process in both efficiency and accuracy. GIS has allowed large volumes of data to be managed and analyzed in a very short time and has been utilized in various landslide mapping studies (Yalcin and Bulut 2007). Despite the advances in GIS capabilities landslide susceptibility studies are still mostly being conducted at a single scale. The objectives of this study are to (1) develop a multiscale MCE model for landslides, (2) implement the modeling approach at a regional, municipal and local spatial scale, and to (3) test the approach using data from the Metro Vancouver area, District of North Vancouver (DNV), and locally on the Berkley Escarpment in the DNV. The spatial resolutions of the Metro Vancouver, DNV, and Berkley Escarpment study areas are 50 m, 10 m, and 1 m, respectively.

There are many techniques available to produce landslide susceptibility maps and these can be categorized into quantitative methods, semi-quantitative methods, and qualitative methods. Quantitative methods such as deterministic models (Wu and Sidle 1995; Luzi and Pergalani 1996; Van Westen and Terlien 1996; Gorsevski et al. 2006; Gomes et al. 2008; Santini et al. 2009) and probabilistic and statistical models (Dai and Lee 2003; Ohlmacher and Davis 2003; Ayalew and Yamagishi 2005; Ercanoglu 2005; Yilmaz 2009; Yilmaz and Keskin 2009) have minimal dependence on human judgment and expert opinion to produce output maps. However, quantitative techniques require large volumes of detailed data derived from laboratory tests and field surveys making them highly unsuitable for regional scale studies (Van Westen et al. 2006). Heuristic methods (both qualitative and semi-quantitative) range from direct field mapping methods to complex logical and computer-based systems that incorporate human judgment and expert opinions (Van Westen et al. 2003; Lee and Choi 2004; Castellanos Abella and Van Westen 2008). A common heuristic approach linking GIS and multicriteria evaluation (MCE) (Jankowski 1995) uses expert opinions on multiple criteria and the resulting landslide maps are categorized into zones of “very low”, “low”, “medium”, “high”, and “very high” categories of susceptibility. A mixture of criteria weighting tools such as the Analytical Hierarchy Process (AHP) and criteria integration tools such as Weighted Linear Combination (WLC) are then used to generate the landslide susceptibility maps (Gorsevski et al. 2006; Akgun and Bulut 2007; Yalcin 2008; Akgun and Turk 2010). Heuristic analysis has proven to be a cost-effective solution for large study areas having limited available data (Van Westen et al. 2006).

Selecting the appropriate scale of analysis is always problematic when producing a susceptibility map as it is often a compromise between the desired scale and data availability. Landslide susceptibility studies usually generate a single map at a fixed scale based on data convenience. However, the scale of observation affects the analysis, outputs and consequently their interpretation. For example, at a country level scale topography will explain the broad patterns of slope, aspect, and flow accumulation and mask local variations that occur at a finer scale. As the scale changes, so do associated patterns of spatial processes and this has implications for understanding any phenomena and the applicability of methods and results from one scale to another (Hay et al. 2001). Understanding the behaviour of phenomena at multiple scales is imperative to determine the effect of scale on spatial processes (Wu et al. 2000).

In the literature, only one analysis has used a multiscale MCE approach to evaluate landslides. The work developed a landslide risk index map at the national level with additional analyses at provincial and municipal levels (Castellanos Abella and Van Westen 2007). One challenge was the lack of available data for the entire country and hence the authors were forced to exclude deterministic landslide hazard assessment methods from their analysis. They compromised by using MCE and AHP methods to produce a qualitative landslide risk index. Further, from this national level risk map they identified areas of high risk at the provincial and municipal levels for additional statistical analysis once relevant data becomes available or accessible. While the authors have produced a useful representation of landslides at the national level, it is clear the methods used and the scale of analysis was conditioned on data availability.

In this study, we have integrated a multiscale analysis into a GIS-based fuzzy multicriteria evaluation (MCE) approach to determine landslide susceptibilities in the Metro Vancouver region, British Columbia, Canada. The ability to model landslide susceptibility across multiple scales allows various levels of decision makers to target susceptibility hotspots and allocate resources and services on a needs basis. The next sections of the paper provide relevant background to the tools and parameters used, outline the multiscale GIS-based fuzzy MCE approach developed, and implement the developed approach at three scales of analysis. The implications of the work are then discussed and some general conclusions stated.

3.3 Background

3.3.1 Geographic Information Systems

Geographic information systems (GIS) has rapidly developed from being a geographic database tool to now being able to provide sophisticated logical and mathematical analysis between multiple map layers (Eastman et al. 1995). GIS gives the ability to store, handle, and transform spatial data efficiently and the integration of additional analytical techniques that can cope with multiple criteria problems has greatly enhanced the functionality of GIS (Carver 1991; Goodchild 2003). As a consequence, GIS is quickly evolving into a decision support system where decisions are made based on mapping outputs generated from the GIS analysis.

Spatial environmental problems with multiple criteria are easier to handle in a raster GIS. In the raster GIS data model, geographic space is represented as a grid of regular cells and each cell is coded with a single attribute value. With this raster GIS model, remote sensing data based on the pixel can now be easily integrated into the GIS as the spatial conceptualization of the pixel is analogous to that of the grid cell (Fisher 1997). Once in the GIS, remote sensing data can then be subjected to advanced spatial data analysis techniques at various scales of analysis.

3.3.2 Multicriteria Evaluation

In multicriteria evaluation (MCE) or multicriteria analysis (MCA) the aim is to investigate a number of choice possibilities given numerous criteria and conflicting objectives (Voogd 1982; Carver 1991; Jankowski 1995). In other words, MCE is primarily concerned with how to combine information from several criteria by standardization to form a single index of evaluation. Criteria are the evidence that the outcome is based on and can be in the form of either factors or constraints. A factor increases or decreases the suitability of a specific alternative for the activity under consideration, while a constraint provides exclusions and limits the alternatives under consideration (Eastman et al. 1995). The degree of suitability of factors can range from either Boolean unsuitable to suitable (i.e. zeros and ones) to varying levels of certainty (i.e. a continuous scale from zero and one), which can be attributable to the type of data used and the subjectiveness of each expert (Malczewski 1999). Fuzzy set theory was developed to deal with the inherent uncertainty of data by allowing membership of data belonging to a set along a continuous scale, rather than a crisp binary set membership (Zadeh 1965). Compared to linear scaling, fuzzy sets are a more realistic standardization approach because using a fuzzy set membership represents a specific relation between the criteria and possible outcomes (Wood and Dragicevic 2007; Gorsevski and Jankowski 2010). When Boolean overlay is used, membership values are reduced to 0 and 1, which assumes crisp boundaries meaning the final outcome is identical to those of Boolean overlay (Jiang and Eastman 2000). Following standardization, the MCE approach requires the expert to construct a matrix that provides the relative importance of each evaluation criteria with respect to the overall objective of the problem (Voogd 1982). By varying and prioritizing criteria, it is possible to generate compromising alternatives and thus rank alternative outcomes by the different expert opinions (Malczewski 2006). Since varying the relative importance of criteria reflects the knowledge of experts, it allows for sensitivity analysis and validation of weights and rankings of alternatives (Jankowski and Richard 1994; Feick and Hall 2004).

MCE provides many advantages for use in defining landslide susceptibility. Landslide studies often use MCE techniques because the types of data available are commonly qualitative (from expert opinion) and quantitative (from observed relationships between parameters and landslides), therefore requiring a semi-quantitative method that incorporates both types of data (Ayalew et al. 2004). These methods involve assigning weights to the different parameters affecting landslide susceptibility and many techniques exist for determining weights (Akgun and Bulut 2007). The most common approach involves obtaining expert opinion to assigning weights in a procedure known as Analytical Hierarchy Process (AHP) and then combining weights additively by weighted linear combination (WLC) to produce landslide susceptibility maps (Ayalew et al. 2005; Komac 2006; Yalcin and Bulut 2007; Akgun et al. 2008).

3.3.3 Landslide-Conditioning Parameters

Landslides are generated from complex processes and hence many landslide-controlling parameters are given consideration to improve the accuracy of the susceptibility mapping. However, in practical implementations many parameters may not be needed due to statistical redundancy or impossible to include due to the unavailability of detailed data. For example, high resolution soil depths and soil properties are not readily available. For these reasons, this study used parameters derived from topographic attributes, vector lines of road, and stream networks. The specific landslide-conditioning parameters considered were: slope gradient, aspect gradient, stream power index (SPI), topographic wetness index (TWI), elevation, distance to road networks, and distance to stream networks.

3.3.4 Slope and Aspect Gradient

Slope gradient is widely used in landslide susceptibility studies because it is known that the movement of landslide material is directly related to slope (Dai et al. 2001; Lee and Min 2001; Van Westen et al. 2003). Specifically, shear stresses on the slope material increases as the slope gradient increases and it is generally expected that landslides occur on the steepest slopes. The slope for each raster cell is calculated as a function of the cell resolution and neighbouring cells (Monmonier 1982). Aspect gradient affects slope material in a indirect relationship because aspect determines the exposure of a landscape to rainfall and solar radiation, and therefore the propensity of vegetation to grow, which in turn effects the soil stability (Carrara et al. 1991). The aspect for each raster cell is calculated as the direction in which the maximum slope faces.

3.3.5 Stream Power Index

The stream power index (SPI) is widely used as a conditioning parameter (Duman et al. 2006; Conoscenti et al. 2008; Yilmaz 2009). The index describes a measure of erosive power of flowing water based on the assumption that runoff is directly proportional to the upslope contributing area (Moore et al. 1991). In terms of each grid cell in the raster GIS, SPI is a function of erosive power of runoff acting on each cell. SPI is defined as:

$$SPI = A_s \times \tan\beta \quad \text{(Equation 3-1)}$$

where A_s = specific catchment area (m^2/m) and β = slope gradient (°).

As A_s and β increase, it is assumed that the amount of water provided by upslope areas and the flow velocity of water increase, thereby increasing SPI and slope-erosion risk.

3.3.6 Topographic Wetness Index

The topographic wetness index (TWI) describes the effect of topography on the location and size of saturated areas of runoff generation (Moore et al. 1991). In other words, this index can be used as an estimation of spatial patterns for soil moisture because topography controls the hydrological conditions where surface runoff and groundwater flow. TWI is defined as:

$$TWI = ln\frac{A_s}{tan\beta} \quad \text{(Equation 3-2)}$$

where A_s = specific catchment area (m^2/m) and β = slope gradient (°).

Steady state conditions and uniform soil properties are assumed. The equation gives predicted values for areas of saturation where A_s is large and β is small; typically these conditions occur at converging slopes in the landscape combined with gentle slope gradient areas.

3.3.7 Elevation

There is overwhelming evidence that elevation is a strong indicator of landslide susceptibility (Pachauri and Pant 1992; Gokceoglu et al. 2005; Duman et al. 2006). Landslides typically occur in the intermediate elevations as slopes tend to be covered by a layer of thin colluvium, which is prone to landslides (Dai and Lee 2002). Landslides are less likely to occur at very high elevations because only weathered rocks are found due to their shear strength being much higher. In the lower elevations, slopes are gentle and covered by thicker colluvium. The chance of landslides occurring is lower, unless the water table rises to initiate slope failure.

3.3.8 Distance to Road Networks

Gravel materials used for roads are engineered and compacted to withstand heavy loads making the surfaces flat and impermeable. During periods of heavy rainfall, road surfaces allow little to no infiltration thereby rapidly achieving overland flow and surface runoff (Horton 1945). Roads can have an major impact on surrounding areas as they have the ability to allow water to pool, which can overload, undercut, and saturate slopes (Guthrie 2002). In addition to increasing the susceptibility for landslide initiation, roads also intercept, store, and produce sediment, which influences downstream hillslopes not necessarily near initiation sites (Wemple et al. 2001).

3.3.9 Distance to Drainage Networks

Landslides have been associated with proximity to drainage network lines because terrain modification caused by stream erosion and undercutting of slopes can influence landslide initiation (Dai and Lee 2002). Also, the presence of streams has the effect of raising water tables in the surrounding areas in close proximity. It is generally accepted that landslide frequency decreases as distance from drainage network lines increases.

3.4 Methods

In order to combine the selected landslide parameters and generate realistic output susceptibility maps, a unique multiscale GIS-based approach was developed using MCE and fuzzy sets. Each landslide-conditioning parameter affects the landslide process and final output maps so it is necessary to determine the relative importance of each parameter. The parameters are standardized to a common measurement scale using fuzzy set membership functions (Zadeh 1965) and the Analytical Hierarchy Process (AHP) calculates the weight values for each parameter (Saaty 1980). Final landslide susceptibility maps are then produced by combining the weighted standardized parameter maps using the weighted linear combination (WLC) method (Voogd 1983). The above approach is applied successively to identify susceptible areas at increasing scales and spatial resolutions (Figure 3-1). This multiscale MCE approach is applied to regional, municipal, and local scales at increasing spatial resolutions of 50 m, 10 m, and 1 m, respectively (Figure 3-2). These finer scales allow for the systematic identification of susceptibility ranging from the national level down to the community level. The susceptibility maps produced at each of the scales can be used in comparative analysis because common important parameters are used even though the scales are varying.

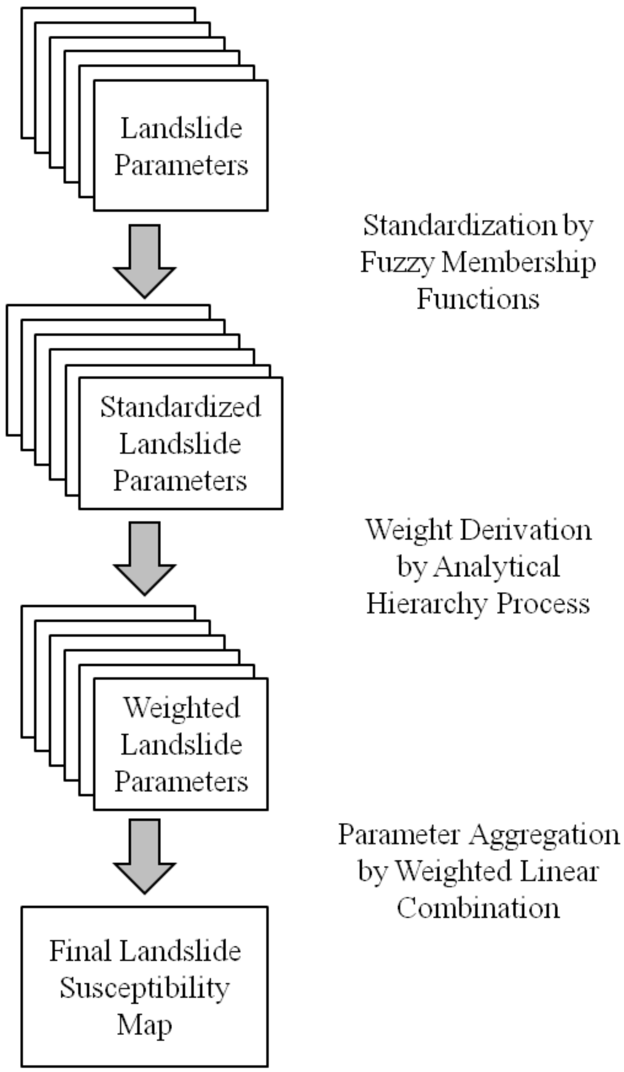

Figure 3-1. Overview of MCE components for each scale.

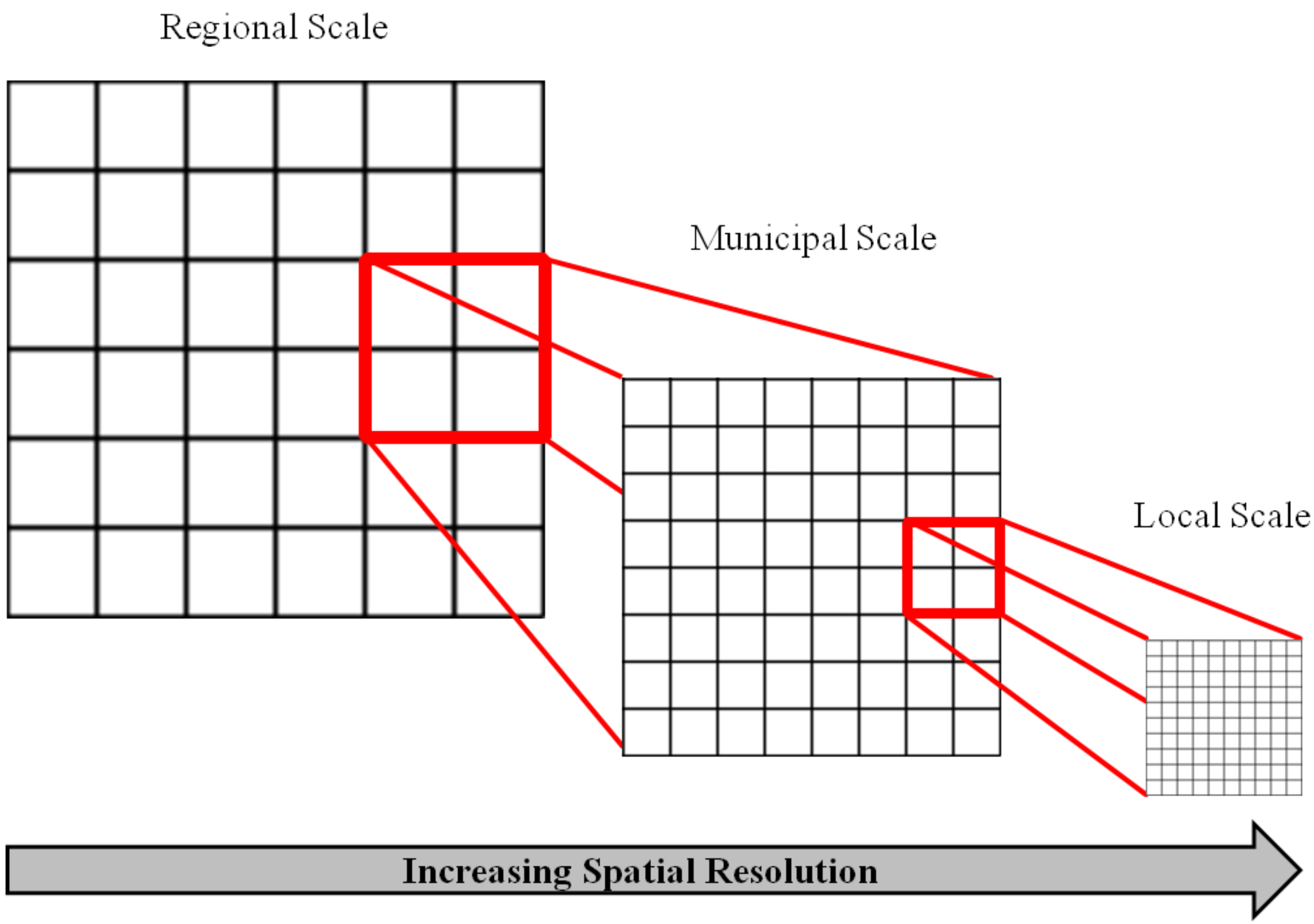

Figure 3-2. Interaction of MCE procedures between scale levels.

3.4.1 Defining Scale-Specific Landslide-Conditioning Parameters

The set of landslide-conditioning parameters for each individual scale was selected based on the relevance and the effect the parameters have at the specific scale of analysis. Topographic variables calculated from the DEM, such as slope gradient, aspect gradient, SPI, and TWI can be used at all three scales of analysis. These variables calculated at different spatial resolutions represent the topography over the length of the cell size. For example, slope gradient derived using a spatial resolution of 50 m is calculated by the average change in height over a cell length of 50 m. For finer spatial resolutions, the slope gradient calculation is the same except it is done at shorter distances. The same is true for other topographic variables except elevation.

The use of elevation is suitable for a study area if the variation in altitude is sufficiently large. A small to medium scale study area would likely provide enough separation in landslide classes between elevations. However, a large scale study focusing on a hillslope or escarpment will not yield significant rise and fall in elevation. In other words, the use of elevation as a landslide-conditioning parameter is limited to scales that exhibit a certain level of topographic variability. Distance away from roads is another parameter that possesses limitations due to spatial resolution. A coarse resolution of 50 m will incorrectly represent a single lane road that typically spans 6 m across. A spatial resolution of 50 m would still be too large even for double-lanes in both directions that typically spans 12 m totally. For each landslide factor, consideration is given to whether its inclusion makes logical sense at a given scale and spatial resolution.

3.4.2 Standardization of Parameters Using Fuzzy Sets

Data standardization is needed prior to GIS-based landslide susceptibility mapping because the gathered and derived data sources are often measured in different units and different scales of measurement. In addition, standardizing the data to a common scale allows comparisons between fuzzy sets because it allows the degree of membership for data to be measured on the same continuous scale between 0 and 1 (Zadeh 1965). Traditionally, GIS applications have operated with crisp sets where spatial information captured from reality are represented as discrete objects in space with a discrete definition. When maps of landslides susceptibility are produced using information based on crisp sets with membership values being 0 or 1, the final outcome is identical to a Boolean overlay analysis. The fuzzification is also considered as a way to handle uncertainty arising from quantifying continuous scale data. Compared to linear scaling, fuzzy sets give a more realistic standardization output as using a fuzzy set membership represents a specific relation between the criteria and possible outcomes (Jiang and Eastman 2000).

The assumption of fuzzy set theory is that any transition between categories is rarely a step function between non-membership to membership. Rather, there is a gradual change in the degree of membership following a specified function. In this study, the landslide parameters are standardized from 0 to 1, where 0 represents the least susceptible areas and 1 represents the most susceptible area. The specific fuzzy membership function used is the sigmoidal or s-shaped membership produced using a cosine function (Eastman 2009). The function for each parameter is constructed by four control points (a, b, c, d) representing the inflection points of the curve. Information from published literature, local slope assessment reports, and expert knowledge were used to establish a relationship between parameters and landslides that aided in the assignment of the fuzzy function control points (BGC Engineering 2006; Akgun and Bulut 2007; BGC Engineering 2010). The resulting curves representing the degree of susceptibility, μ(x), are characterized as monotonically increasing, monotonically decreasing, and symmetric. The most commonly used and relevant membership function is the sigmoidal function given by:

$$\mu(x) = cos^2\alpha \quad \text{(Equation 3-3)}$$

where, in the case of a monotonically decreasing function:

$$\alpha = \left(\frac{x-c}{d-c}\right)\frac{\pi}{2} \quad \text{(Equation 3-4)}$$

when $x < c$, $\mu(x) = 1$. In the case of a monotonically increasing function:

$$\alpha = \left(1 - \frac{x-a}{b-a}\right)\frac{\pi}{2} \quad \text{(Equation 3-5)}$$

when $x > b$, $\mu(x) = 1$.

3.4.3 Weighted Linear Combination

In producing a final susceptibility map, the weighted linear combination (WLC) method is frequently used for aggregating factor maps (Akgun et al. 2008). The WLC method used in this study is expressed by $S = \sum w_i \cdot x_i$, where *S* is the final susceptibility, w_i is the standardized weight of the factor i and x_i is criterion score of factor i. The standardized parameter maps created using fuzzy membership functions are multiplied by the weight of each parameter. The set of weights must sum to one in order for the resulting susceptibility map to have the same range of values as the standardized factor maps. The weighted parameter maps are then combined by summation to produce the susceptibility map. WLC is an effective way to combine primary level weights (fuzzy standardized parameters) with secondary-level weights (parameter importance) to produce an overall result. Constraints in the form of qualitative criteria, such as locations of water bodies, can be masked by Boolean overlay as unsuitable areas. The main issue is to define the set of weights that represent the relative importance of each parameter in conditioning landslides. AHP is used to assign weights in this study (Ayalew et al. 2004).

3.4.4 Analytical Hierarchy Process

As the number of parameters increase, it becomes a challenge to evaluate their importance and to assign appropriate weights. Analyzing and comparing two parameters at a time in an organized manner helps to breakdown the assignment of weights into smaller entities. Performing multiple one-to-one pairwise comparisons is a much simpler and intuitive process to determine a hierarchy of landslide influencing factors than trying to evaluate all parameters as a whole. The technique implemented in this study is the Analytical Hierarchy Process (AHP). AHP is useful since it has the capability to handle both qualitative and quantitative criteria (Ayalew et al. 2004). The technique operates irrespective of the data type because the fundamental input given by the user is the expert judgment in answer to the question: How important is parameter A compared to parameter B? The relative importance of parameters is translated to a 9 point continuous rating scale and entered into a pairwise comparison matrix (Saaty 1980) (Table 3-1). Ratings are given by 1, 3, 5, 7, and 9 starting with equal importance to increasing importance, with 2, 4, 6, and 8 as intermediate values. Comparing a parameter with itself generates an equal rating of 1. Reciprocals represent the comparison of a pair of parameters in reverse. For example, if parameter A was extremely more important relative to parameter B a rating of 9 is given. The comparison in reverse of parameter B in relation to parameter A is given a rating of 1/9. Once every possible pair of parameters has been given a rating weights are calculated by matrix algebra using the eigenvector method to find the maximum or principal eigenvector of the matrix (Eastman 2009). The sum of weights must equal 1, which is a requirement of WLC in producing the final susceptibility map. The weight values calculated in this way are considered the average of all possible ways of comparing the parameters and represent the importance of parameters to each other (Malczewski 1999).

Table 3-1. Nine point continuous rating scale.

<table>
<tr><th>Rating</th><th colspan="2">Comparison</th></tr>
<tr><td>1/9</td><td>Extremely</td><td rowspan="4">Less important</td></tr>
<tr><td>1/7</td><td>Very strongly</td></tr>
<tr><td>1/5</td><td>Strongly</td></tr>
<tr><td>1/3</td><td>Moderately</td></tr>
<tr><td>1</td><td>Equally</td><td></td></tr>
<tr><td>3</td><td>Moderately</td><td rowspan="4">More important</td></tr>
<tr><td>5</td><td>Strongly</td></tr>
<tr><td>7</td><td>Very strongly</td></tr>
<tr><td>9</td><td>Extremely</td></tr>
</table>

Since calculating weights using a pairwise comparison matrix may result in many variations, a degree of consistency is determined for the development of ratings. Saaty

(1977) proposed an index of consistency known as the consistency ratio (CR). The CR is a measure of the probability the matrix ratings were randomly generated. As a rule of thumb, a CR value of less than 10% is considered acceptable. Other values warrant further evaluation in the matrix ratings.

3.4.5 Software

The GIS software used in this study were Idrisi Taiga (Eastman 2009) and ArcGIS 9.3 (ESRI 2009). Idrisi Taiga was used as the analyzing platform for data manipulation and multi-criteria evaluation. ArcGIS was used for digitization, visualization, and cartographic output.

3.5 Results and Discussion

In the sections that follow, the practical implementation and resulting outputs of the developed GIS-based MCE fuzzy set approach at three different scales of analysis are presented.

3.5.1 Regional Scale – Metro Vancouver

3.5.1.1 Study Area

There have been roughly 200 reported incidences of landslides in the Metro Vancouver Region since 1909 (BGC Engineering 2011). Most of these are weather related in that the likely trigger was an accumulation of precipitation in preceding days or an onset of intense precipitation in a short period of time. Vancouver receives on average just less than 1300 mm of precipitation per year. The majority of this precipitation, mostly rainfall, occurs from November to March. Landslides occurrences are strongly correlated with these months.

3.5.1.2 Geospatial Data

The data for the Metro Vancouver Region was derived from a 1:50,000 DEM provided by the National Topographic Data Base (NTDB). The spatial resolution of the DEM is 50 m. Slope gradient, aspect gradient, SPI, and TWI were generated from the DEM. The drainage network at a 1:50,000 scale was obtained from the National Hydro Network (NHN) as vector lines and polygons. Finally, a landslide inventory has been compiled, mapped, and maintained using various sources of information. Local newspapers, engineering reports, scientific papers reporting incidences of landslides dating from as far back as 1909 have been documented in the inventory showing point locations (BGC Engineering 2011).

3.5.1.3 MCE

In the regional scale MCE analysis, the following six parameters were taken into consideration: slope gradient, aspect gradient, SPI, TWI, distance to drainage network, and elevation. The control points for each parameter were obtained from a recent survey of the literature employing similar decision-making approaches (Table 3-2). These points were associated to a fuzzy membership for standardization prior to determining parameter weights. In AHP, each parameter is compared with one another and given an individual rating. When each pair is rated, parameter weights are calculated. The measured CR was at 2% meaning the computed weights are well below the acceptable 10% CR threshold. The weight value of slope gradient is highest, followed by SPI, elevation, TWI, distance to drainage network, and aspect gradient in decreasing order. The weighted parameter maps are summated to produce a regional scale landslide susceptibility map for the Metro Vancouver region. The map has a continuous scale of numerical values in the range 0-1 making it difficult for visually interpret. In order to reduce the visual map complexity, the continuous values were categorized into equal intervals showing degrees of susceptibility. The five categories were distinguished as very low, low, medium, high, and very high (Figure 3-3). The resulting susceptibility map shows that the largest proportion of the study area has low susceptibility occupying 37.53% of the entire area. The very low, medium, and high susceptible classes make up 10.72%, 20.40%, and 23.72% respectively. The very high susceptibilities account for 7.64% of the study area. The point locations of past landslides have been mapped and are used to perform the validation of this susceptibility map. The validation technique used is the seed cell area index (SCAI) proposed by Suzen and Doyuran (2004). SCAI is calculated by normalizing the area percentages for each landslide susceptibility class by the landslide seed cell percentages. It is desired that the high and very high susceptibility classes to have very small SCAI values. Conversely, low and very low susceptibility classes should have higher SCAI values. The SCAI values calculated indicate that the generated map for the Berkley Escarpment is accurate because the high and very high susceptibly classes have very low SCAI values, whereas the very low and low susceptibility classes are relatively higher (Figure 3-4).

Table 3-2. Regional scale parameter standardization and pairwise comparison matrix.

Parameter	**Membership Function**	**Type**	**Control Points**
Aspect	Sigmoidal	Monotonically decreasing	c=90°, d=360°
Distance to drainage	Sigmoidal	Monotonically decreasing	c=50m, d=1000m
Elevation	Sigmoidal	Symmetric	a=100m, b=250m, c=750m, d=800m
Slope	Sigmoidal	Symmetric	a=3°, b=20°, c=30°, d=40°
Stream Power Index	Sigmoidal	Monotonically increasing	a=0, b=300
Topographic Wetness Index	Sigmoidal	Monotonically increasing	a=1, b=12

	Aspect	**Drainage**	**Elevation**	**Slope**	**SPI**	**TWI**	**Weights**
Aspect	1						0.0448
Drainage	2	1					0.0688
Elevation	5	3	1				0.1706
Slope	7	5	3	1			0.4083
SPI	3	3	1	1/3	1		0.1772
TWI	3	2	1	1/3	1/2	1	0.1303

CR = 0.02 < 0.1

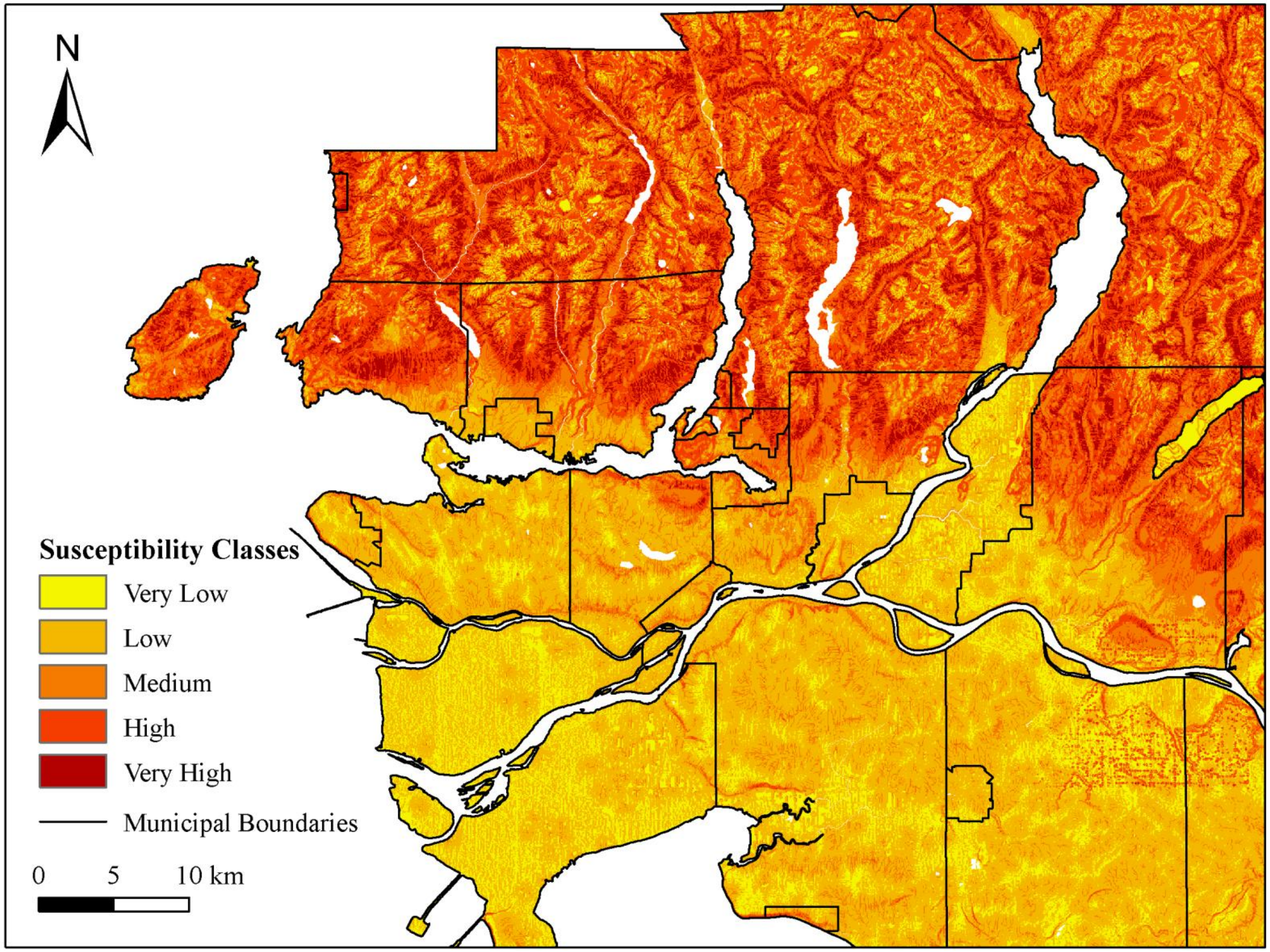

Figure 3-3. Landslide susceptibility at a regional scale: the case of the Metro Vancouver Region.

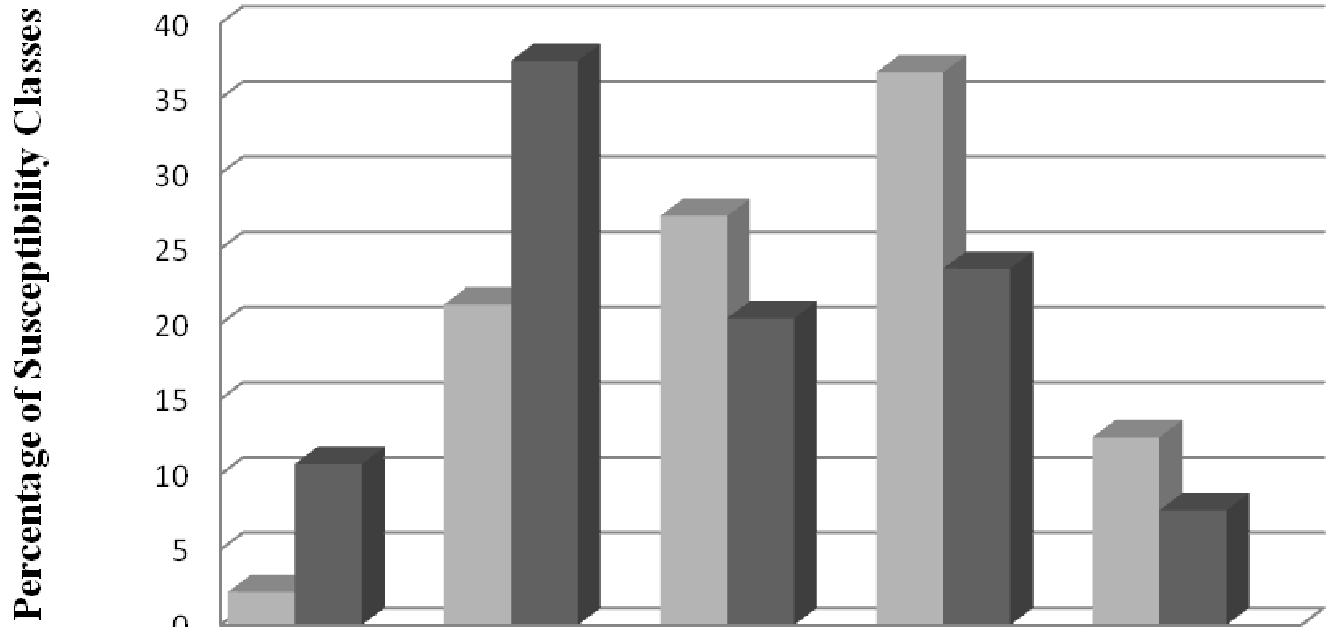

	Very Low	Low	Medium	High	Very High
Seed (%)	2.21	21.32	27.21	36.76	12.50
Area (%)	10.72	37.53	20.40	23.72	7.64
SCAI	4.86	1.76	0.75	0.65	0.61

Figure 3-4. Densities of actual landslides among landslide susceptibility classes and calculated SCAI values for the Metro Vancouver Region.

3.5.2 Municipal Scale – District of North Vancouver

3.5.2.1 Study Area

The District of North Vancouver (DNV) is located at the base of the Coast Mountain Range just north of the City of Vancouver, British Columbia. Several neighbourhoods in the District are built along the crests and bases of slopes and this may place residents at risk. To compound this problem, some property owners try to extend their properties by placing fill on the tops of slopes. This action over steepens already unstable slopes. In addition, when neighbourhoods were developed prior to 1980, most storm water was directed over the edge of escarpments instead of being diverted into the municipal storm drainage system (Eisbacher and Clague 1981).

3.5.2.2 Geospatial Data

The data used at this scale was provided by the DNV GIS Department. The data include a 10 m spatial resolution DEM as well as drainage networks and road networks. From these datasets, slope gradient, aspect gradient, SPI, TWI, and distances to drainage and roads were calculated. The landslide inventory dataset is identical to that used in the regional scale study.

3.5.2.3 Multicriteria Evaluation Analysis

In the case of the municipal scale study on the DNV, the following seven parameters were chosen as landslide influencing factors: slope gradient, aspect gradient, SPI, TWI, distance to drainage network, distance to road network, and elevation. The control points for each parameter are shown in Table 3-3. These points were used in the standardization procedure using fuzzy sets. Parameter weights were then calculated by

AHP pairwise comparison. The measured CR was 3%, which is below the acceptable threshold value. The weight value of slope gradient is highest, followed by elevation, SPI, distance to road network, TWI, distance to drainage network, and aspect gradient in decreasing order (Table 3-3). The landslide susceptibility map for the DNV was then produced by combining the weighted parameters. The map results in a continuous scale of numerical values (i.e. 0-1) and the susceptibilities categorized into equal intervals for better visual interpretation. Five categories were distinguished as very low, low, medium, high, and very high (Figure 3-5). From the susceptibility map, the largest proportion of the study area has medium susceptibility, occupying 31.47 % of the entire area. The very low and low susceptibility classes make up 12.95% and 30.38%, while 21.20% is occupied by high susceptibility areas. The very high susceptibilities account for 4.00% of the study area. Again, to validate the susceptibility map past point locations of landslides were used to calculate the SCAI. The SCAI values indicate that the generated map for the DNV is accurate since SCAI values are highest from the lowest susceptibilities to lowest in the highest susceptibilities (Figure 3-6).

Table 3-3. Municipal scale parameter standardization and pairwise comparison matrix.

Parameter	**Membership Function**	**Type**	**Control Points**
Aspect	Sigmoidal	Monotonically decreasing	c=90°, d=360°
Distance to drainage	Sigmoidal	Monotonically decreasing	c=50m, d=1000m
Distance to roads	Sigmoidal	Monotonically decreasing	c=50m, d=150m
Elevation	Sigmoidal	Symmetric	a=5m, b=200m, c=450m, d=700m
Slope	Sigmoidal	Symmetric	a=3°, b=20°, c=30°, d=40°
Stream Power Index	Sigmoidal	Monotonically increasing	a=0, b=300
Topographic Wetness Index	Sigmoidal	Monotonically increasing	a=1, b=12

	Aspect	**Drainage**	**Road**	**Elevation**	**Slope**	**SPI**	**TWI**	**Weights**
Aspect	1							0.0423
Drainage	2	1						0.0577
Road	2	3	1					0.1255
Elevation	5	3	2	1				0.1640
Slope	7	5	2	3	1			0.3432
SPI	3	3	1	1	1/3	1		0.1510
TWI	3	2	1	1	1/3	1/2	1	0.1163

CR = 0.03 < 0.1

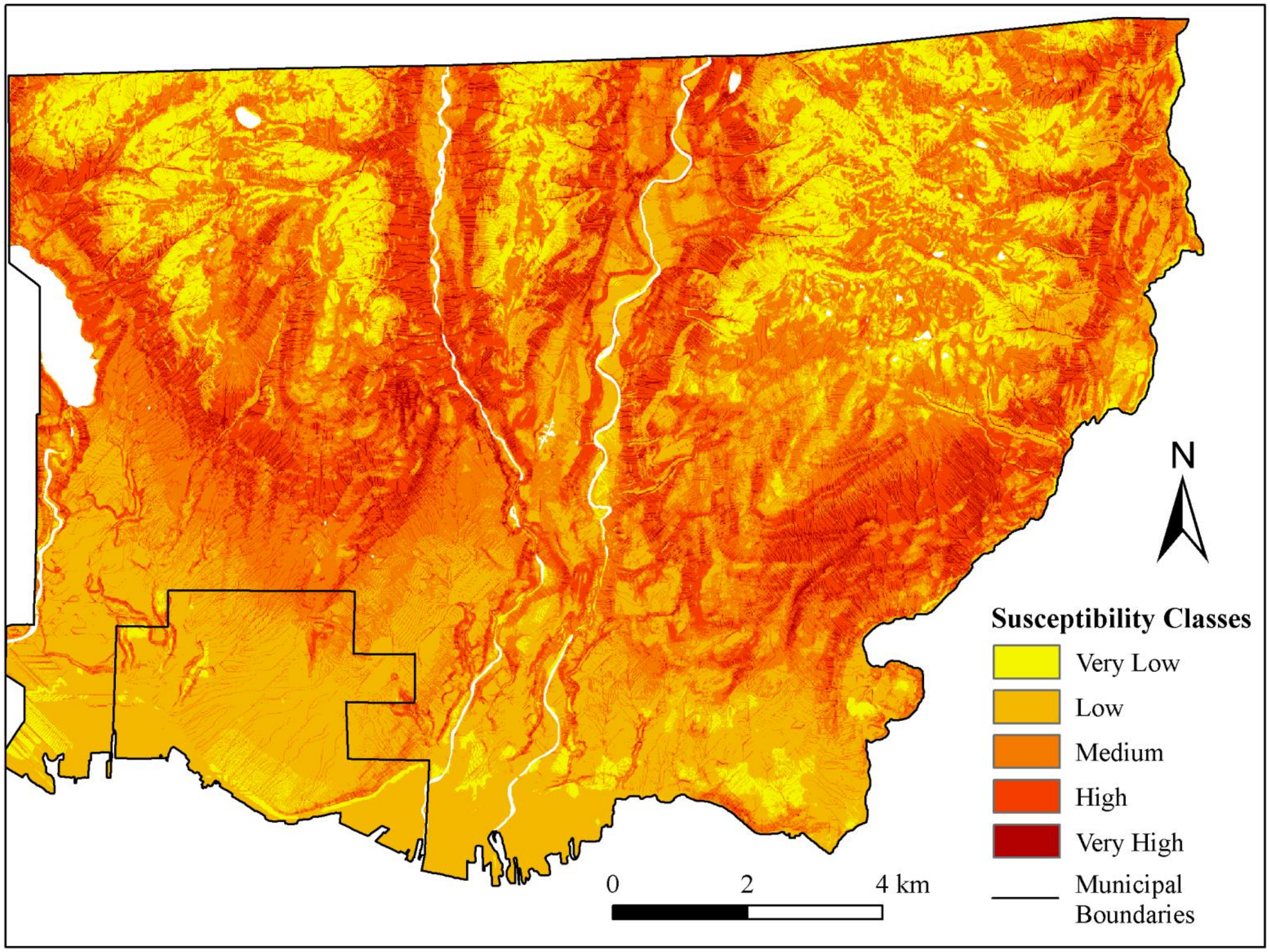

Figure 3-5. Landslide susceptibility at the municipal scale: the case of the District of North Vancouver.

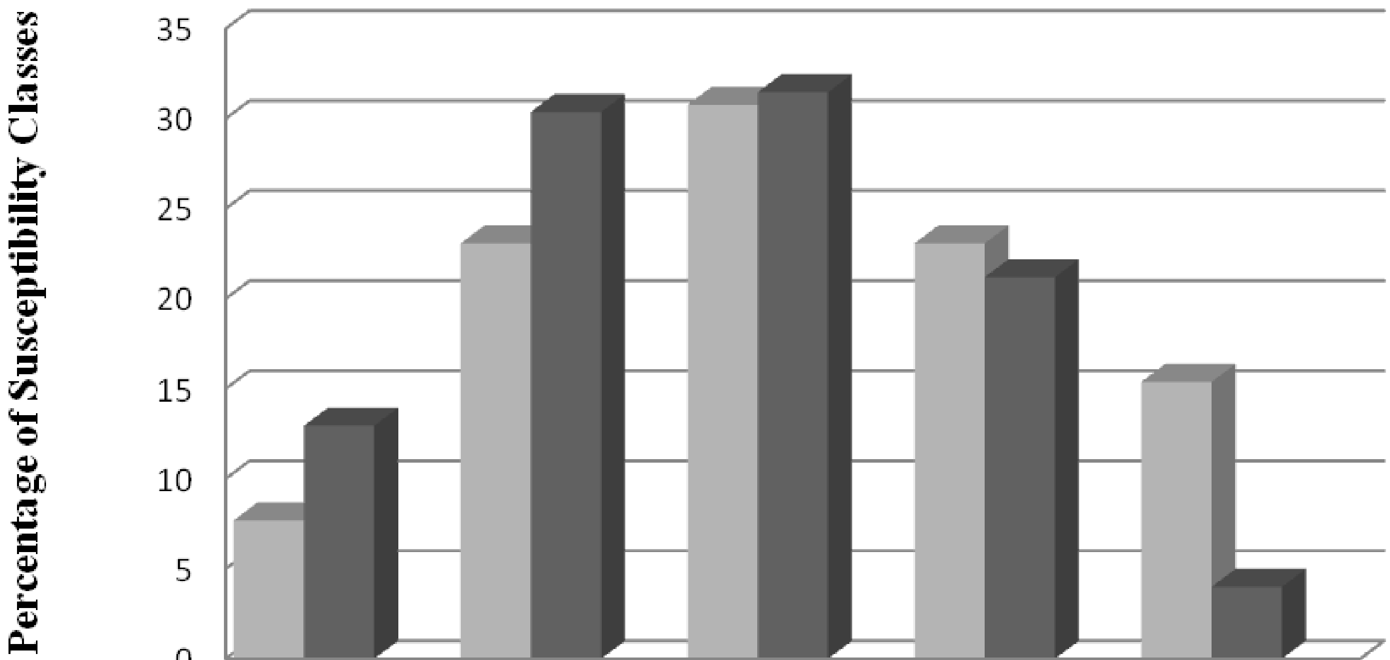

	Very Low	Low	Medium	High	Very High
Seed (%)	7.69	23.08	30.77	23.08	15.38
Area (%)	12.95	30.38	31.47	21.20	4.00
SCAI	1.68	1.32	1.02	0.92	0.26

Figure 3-6. Densities of actual landslides among the landslide susceptibility classes and calculated SCAI values for the District of North Vancouver.

3.5.3 Local Scale – Berkley Escarpment

3.5.3.1 Study Area

The Berkley Escarpment is located in the DNV and runs along a ridge east of the lower Seymour River area. Houses have been constructed at the top and bottom of the escarpment slopes. Some houses have been built too close to the crest and others are built on top of loose fill added during construction and this increases the local slope and landslide potential. Due to these reasons, this particular residential area has been susceptible to urban landslides in the past. Since the 1970s, six landslides have originated from the crest of this escarpment, leading to loss of life and causing extensive property damage (Figure 3-7). The landslides that have occurred were caused by periods of intense rainfall. The latest failure occurred in 2005, which prompted the Provincial Government of British Columbia and the DNV to order evacuations and purchase at-risk homes.

3.5.3.2 Geospatial Data

The data for the Berkley Escarpment were derived from a topographic base map (scale 1:2,000) consisting of 2 m elevation contour intervals commissioned by the DNV on 6th March 2006. Digitization, conversion, and interpolation of the contour intervals produced a detailed DEM at a spatial resolution of 1 m. Slope gradient, aspect gradient, SPI, TWI, and the distance to the slope crest were calculated directly from the DEM. The stream network and road network for the area were provided by the DNV in the form of maps at a scale of 1:2,000. The areal extents of the landslides were also obtained from DNV maps at the same scale.

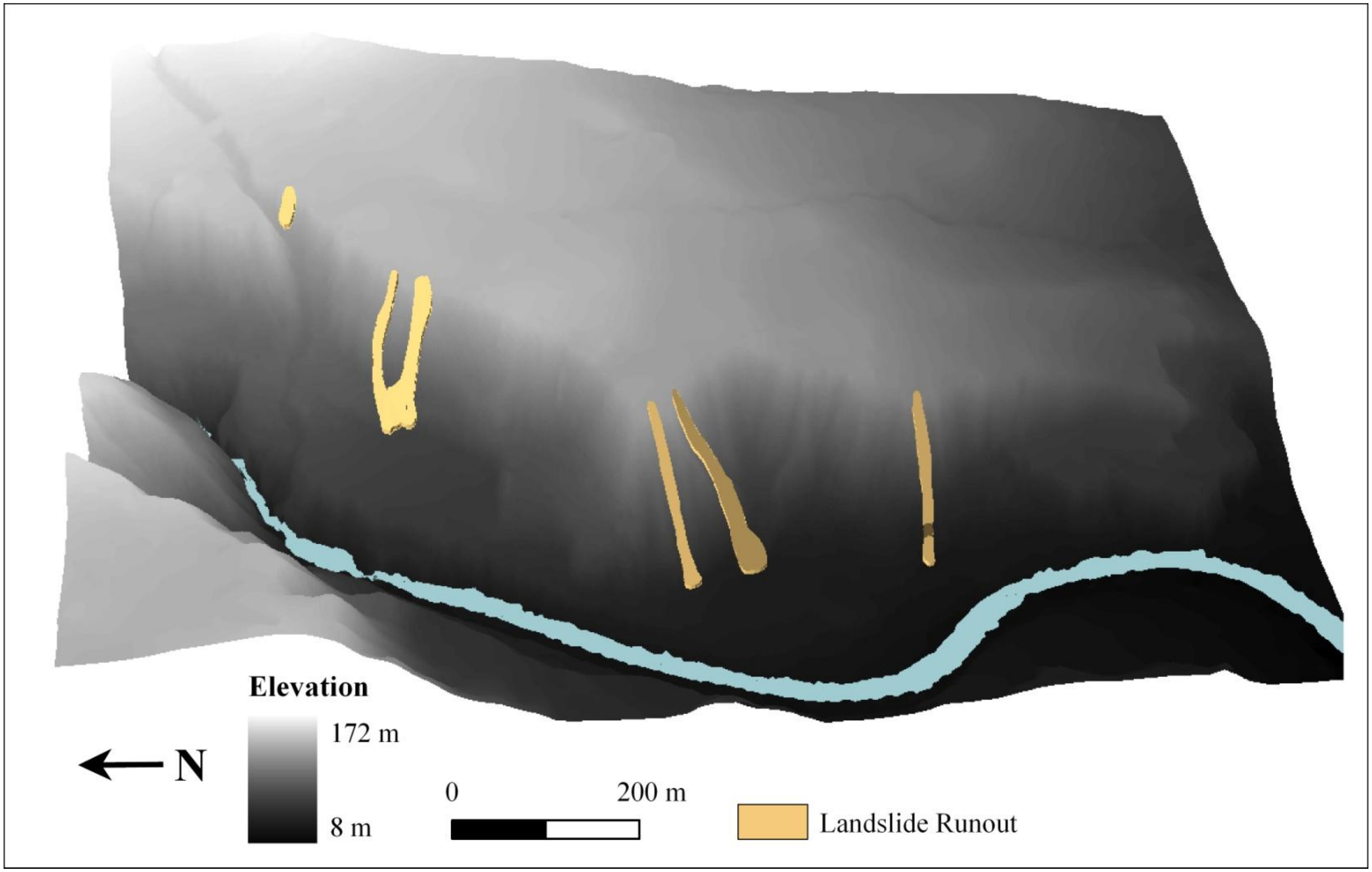

Figure 3-7. Locations of past landslide events on the Berkley Escarpment.

3.5.3.3 Multicriteria Evaluation Analysis

In this local scale study, the following seven parameters were taken into consideration: slope gradient, aspect gradient, SPI, TWI, distance to drainage network, distance to road network, and distance to the escarpment crest. The elevation parameter was removed at this local scale because variation in elevation was very low, being less than 100 m variation between maximum and minimum. Distance from the crest was only used at this scale because this area was localized at a single escarpment, allowing the precise delineation of the crest line to be straightforward. The control points for each parameter are adapted from those of the regional and municipal studies (Table 3-4). These points were used to relate parameter values to their fuzzy membership. The assignment of weights was achieved by pairwise comparison using the AHP method and the individual ratings and parameter weights are presented in (Table 3-4). The measured CR was at 4% meaning the computed weights are acceptable. The weight value of slope gradient is highest, followed by SPI, TWI, distance to escarpment crest, distance to road network, aspect gradient, and distance to drainage network, in decreasing order. The weighted parameter maps are summated to produce a local scale landslide susceptibility map for the Berkley Escarpment. Continuous values of susceptibility were then categorized into equal intervals producing the following five classes (Figure 3-8): very low, low, medium, high, and very high. From the susceptibility map, the largest proportion of the study area has very low susceptibility, occupying 54.34% of the entire area. The low, medium, and high susceptible classes make up 19.87%, 12.01%, and 12.16%, respectively. The very high susceptibilities account for 1.62% of the study area. The locations of past landslides and their runouts have been mapped and are used to perform the validation of this susceptibility map. The technique used is the seed cell area index (SCAI). The calculated SCAI values show that the generated map for the Berkley Escarpment is accurate because the high and very high susceptibly classes have very low SCAI values, whereas the very low and low susceptibility classes are relatively much higher (Figure 3-9).

Table 3-4. Local scale parameter standardization and pairwise comparison matrix.

Parameter	**Membership Function**	**Type**	**Control Points**
Aspect	Sigmoidal	Symmetric	a=180°, b=270°, c=270°, d=360°
Distance to crest	Sigmoidal	Monotonically decreasing	c=5m, d=100m
Distance to drainage	Sigmoidal	Monotonically decreasing	c=50m, d=1000m
Distance to roads	Sigmoidal	Monotonically decreasing	c=40m, d=100m
Slope	Sigmoidal	Symmetric	a=5°, b=20°, c=30°, d=40°
Stream Power Index	Sigmoidal	Monotonically increasing	a=0, b=300
Topographic Wetness Index	Sigmoidal	Monotonically decreasing	c=2, d=4

	Aspect	Crest	Drainage	Road	Slope	SPI	TWI	Weights
Aspect	1							0.0461
Crest	3	1						0.1074
Drainage	1	1/3	1					0.0409
Road	1	1/3	3	1				0.0572
Slope	7	3	7	7	1			0.3824
SPI	4	3	4	4	1/3	1		0.2105
TWI	3	3	3	3	1/3	1/2	1	0.1554

CR = 0.04 < 0.1

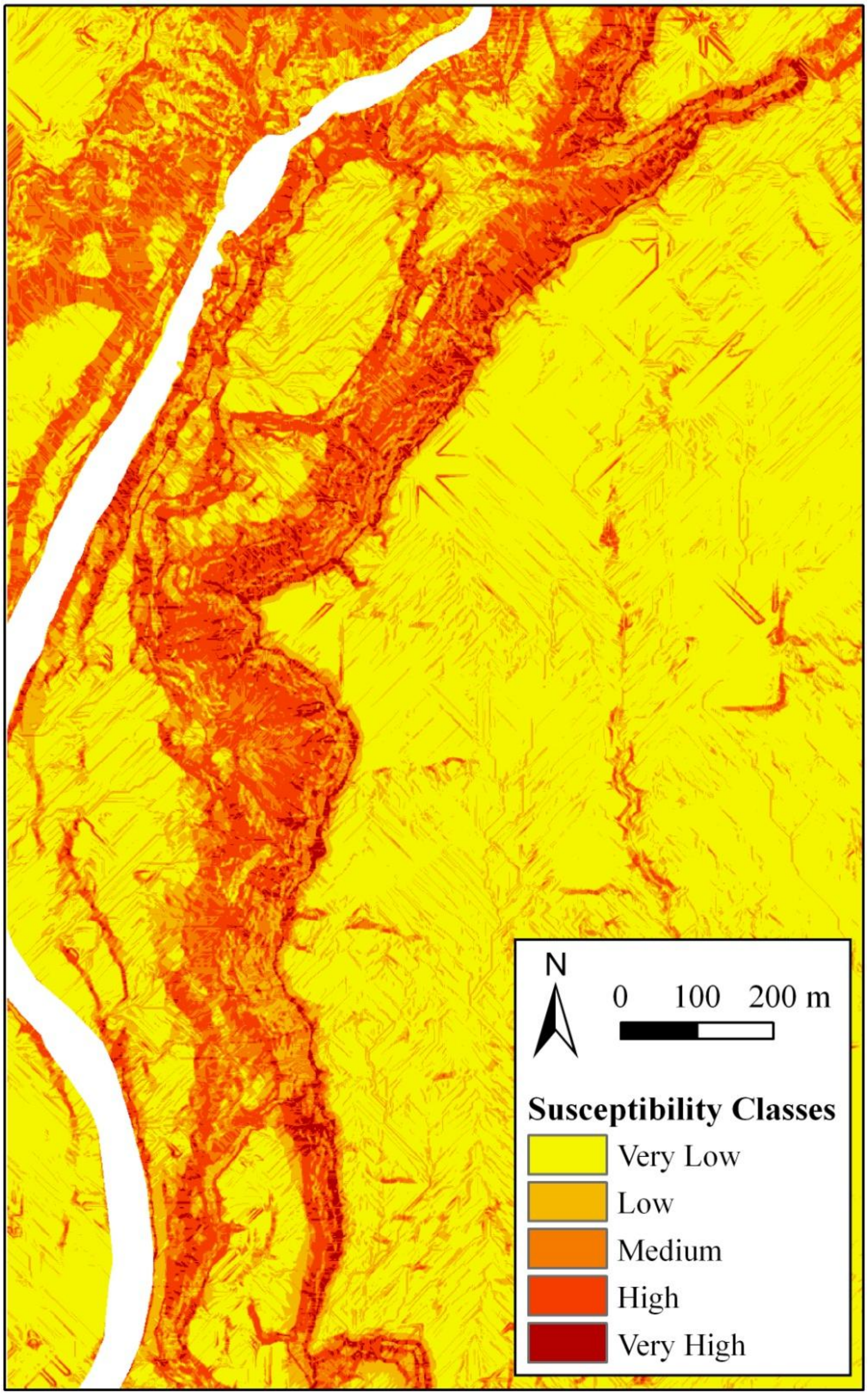

Figure 3-8. Landslide susceptibility at the local scale: the case of the Berkley Escarpment.

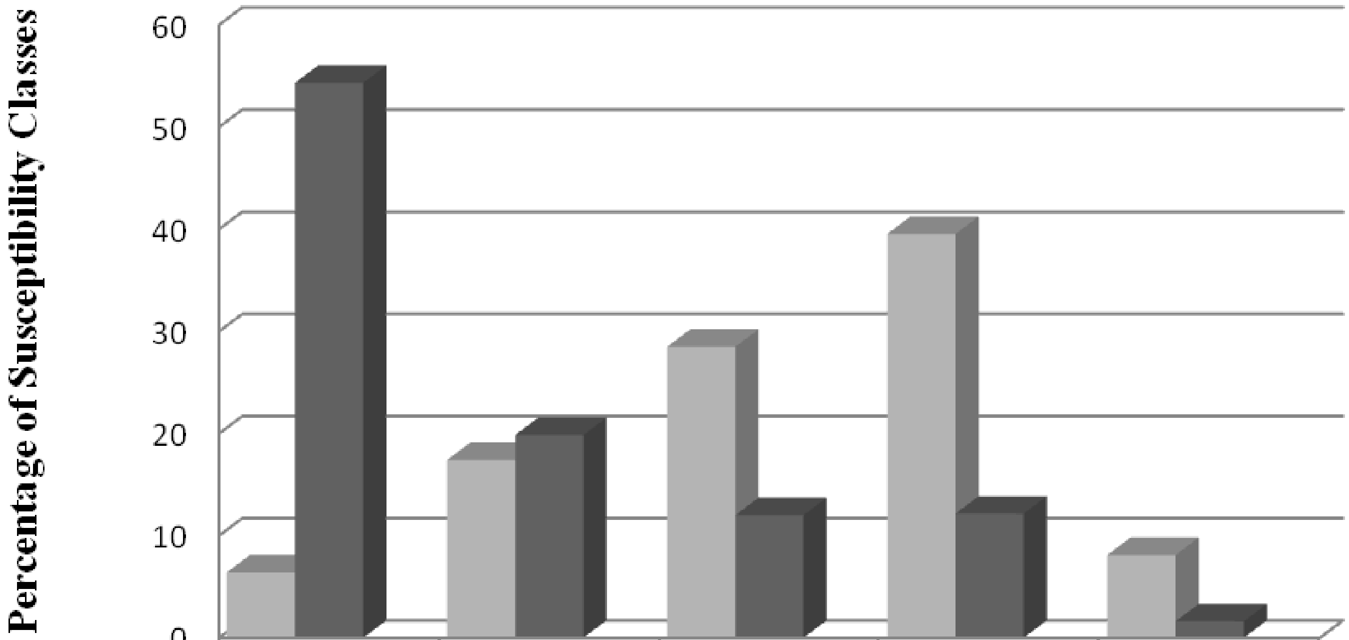

	Very Low	Low	Medium	High	Very High
Seed (%)	6.42	17.41	28.50	39.55	8.12
Area (%)	54.34	19.87	12.01	12.16	1.62
SCAI	8.47	1.14	0.42	0.31	0.20

Figure 3-9. Densities of actual landslides among the landslide susceptibility classes and calculated SCAI values for the Berkley Escarpment.

3.6 Validation

The validation technique used to evaluate the susceptibility maps at each scale is the seed cell area index (SCAI). It is calculated by normalizing the area percentages for each landslide susceptibility class by the landslide seed cell percentages. It is expected that the calculated SCAI decreases on the spectrum of very low susceptibility to very high susceptibility. The SCAI values given in Figure 3-4, Figure 3-6, and Figure 3-9 indicate the generated maps are reliable since the high and very high susceptibility classes have very low SCAI values, whereas the SCAI values of the very low and low susceptibility classes are higher. Further, these results indicate the evaluation technique across multiple scales was consistent. This provides strong reason to perform multiscale analyses as they provide a powerful basis for evaluating the robustness and persistence of findings across scales. The spatial resolution of data is also an important factor when performing analyses. Figure 3-10 shows the comparison between resolutions of 1 m, 10 m, and 50 m over the same area. Visual comparison indicated that the overlay of these different resolutions verify the susceptibility results over different scales and resolutions. For example, there is no doubt the escarpment poses the highest landslide risk and flat residential areas east of the escarpment has low landslide risk.

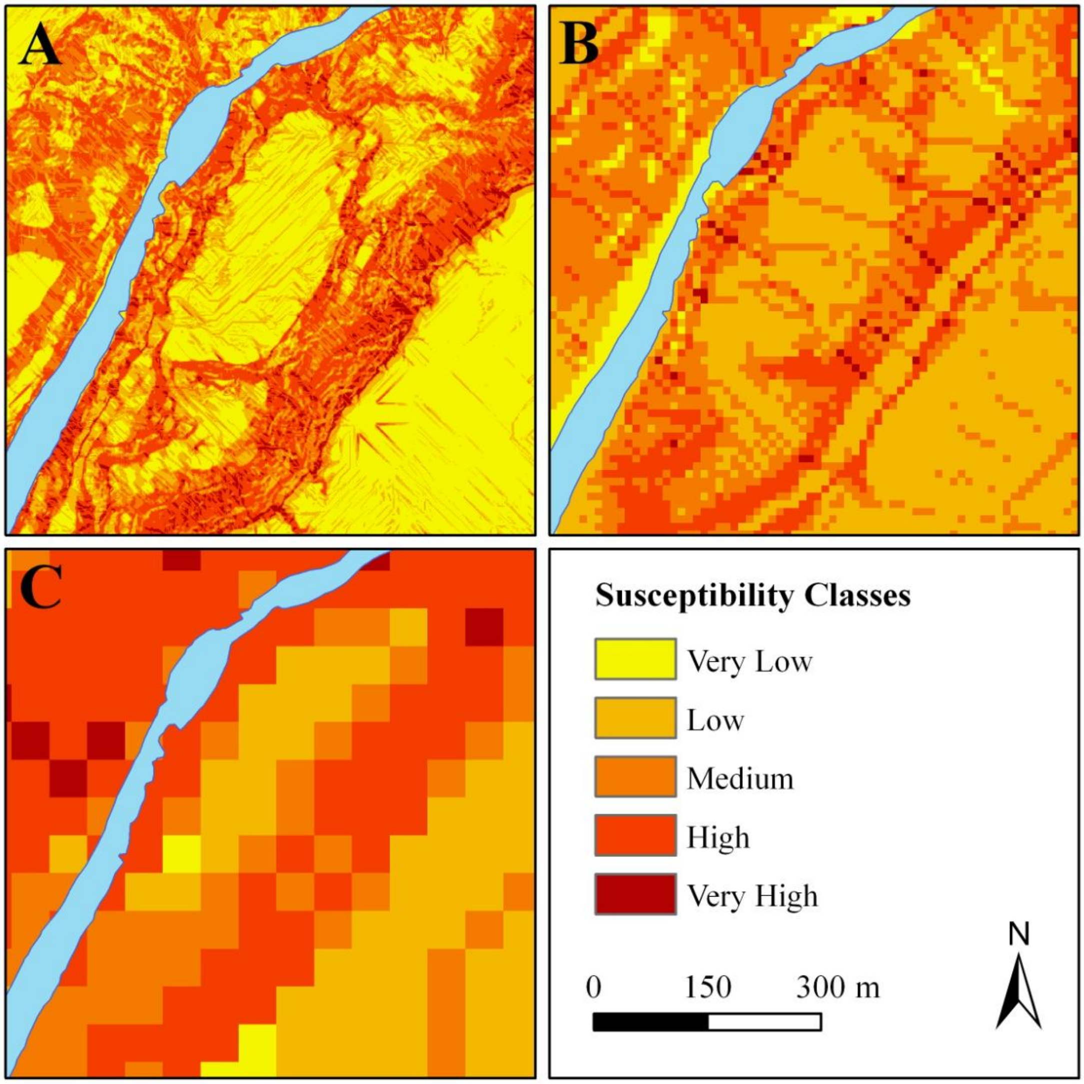

Figure 3-10. Comparison of susceptibilities generated under various spatial scales and resolutions. a) local scale at 1 m resolution; b) municipal scale at 10 m resolution; and c) regional scale at 50 m resolution.

3.7 Conclusion

The developed GIS-based fuzzy multicriteria evaluation and multiscale approach was implemented on the Metro Vancouver Region, the DNV, and the Berkley Escarpment as a novel and comprehensive means to analyze landslide susceptibility at multiple spatial scales and resolutions. In particular, the MCE utilizing Analytical Hierarchy Process (AHP) and weighted linear combination (WLC) methods were applied successively to study areas with cell resolutions of 50 m, 10 m, and 1 m. Careful consideration was given to the definition of relevant parameters across different scales since the size of each grid cell is a limiting factor for certain parameters. The developed approach produced three landslide susceptibility maps at different spatial resolutions with each susceptibility map validated using the seed cell area index (SCAI) technique. The maps have been found to be reliable and internally consistent between and within scales. This makes them suitable for comparative analysis. The multiscale MCE can be useful for planning landslide mitigation studies beginning at a regional scale and moving to finer scales because results at varying scales will have different impacts on the decision-making process.

Acknowledgements

This study was fully supported by a Natural Sciences and Engineering Research Council (NSERC) of Canada Discovery Grant awarded to Suzana Dragićević. The District of North Vancouver (DNV) GIS Department, British Columbia, Canada provided elevation base maps and contour maps. Mark Leir and Neil Ripley of BGC Engineering provided the landslide inventory of the Metro Vancouver Region.

3.8 References

Akgun, A. and F. Bulut (2007). "GIS-based landslide susceptibility for Arsin-Yomra (Trabzon, North Turkey) region." Environmental Geology **51**(8): 1377-1387.

Akgun, A., S. Dag, et al. (2008). "Landslide susceptibility mapping for a landslide-prone area (Findikli, NE of Turkey) by likelihood-frequency ratio and weighted linear combination models." Environmental Geology **54**(6): 1127-1143.

Akgun, A. and N. Turk (2010). "Landslide susceptibility mapping for Ayvalik (Western Turkey) and its vicinity by multicriteria decision analysis." Environmental Earth Sciences **61**(3): 595-611.

Ayalew, L. and H. Yamagishi (2005). "The application of GIS-based logistic regression for landslide susceptibility mapping in the Kakuda-Yahiko Mountains, Central Japan." Geomorphology **65**(1-2): 15-31.

Ayalew, L., H. Yamagishi, et al. (2005). "Landslides in Sado Island of Japan: Part II. GIS-based susceptibility mapping with comparisons of results from two methods and verifications." Engineering Geology **81**(4): 432-445.

Ayalew, L., H. Yamagishi, et al. (2004). "Landslide susceptibility mapping using GIS-based weighted linear combination, the case in Tsugawa area of Agano River, Niigata Prefecture, Japan." Landslides **1**(1): 73-81.

BGC Engineering (2006). District of North Vancouver, Berkley Landslide Risk Management: Phase 2 Assessment of Risk Control Options, May 11, 2006.

BGC Engineering (2010). District of North Vancouver, Landslide Risk Summary, November 12, 2010.

BGC Engineering (2011). Metro Vancouver Landslide Inventory [shapefile].

Brabb, E. E., E. H. Pampeyan, et al. (1972). Landslide susceptibility in San Mateo County, California, U.S. Geol. Surv., Misc. Field Studies**:** Map MF-360.

Carrara, A., M. Cardinali, et al. (1991). "GIS techniques and statistical models in evaluating landslide hazard." Earth Surface Processes and Landforms **16**(5): 427-445.

Carver, S. J. (1991). "Integrating multi-criteria evaluation with geographical information systems." International Journal of Geographical Information Systems **5**(3): 321-339.

Castellanos Abella, E. A. and C. J. Van Westen (2007). "Generation of a landslide risk index map for Cuba using spatial multi-criteria evaluation." Landslides **4**(4): 311-325.

Castellanos Abella, E. A. and C. J. Van Westen (2008). "Qualitative landslide susceptibility assessment by multicriteria analysis: A case study from San Antonio del sur, Guantanamo, Cuba." Geomorphology **94**(3-4): 453-466.

Conoscenti, C., C. Di Maggio, et al. (2008). "GIS analysis to assess landslide susceptibility in a fluvial basin of NW Sicily (Italy)." Geomorphology **94**(3-4): 325-339.

Dai, F. C. and C. F. Lee (2002). "Landslide characteristics and slope instability modeling using GIS, Lantau Island, Hong Kong." Geomorphology **42**(3-4): 213-228.

Dai, F. C. and C. F. Lee (2003). "A spatiotemporal probabilistic modelling of storm-induced shallow landsliding using aerial photographs and logistic regression." Earth Surface Processes and Landforms **28**(5): 527-545.

Dai, F. C., C. F. Lee, et al. (2001). "Assessment of landslide susceptibility on the natural terrain of Lantau Island, Hong Kong." Environmental Geology **40**(3): 381-391.

Drennon, C. B. and W. G. Schleining (1975). "Landslide hazard mapping on a shoestring." Journal of the Surveying and Mapping Division **101**(1): 107-114.

Duman, T. Y., T. Can, et al. (2006). "Application of logistic regression for landslide susceptibility zoning of Cekmece Area, Istanbul, Turkey." Environmental Geology **51**(2): 241-256.

Eastman, J. R. (2009). IDRISI Taiga. Worcester, MA, Clark University.

Eastman, J. R., W. G. Jin, et al. (1995). "Raster procedures for multi-criteria/multi-objective decisions." Photogrammetric Engineering and Remote Sensing **61**(5): 539-547.

Eisbacher, G. H. and J. J. Clague (1981). "Urban landslides in the vicinity of Vancouver, British Columbia, with special reference to the December 1979 rainstorm." Canadian Geotechnical Journal **18**(2): 205-216.

Ercanoglu, M. (2005). "Landslide susceptibility assessment of SE Bartin (West Black Sea region, Turkey) by artificial neural networks." Natural Hazards and Earth System Sciences **5**(6): 979-992.

ESRI (2009). ArcGIS 9.3. Redlands, California, Environmental Systems Research Institute.

Feick, R. D. and G. B. Hall (2004). "A method for examining the spatial dimension of multi-criteria weight sensitivity." International Journal of Geographical Information Science **18**(8): 815-840.

Fell, R., J. Corominas, et al. (2008). "Guidelines for landslide susceptibility, hazard and risk zoning for land-use planning." Engineering Geology **102**(3-4): 99-111.

Fisher, P. (1997). "The pixel: A snare and a delusion." International Journal of Remote Sensing **18**(3): 679-685.

Gokceoglu, C., H. Sonmez, et al. (2005). "The 17 March 2005 Kuzulu landslide (Sivas, Turkey) and landslide-susceptibility map of its near vicinity." Engineering Geology **81**(1): 65-83.

Gomes, R. A. T., R. F. Guimaraes, et al. (2008). "Identification of the affected areas by mass movement through a physically based model of landslide hazard combined with an empirical model of debris flow." Natural Hazards **45**(2): 197-209.

Goodchild, M. E. (2003). "Geographic information science and systems for environmental management." Annual Review of Environment and Resources **28**: 493-519.

Gorsevski, P. V., P. E. Gessler, et al. (2006). "Spatially and temporally distributed modeling of landslide susceptibility." Geomorphology **80**(3-4): 178-198.

Gorsevski, P. V. and P. Jankowski (2010). "An optimized solution of multi-criteria evaluation analysis of landslide susceptibility using fuzzy sets and Kalman filter." Computers & Geosciences **36**(8): 1005-1020.

Gorsevski, P. V., P. Jankowski, et al. (2006). "An heuristic approach for mapping landslide hazard by integrating fuzzy logic with analytic hierarchy process." Control and Cybernetics **35**(1): 121-146.

Guthrie, R. H. (2002). "The effects of logging on frequency and distribution of landslides in three watersheds on Vancouver Island, British Columbia." Geomorphology **43**(3-4): 273-292.

Hay, G. J., D. J. Marceau, et al. (2001). "A multiscale framework for landscape analysis: Object-specific analysis and upscaling." Landscape Ecology **16**(6): 471-490.

Horton, R. E. (1945). "Erosional development of streams and their drainage basins; hydrophysical approach to quantitative morphology." Geological Society of America Bulletin **56**(3): 275-370.

Jankowski, P. (1995). "Integrating geographical information systems and multiple criteria decision-making methods." International Journal of Geographical Information Systems **9**(3): 251-273.

Jankowski, P. and L. Richard (1994). "Integration of GIS-based suitability analysis and multicriteria evaluation in a spatial decision support system for route selection." Environment and Planning B-Planning & Design **21**(3): 323-340.

Jiang, H. and J. R. Eastman (2000). "Application of fuzzy measures in multi-criteria evaluation in GIS." International Journal of Geographical Information Science **14**(2): 173-184.

Komac, M. (2006). "A landslide susceptibility model using the Analytical Hierarchy Process method and multivariate statistics in penialpine Slovenia." Geomorphology **74**(1-4): 17-28.

Lee, S. and J. Choi (2004). "Landslide susceptibility mapping using GIS and the weight-of-evidence model." International Journal of Geographical Information Science **18**(8): 789 - 814.

Lee, S. and K. Min (2001). "Statistical analysis of landslide susceptibility at Yongin, Korea." Environmental Geology **40**(9): 1095-1113.

Luzi, L. and F. Pergalani (1996). "Applications of statistical and GIS techniques to slope instability zonation (1:50.000 Fabriano geological map sheet)." Soil Dynamics and Earthquake Engineering **15**(2): 83-94.

Malczewski, J. (1999). GIS and multicriteria decision analysis. New York, Wiley.

Malczewski, J. (2006). "GIS-based multicriteria decision analysis: a survey of the literature." International Journal of Geographical Information Science **20**(7): 703-726.

Monmonier, M. (1982). Computer-assisted cartography: Principles and prospects. Englewood Cliffs, N.J., Prentice-Hall, Inc.

Moore, I. D., R. B. Grayson, et al. (1991). "Digital terrain modelling: A review of hydrological, geomorphological, and biological applications." Hydrological Processes **5**(1): 3-30.

Ohlmacher, G. C. and J. C. Davis (2003). "Using multiple logistic regression and GIS technology to predict landslide hazard in northeast Kansas, USA." Engineering Geology **69**(3-4): 331-343.

Pachauri, A. K. and M. Pant (1992). "Landslide hazard mapping based on geological attributes." Engineering Geology **32**(1-2): 81-100.

Saaty, T. L. (1977). "Scaling method for priorities in hierarchical structures." Journal of Mathematical Psychology **15**(3): 234-281.

Saaty, T. L. (1980). The analytical hierarchy process: Planning, priority setting, resource allocation. New York, McGraw-Hill.

Santini, M., S. Grimaldi, et al. (2009). "Pre-processing algorithms and landslide modelling on remotely sensed DEMs." Geomorphology **113**(1-2): 110-125.

Sidle, R. C. and H. Ochiai (2006). Landslides: Processes, Prediction, and Land Use. Washington, DC, American Geophysical Union.

Suzen, M. L. and V. Doyuran (2004). "A comparison of the GIS based landslide susceptibility assessment methods: multivariate versus bivariate." Environmental Geology **45**(5): 665-679.

Van Westen, C. J., N. Rengers, et al. (2003). "Use of geomorphological information in indirect landslide susceptibility assessment." Natural Hazards **30**(3): 399-419.

Van Westen, C. J. and M. T. J. Terlien (1996). "An approach towards deterministic landslide hazard analysis in GIS. A case study from Manizales (Colombia)." Earth Surface Processes and Landforms **21**(9): 853-868.

Van Westen, C. J., T. W. J. Van Asch, et al. (2006). "Landslide hazard and risk zonation - why is it still so difficult?" Bulletin of Engineering Geology and the Environment **65**(2): 167-184.

Voogd, H. (1982). "Multicriteria evaluation with mixed qualitative and quantitative data." Environment and Planning B-Planning & Design **9**(2): 221-236.

Voogd, H. (1983). Multicriteria evaluation for urban and regional planning. London, Pion.

Wemple, B. C., F. J. Swanson, et al. (2001). "Forest roads and geomorphic process interactions, Cascade Range, Oregon." Earth Surface Processes and Landforms **26**(2): 191-204.

Wood, L. J. and S. Dragicevic (2007). "GIS-Based multicriteria evaluation and fuzzy sets to identify priority sites for marine protection." Biodiversity and Conservation **16**(9): 2539-2558.

Wu, J. G., D. E. Jelinski, et al. (2000). "Multiscale analysis of landscape heterogeneity: scale variance and pattern metrics." Geographic Information Sciences **6**(1): 6-19.

Wu, W. M. and R. C. Sidle (1995). "A distributed slope stability model for steep forested basins." Water Resources Research **31**(8): 2097-2110.

Yalcin, A. (2007). "Environmental impacts of landslides: A case study from East Black Sea Region, Turkey." Environmental Engineering Science **24**(6): 821-833.

Yalcin, A. (2008). "GIS-based landslide susceptibility mapping using analytical hierarchy process and bivariate statistics in Ardesen (Turkey): Comparisons of results and confirmations." Catena **72**(1): 1-12.

Yalcin, A. and F. Bulut (2007). "Landslide susceptibility mapping using GIS and digital photogrammetric techniques: a case study from Ardesen (NE-Turkey)." Natural Hazards **41**(1): 201-226.

Yilmaz, I. (2009). "Landslide susceptibility mapping using frequency ratio, logistic regression, artificial neural networks and their comparison: A case study from Kat landslides (Tokat-Turkey)." Computers & Geosciences **35**(6): 1125-1138.

Yilmaz, I. and I. Keskin (2009). "GIS based statistical and physical approaches to landslide susceptibility mapping (Sebinkarahisar, Turkey)." Bulletin of Engineering Geology and the Environment **68**(4): 459-471.

Zadeh, L. A. (1965). "Fuzzy sets." Information and Control **8**(3): 338-353.

CHAPTER 4 INTEGRATION OF MULTICRITERIA EVALUATION AND CELLULAR AUTOMATA METHODS FOR LANDSLIDE SIMULATION MODELLING[3]

4.1 Abstract

The most common way of representing and modelling physical and natural systems requires the use of partial differential equations. Physical processes including flooding, tsunamis, avalanches, earthquakes and landslides and others have undeniably complex systems behaviours. It can be argued that these physical processes are non-linear, random, and evolve spatially as local interactions occur, and are sometimes almost impossible to predict. However, capturing the geocomplexity of such phenomena, the use of complex system theory, more particularly cellular (CA) automata is considered necessary. In this study the novel approach that combines geographic information systems (GIS), multicriteria evaluation (MCE) and CA is developed for simulation modelling of urban landslide flows. The landslide susceptibility map produced from the MCE model provides the input for use in the CA model. The input data for this coupled approach is a high-resolution digital elevation model in which topographic variables such as slope, aspect, stream power index, topographic wetness index, and flow direction are calculated. The proposed MCE-CA simulation model was tested on historical landslide data in Metro Vancouver, Canada. When spatial extents of the landslide simulations were

[3] The following chapter will be submitted for publication to *Landslides* under the co-authorship of Suzana Dragicevic and Margaret Schmidt.

compared by map overlay analysis, an average of 89% of the cells were accurately predicted, while 11% of cells were missed predictions and 13% were over-predicted. The flexibility of this model in terms of modifying existing or adding new expert knowledge to the MCE model allows the transition rules in the CA to be tailored to a specific study site. The proposed simulation model can be used by urban planners who face landslide hazards.

4.2 Introduction

Urban landslides in Metro Vancouver, Canada, have occurred since the development of the area in the 1800s. The reason for this is a combination of high relief, steep slopes, heavy rainfall, seismicity, and landslide-prone materials that have posed a significant hazard to land use development (Evans and Savigny 1994). In the past, landslides were triggered by intense fall and winter rainstorms and occurred most commonly along escarpments. The lack of available flat land has necessitated the need to increasingly develop on steeper, potentially unstable slopes surrounding populated areas, thereby increasing the vulnerability of failures near human activity (Eisbacher and Clague 1981).

Modelling and simulation have been applied to landslides for many years, particularly to predict landslide susceptibility and behaviour. Generally, computer modelling using a single approach or a combination of techniques has been a preferred choice simply because it is the most practical way to replicate a complex spatial phenomena (Santini et al. 2009). Traditionally, the study of landslide prediction has incorporated the infinite slope model, which is an analysis of the ratio between resisting forces of slope movement and driving forces that make the slope fail (Van Westen and

Terlien 1996; Wu and Sidle 1995; Shou and Wang 2003). The calculation takes into account properties of soil, vegetation, topography, and hydrology (Paulin and Bursik 2009). The dimensionless ratio value is known as the factor of safety and a value of 1 implies the slope is in a balanced state (Iverson 2000). Values greater than 1 predict stable slopes, whereas unstable slopes are characterized by a factor of safety ratio of less than 1. The general form of the infinite slope model changes and becomes more complex as groundwater and the variability of the terrain is fully considered (Wilkinson et al. 2002). For example, the equations change from the simple case of a dry slope, to varying levels of saturation, and finally to full saturation.

Describing a physical system entirely using partial differential equations, without vast simplification, presents a challenge because a system of many differential equations is computationally intensive (Karafyllidis and Thanailakis 1997). In addition, representing a physical system that is inherently spatial and temporal using differential equations requires new dimensions to be added to the analysis (i.e. 2- or 3-dimensional). Spatial and temporal 3-dimensionality can be alternatively handled by viewing the event of a landslide as a complex system in which the relationships of the parts to the environment affect the collective behaviour of the system. Many natural systems, such as landslide flow, can be seen as complex systems with characteristics such as organization, evolution, bifurcation, and others (Rundle et al. 2000; Manson 2001). Cellular automata (CA) modelling is one such approach designed to characterize complex systems (von Neumann 1966). CA models are an alternative to using differential equations and have been applied successfully in modelling physical systems and processes (Toffoli 1984). When a landslide occurs, the front of the slide is influenced by the surrounding environment which determines whether flow occurs and in which direction; this interaction provides the basis for which CA representation is justified.

The CA approach is extremely relevant because its inherent simplicity has great potential for modelling complexity. Transition rules control a grid of cells that update the state they are in at each increment in time. In geography, CA has largely been developed over the past two decades for modelling urban growth and land use change (Clarke et al. 1997; Batty and Xie 1994; White et al. 1997; White and Engelen 2000; Yeh and Li 2001; Wu 2002; Barredo et al. 2003).

It has also been found that CA is an excellent way to analyze many natural phenomena. Many of these have anthropogenic links, such as deforestation (Moreno et al. 2007), forest fires (Karafyllidis and Thanailakis 1997; Yassemi et al. 2008), insect infestations (Bone et al. 2006), and oil spills (Karafyllidis 1997). In the geological context, the term geocomplexity (geological complexity) has been used as an alternative approach to explain the complexity exhibited by earth systems (Turcotte 2006). It is recognized that the patterns generated by the CA approach can provide an understanding to a wide range of geological phenomena. For example, CA approaches have been applied in the context of geocomplexity to earthquakes (Rundle et al. 2000; Weatherley et al. 2000), lava flows (Crisci et al. 2008; Rongo et al. 2008), density currents (Salles et al. 2007), surface water flows (Thomas and Nicholas 2002; Parsons and Fonstad 2007; Coppola et al. 2007; Doeschl-Wilson and Ashmore 2005), flooding (Dalponte et al. 2007), and the formation of aeolian features (Nield and Baas 2008; Anderson and Bunas 1993; Mehta and Barker 1994). A reason that CA has been so useful in analyzing natural physical phenomena is that most physical processes are local in nature and interactions can be modelled in separate components.

In respect to CA modelling of landslides as reported in the literature, Malamud and Turcotte (2000) presented a simple CA “sand pile” model applied to landslides. Guthrie et al. (2008) developed a CA model that modelled landslide flow based on aspect ranking. SCIDDICA (Smart Computational Innovative method for the Detection of Debris/mud flow path with Interactive Cellular Automata) is an example of a successful model applied to landslides for several locations (Avolio et al. 2000; D'Ambrosio et al. 2002; D'Ambrosio et al. 2003; Di Gregorio et al. 1999; Iovine et al. 2003). SCIDDICA breaks landslide flow into elementary processes such as outflows from each cell, run-up from momentum, mobilisation, water loss, and solidification. Each of these components requires an abundance of data from a set of global parameters specific to each study site. The drawback of SCIDDICA is that the formalization of transition rules requires an extensive amount of data. The simplification of transition rules would prove advantageous as it was shown that a model based on simple slope-based rules, while requiring relatively low data requirements, can still achieve high accuracy and efficiency (Benda and Cundy 1990).

The rules representing the local interactions, more aptly known as CA transition rules, govern cell state changes. They are at the core of how a CA operates and can be derived empirically or from a function that represents the system. In order to determine functions that realistically represent the system, transition rules can be determined when combined with an additional approach such as integrating logistic regression (Soares et al. 2002; Fang et al. 2005), neural networks (Li and Yeh 2001; Almeida et al. 2008; Li and Yeh 2002), Bayesian networks (Kocabas and Dragicevic 2007), fuzzy sets (Liu and Phinn 2003), and others.

Another example is the integrated approach of multicriteria evaluation (MCE) and CA, wherein the decision-making capability of the MCE derives the non-deterministic transition rules for the CA. This approach has been used to simulate urban land use change (Wu and Webster 1998), alpine tundra vegetation dynamics (Zhang et al. 2008), and desertification (Wang et al. 2007). Despite its application, to this date the integrated approach of MCE and CA has not been applied to landslide modelling. The use of MCE coupled with the CA approach relies on the expert knowledge provided in the MCE. This multiple criteria evaluation process determines which landslide conditioning factors most influence landslide flow. The flexibility provided in the MCE process allows this approach to be easily modified for different study sites. Also, the relative ease with which the decision process is carried out with multiple criteria assists in the determination of CA transition rules. Both the MCE and CA approaches are suitable for combination with raster (cell) based geographic information systems (GIS) known for its geospatial data storage, manipulation and analytical capabilities.

Therefore the main objective of this study is to develop and implement a CA model, which integrates a GIS-based MCE approach for simulating landslide flow. The decision-making process incorporates numerous parameters that affect the movement of the landslide front. The approach offers a model that effectively predicts landslide flow without requiring large amounts of data.

4.3 Methods

The methodology for the MCE-CA model was composed of two parts. The first consisted of the development of the MCE model, which produced a map of landslide susceptibility used as an input for the CA model. The second was the development and testing of the CA model for landslide flow prediction, where the output was a series of maps representing landslide flow at discrete times.

4.3.1 Multicriteria Evaluation Model

The objective of the multicriteria evaluation approach used in this study was to classify landslide susceptibility based on numerous conditioning factors in order to produce an input for the CA model to predict landslide flow. The most common MCE factor aggregation procedure is known as weighted linear combination (WLC), where continuous parameters are standardized to a common numeric range, weights are calculated for each parameter, and then combined by weighted averaging for the final landslide susceptibility map (Voogd 1983).

The parameters evaluated individually were slope gradient, aspect gradient, stream power index (SPI), topographic wetness index (TWI), distance to drainage, distance to roads, and distance to escarpment crest. Due to the different measurement units and scales for each parameter, it was essential to utilize a standardization procedure (Jiang and Eastman 2000). Traditional GIS applications have used crisp Boolean sets, where spatial information represented discrete objects in a discrete definition; however, transition from membership to non-membership is rarely a step function. Rather, there is a gradual change represented as fuzzy sets (Zadeh 1965) and it is characterized by a membership function $f(\mu(x))$ where $\mu(x) \in [0,1]$ is a degree of membership to a particular set. In this study, fuzzy sets were used to represent individual landslide conditioning parameters and their relationship to landslide susceptibility. This membership for each landslide parameter is standardized on a byte scale from 0 to 1, where 0 represents the least susceptible and 1 represents the most susceptible. The fuzzy membership function used in this study is the sigmoidal or s-shaped membership, which follows a cosine function. The sigmoidal membership function is most commonly used in GIS applications and especially where the grade of membership is a function of distance from a location or object (Robinson 2003). Four control points that represent the inflection points of the curve describe the susceptibility of each parameter. The assignment of these control points required expert knowledge gained through local slope assessment reports and a review of landslide literature.

Once landslide-conditioning parameters were standardized by fuzzy sets, the importance of each parameter was evaluated and assigned weights in consideration of other parameters, which was difficult since there are many parameters. The most commonly used technique for assigning weights is the Analytical Hierarchy Process (AHP), developed by Saaty (1977) and first introduced to GIS by Rao (1991). AHP involves comparing pairs of parameters at a time in an organized manner, rather than evaluating all parameters as a whole (Saaty 1990). The fundamental input provided by expert knowledge is deciding how important one parameter is to another. The relative importance is translated to a 9 point continuous rating scale, and then entered into a pairwise comparison matrix (Saaty 1980). A rating of 1 denotes equal importance between two parameters (or with itself) and an increasing rating, up to a value of 9, represents an increasing level of importance of one parameter over the other. The reciprocal of the rating given to the same pair represents the comparison in reverse. For example, parameter A is much more important than parameter B, thus deserving a rating of 9. By the same comparison, parameter B is much less important than parameter A and the rating becomes 1/9. This comparison procedure is performed until all possible pairs of parameters have been assigned a rating. Weights are then calculated by matrix algebra using the eigenvector method, which calculates the maximum or principal eigenvector of the matrix (Eastman 2009). These weights must sum to one and they represent the relative importance and contribution that each parameter has on landslide susceptibility.

The procedure used to combine information from multiple criteria for continuous factors is WLC, which can be expressed by $S = \sum w_i \cdot x_i$, where S is the landslide susceptibility, w_i is the weight of the parameter i, and x_i is the criterion score of parameter i. In other words, parameters are combined by applying a weight, calculated by AHP, to each followed by a summation of the results to yield a susceptibility map.

4.3.2 Cellular Automata Model

Space and time are represented in CA models as discrete components and the evolution of change is dictated by transition rules that mimic the process interactions at a local scale. The landslide CA model is characterized by five properties: 1) a grid of cells, 2) a set of cell states, 3) the neighbourhood, 4) transition rules, and 5) a sequence of time steps as cell states are updated (White and Engelen 2000).

The grid space defines the spatial region consisting of a number of cells with identical shape and size. In this study, a regular two-dimensional square lattice was utilized for its compatibility with raster-based GIS data. The spatial resolution of the raster grid determines the lower limit of distance travelled as a landslide flow occupies a single cell. For each grid cell, the set of possible cell states is simply defined as the presence or absence of landslide flow.

The neighbourhood refers to a defined collection of cells surrounding each individual cell that will have an influence on the state of that cell. This defined area can consist of cells in the cardinal directions (i.e. north, east, south, and west) of each individual cell, which is known as the von Neumann neighbourhood (4 cells around a central cell). Another common neighbourhood is the Moore neighbourhood, which considers all eight cells directly adjacent (i.e. north, northwest, west, southwest, south, southeast, east, and northeast), to each central cell. The above definitions describe a radius of influence that spans one cell from each individual cell (r = 1); however, both neighbourhood types can be extended to reach over the distance of multiple adjacent cells (r = 1, 2, 3 ... n). Since the neighbourhood type and size are reflective of the influence area of local interactions occurring within the physical system, there is a need to investigate the effects when they are varied (Kocabas and Dragićević 2006; Ménard and Marceau 2005). In other words, a sensitivity analysis on the neighbourhood type and size should be carried out prior to modelling. This is a way to assess the model behaviour and the agreement between the model and the real world. The von Neumann neighbourhood is not used in this study because of the lack of diagonal cells that are important for description of the process of flow of the landslides. Instead, extended Moore neighbourhoods of various radii (r = 1, 2, 3) were tested to justify the chosen neighbourhood size.

The transition rules represent the interactions that occur at a local spatial scale. These rules govern how the states of neighbourhood cells will affect the future state of a cell. Rules can be determined from a physical basis or an empirical approach. Applying simple rules mimicking the logic of the modelled processes at local scales generate complex patterns of the system at larger spatial extents (Packard and Wolfram 1985). Transition rules that govern landslide flow were derived from the susceptibility map produced in the MCE model and consider flow directions from the local DEM.

The time step is a single application of the defined transition rules to all cell states in the grid space and the updating of cells simultaneously (or "synchronously"). In this manner, the repeated application or iteration of transition rules provides a discrete representation of time as the phenomenon evolves (Wolfram 1983). The number of time steps taken to model landslide flow from initiation to stoppage is known as the temporal extent of the model. Therefore the dynamics of the landslide process is represented both spatially and temporally.

4.4 Model Implementation

4.4.1 Study area

The District of North Vancouver (DNV), comprised of urbanized and undeveloped land with a population of roughly 88 000, is located in Metro Vancouver, Canada (BC Stats 2010). The Berkley Escarpment is located within the DNV, east of the Seymour River in a residential neighbourhood (Figure 4-1). It is approximately 2 km long and 60 m from the bottom to the top of the escarpment. Houses have been built close to the crest and loose fill was placed at the top of the escarpment, locally raising the elevation and oversteepening the top of the slope. This in turn increases the potential for landslide failures. Historically, landslide failures triggered by intense storm rainfall have occurred along the escarpment crest. Four storms which occurred in December 1972, December 1979, January 1999, and most recently January 2005 triggered six landslides near the crest of the Berkley Escarpment.

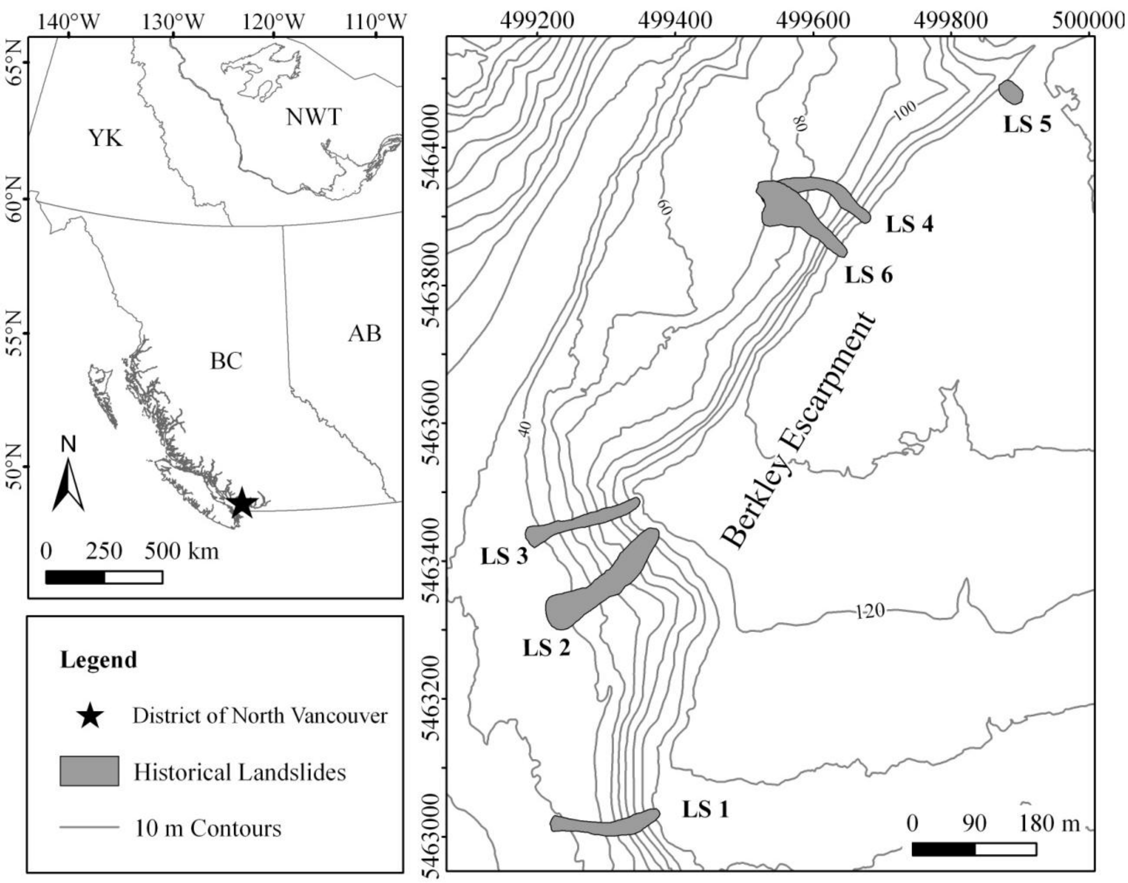

Figure 4-1. Location of six historical landslides on the Berkley Escarpment.

4.4.2 Geospatial Data

Two meter contours from topographic maps (1:2000) produced in March 2006 by the DNV were used to generate a high-resolution digital elevation model (DEM). The software used to perform the conversion of and interpolation between contour intervals was raster GIS Idrisi Taiga (Eastman 2009). The linear interpolation between contours produced a DEM with a cell resolution of 1 m. The implication of this high level of detail dictates that CA transition rules may be applied to a very fine spatial scale, allowing landslide movement to occur at 1 m increments.

Various topographic variables were derived from the raster GIS using the high resolution DEM, such as slope gradient, aspect gradient, stream power index (SPI), topographic wetness index (TWI), flow direction, distance to drainage, distance to roads, and distance to escarpment crest. Six historical landslides along the Berkley Escarpment were the subject of the CA modelling in this study, where the distances travelled and the scar area left behind have been measured (Table 4-1). The spatial extents of the six landslide scars were digitized from maps in order to calibrate and test the model on a cell-by-cell basis. From these locations, hypothetical initial failure areas were generated by digitizing polygons with the initial width of respective landslides. The purpose of this was to use these polygons as a starting point for which the CA model could simulate landslide flow, rather than simulate the initiation of slope failure.

Table 4-1. Landslide inventory data.

Landslide	**Scar length (m)**	**Scar size (m^2)**	**Initial Area (m^2)**
LS 1 - December 1972	165	3205	132
LS 2 - December 1979	207	7310	389
LS 3 - December 1979	172	3089	152
LS 4 - December 1979	175	3548	131
LS 5 - January 1999	37	836	159
LS 6 - January 2005	169	5783	328

4.4.3 The MCE-CA Model

The spatio-temporal modelling occurred in the CA model, where the six Berkley Escarpment landslides were simulated, based on information provided from the susceptibility map. The workflow of the MCE-CA model is presented (Figure 4-2).

Several procedures were performed prior to producing the susceptibility map. The landslide conditioning parameters were chosen due to the relevance of these parameters in past landslide studies and also the ease with which the parameters could be calculated given the availability of data (i.e. high resolution DEM). Each of these parameters were standardized by a fuzzy membership according to a set of control points, which were derived from the expert knowledge of previous studies (Jiang and Eastman 2000). The control points determined the relationship each parameter had with landslide susceptibility on a continuous scale from 0 to 1 (Table 4-2). For example, the landslide susceptibility in relation to slope was defined by a symmetric sigmoidal membership function. Control points *a* and *d* represented very low landslide susceptibilities at slopes of 5° and 40°, respectively. The peak of the function was between control points *b* and *c*, which represented very high landslide susceptibilities at slopes of 30° and 40°, respectively. The next crucial step of the MCE process was determining the parameter weighting, which was carried out by the pairwise comparison matrix procedure known as AHP (Table 4-2). Each parameter was individually compared relative to another. Slope was regarded as the most important parameter, therefore any comparison of slope to another parameter yielded a rating greater than 1 (equal). For instance, the comparison from slope to aspect was given a rating of 7. Conversely, any parameter compared to slope was given a rating less than 1. For example, the comparison from SPI to slope yielded a rating of 1/3. Since the weighting process was carried out in a subjective manner, a method was used to evaluate the process. Saaty (1977) proposed a way to determine consistency within the ratings, known as the consistency ratio (CR). It is a measure of probability that the matrix ratings were randomly generated. A value of less than 10% is considered acceptable and a greater value requires further evaluation in the matrix ratings. The resulting CR value obtained was 4%, which was acceptable. The final step was to produce the susceptibility map was to combine the primary level weights (fuzzy standardized parameters) with secondary level weights (AHP derived). The method used for evaluating the effectiveness of a susceptibility map used for landslides is the seed cell area index (Suzen and Doyuran 2004). The index is the ratio between percentage area occupied by a single susceptibility class and the proportion of landslide cells (seed cells) within the susceptibility class. SCAI values in higher susceptibility classes are expected to have very small values as the number of landslide cells should be proportionately larger within higher susceptibilities. On the other hand, a greater area of lower susceptibilities along with fewer landslide cells within them yields a large SCAI value. This susceptibility map was then used as an input for CA modelling.

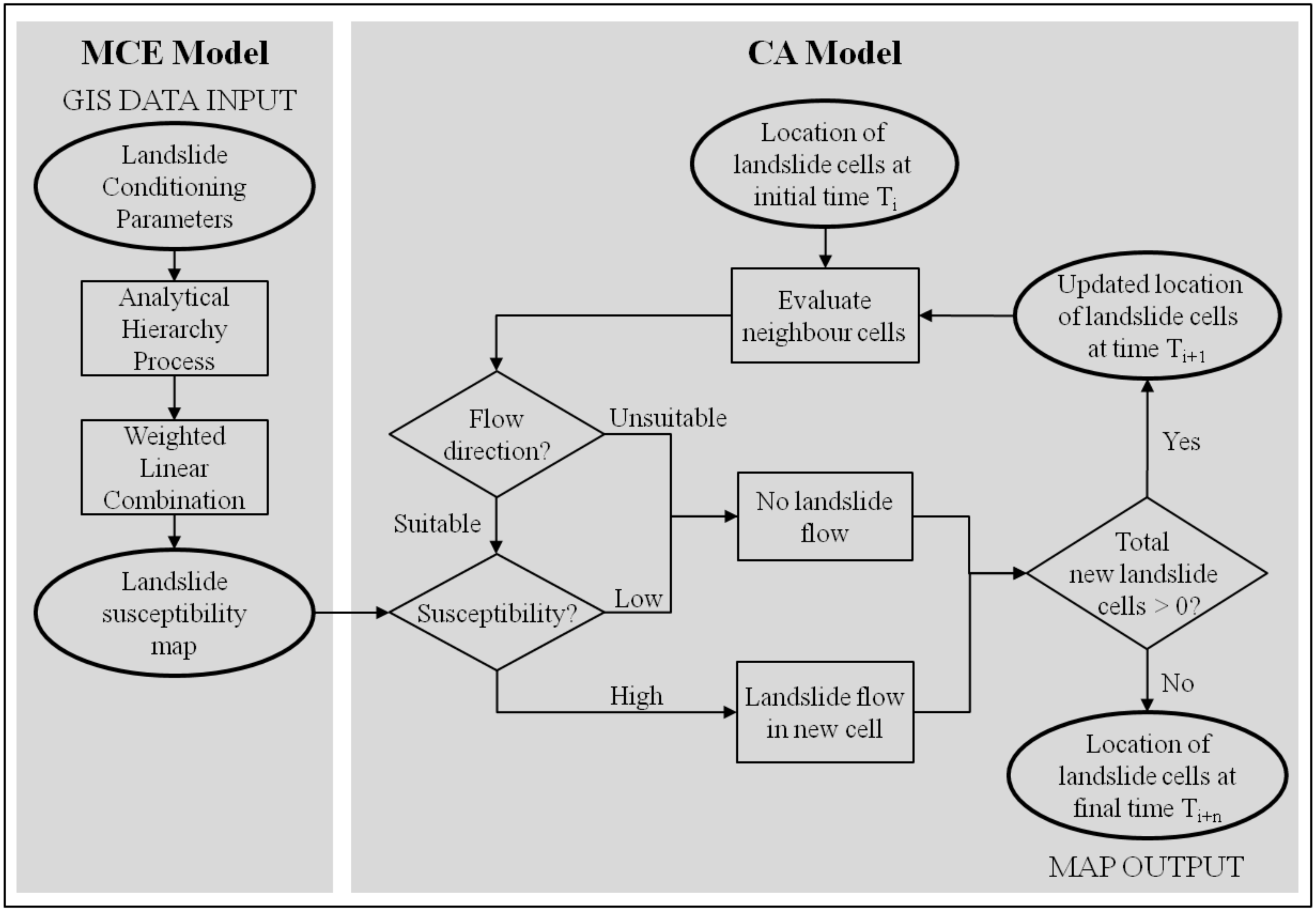

Figure 4-2. Flow chart of MCE-CA modelling components.

4.4.4 Specifying the CA Model

Regardless of neighbourhood size, the CA model employed a regular Moore neighbourhood, which meant each individual cell considered the states of neighbouring cells in all directions. By including neighbours in all directions, the propagation of the landslide focused purely on transition rule elicitation from flow direction and landslide susceptibility.

First, the neighbours of the hypothetical initial polygons were determined and an evaluation process was carried out for each neighbour cell. For each neighbour cell that was directly adjacent to a landslide cell, flow direction logically allowed and constrained whether flow into that cell was possible. For example, a failure that occurred on a west-facing slope would generally travel westward because this direction was downslope. In other words, flow direction controlled the notion that a landslide will not progress upslope under any condition.

Secondly, neighbour cells deemed unsuitable for movement based on flow direction (i.e. typically cells behind the landslide front) automatically resulted in inaction; however, cells that passed that evaluation stage were tested for high landslide susceptibility provided by the MCE model. The landslide susceptibility map explained and predicted areas prone to landslide failure and this information guides the CA model. Highly susceptible areas were typically located on steep slopes that had an affinity for the accumulation of water flow, which would also form channels for landslide flow. On the other hand, low susceptibility areas occurred on gentle slopes, where landslide stoppage and deposition most likely occurred. In essence, the flow direction parameter was coupled with a landslide susceptibility map that did not consider flow direction.

Additionally, including flow direction in the CA model, rather than in the MCE model, avoided duplication of parameters in the process.

Each neighbour cell must pass through two stages of evaluation in order to elicit a change in cell states from non-landslide cell to landslide cell. The transition rules required a suitable flow direction in consideration of existing landslide cells and a high susceptibility of landslide flow. The implementation of these rules also confined landslide flow to lower elevations (i.e. downhill), prevented upslope movement, as well as where the landslide front stopped.

At each time step, the model updated the spatial location of the landslide front and used the updated location as an input for the next application of transition rules. The model iterated until there was a complete stoppage in terms of the number of state transitions from non-landslide cells to landslide cells (i.e. zero new landslide cells). The model outcomes are a series of map layers that depicted the spatial location of the moving landslide front as the model progressed in terms of time steps.

Prior to the implementation of the CA model, calibration was carried out in order to test neighbourhood size on model behaviour. Simulations using three different radii (r = 1, 2, 3 cells) of Moore neighbourhoods were tested in order to determine the area of influence for the CA model (Figure 4-3). The simulations were compared to real landslide datasets in order to choose best model parameters.

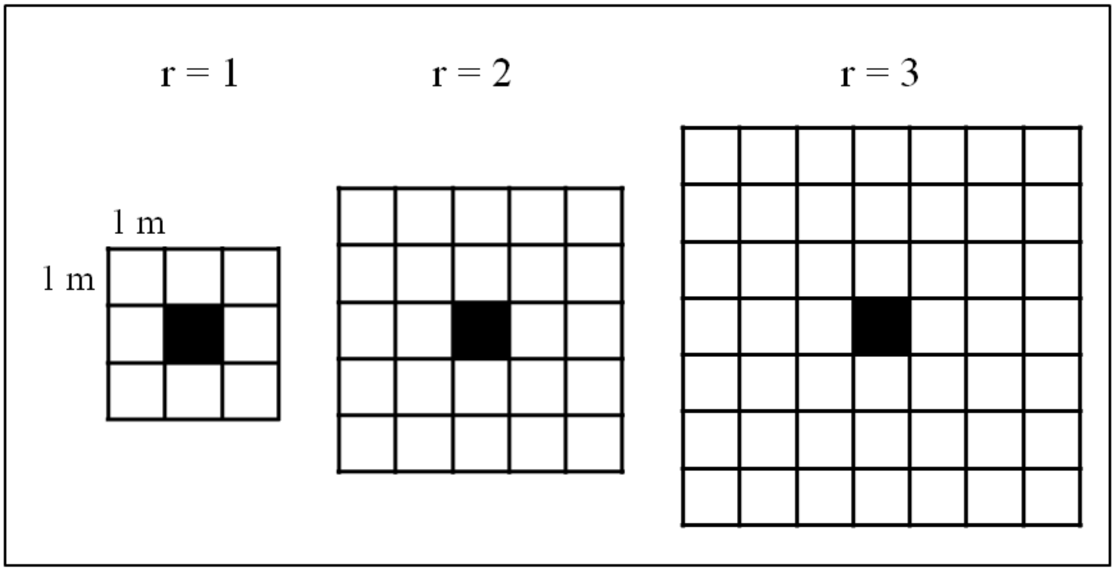

Figure 4-3. Neighbourhood sizes r = 1, 2, 3.

Table 4-2. Fuzzy standardization and pairwise comparison matrix.

Parameter	**Membership Function**	**Type**	**Control Points**
Slope	Sigmoidal	Symmetric	a=5°, b=20°, c=30°, d=40°
Aspect	Sigmoidal	Symmetric	a=180°, b=270°, c=270°, d=360°
Stream power index	Sigmoidal	Monotonically increasing	a=0, b=300
Topographic wetness index	Sigmoidal	Monotonically decreasing	c=2, d=4
Distance to drainage	Sigmoidal	Monotonically decreasing	c=50m, d=1000m
Distance to roads	Sigmoidal	Monotonically decreasing	c=40m, d=100m
Distance to crest	Sigmoidal	Monotonically decreasing	c=5m, d=100m

Parameter importance (Column 1)	**Relative to Parameters (Columns 2-8)**							
	Aspect	Crest*	Drainage*	Road*	Slope	SPI	TWI	Weights
Aspect	1							0.0461
Crest*	3	1						0.1074
Drainage*	1	1/3	1					0.0409
Road*	1	1/3	3	1				0.0572
Slope	7	3	7	7	1			0.3824
SPI	4	3	4	4	1/3	1		0.2105
TWI	3	3	3	3	1/3	1/2	1	0.1554

* refers to distance parameters

CR = 0.04 < 0.1

4.5 Results

The MCE model based on fuzzy sets generated a landslide susceptibility map for the Berkley Escarpment. The map had numerical values from a continuous scale from 0 to 1, which was visually difficult to interpret. In order to address this problem, susceptibility was divided into equal intervals to produce five classes: very low, low, medium, high, and very high (Figure 4-4). As expected, the low susceptibility classes are located primarily on the flat land of the residential areas. Conversely, the very high susceptibility classes occur right at the crest of the escarpment where the slope suddenly steepens. It is impossible to pinpoint exactly where the next landslide failures will occur, but it would likely originate in these highly susceptible areas.

The SCAI values obtained indicated that the generated map for the Berkley Escarpment was accurate because the high (12%) and very high (2%) susceptibly classes had very low SCAI values (0.31 and 0.20, respectively), whereas the very low (54%) and low (20%) susceptibility classes were relatively higher (8.47 and 1.14, respectively).

Calibration was carried out using two of six modelled landslides in order to determine the effect of varying neighbourhood sizes on the CA model outcomes, while every other component remained unchanged. Specifically, a subsample of Landslides 2 and 3 on the Berkley Escarpment were used in the calibration process. This was performed by testing the model using regular Moore neighbourhoods with radii (r) of 1, 2, and 3 cells. In other words, the neighbourhoods were defined 3 by 3 cells, 5 by 5 cells, and 7 by 7 cells, respectively. The resulting number of neighbourhood cells influencing the centre cell is 8 for the 3 by 3 neighbourhood, 24 for the 5 by 5 neighbourhood, and 48 for the 7 by 7 neighbourhood. Since the cell resolution of the geospatial data is 1 m, the

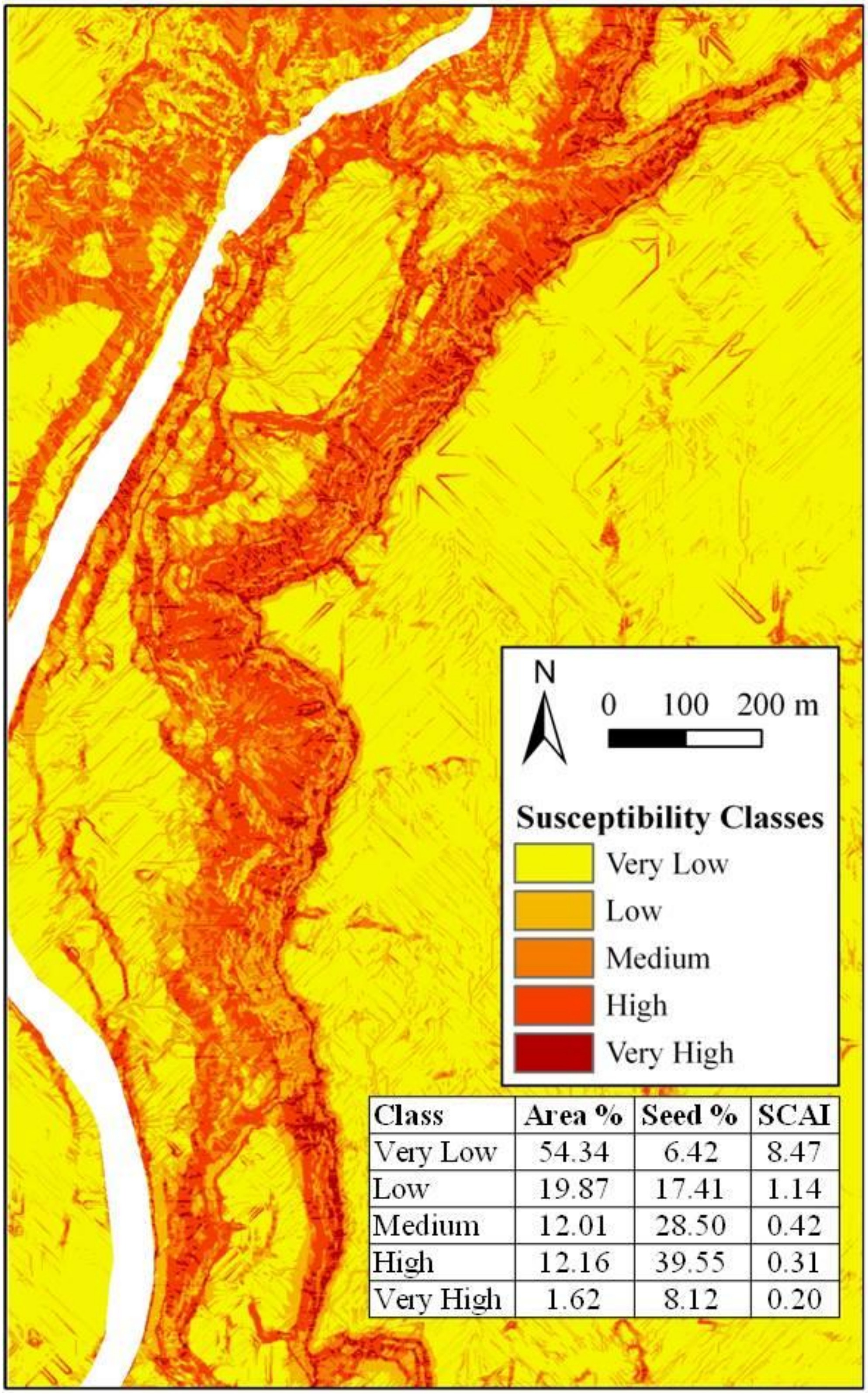

Class	Area %	Seed %	SCAI
Very Low	54.34	6.42	8.47
Low	19.87	17.41	1.14
Medium	12.01	28.50	0.42
High	12.16	39.55	0.31
Very High	1.62	8.12	0.20

Figure 4-4. Susceptibility map for Berkley Escarpment.

areas of influence for each centre cell in the three neighbourhood sizes are 8 m^2, 24 m^2, and 48 m^2, respectively.

The results of the calibration were visually compared by overlaying simulation maps with real landslide data (Figure 4-5). The overlaid simulation maps clearly indicated spatial differences in the landslide simulation outcomes when neighbourhood size changed. By comparing the modelled outcomes and actual extents derived from real landslide datasets, the landslide area not modelled increased with increasing neighbourhood size. This comparison indicated that neighbourhood size has an effect on the CA model outcomes. Without changing other parameters, the model behaviour was consistent and followed the general slope of the topography.

Given the performed calibration procedure, the chosen neighbourhood size for modelling of all six landslides was the 3 cell by 3 cell Moore neighbourhood (r = 1). The justification was drawn from the calibration since this neighbourhood size resulted in the most accurately simulated landslide extents. The CA model performed the simulation using transition rules derived from the susceptibility map and flow direction, which controlled landslide flow for the Berkley Escarpment. The six landslide simulations were evaluated using a raster GIS map overlay method, which compared the extents of the real landslides as digitized from maps with the simulated extents (Figure 4-6-Figure 4-10). Visually, the modelled flow paths provided good correspondence when matched with the actual landslide events. The MCE-CA model handled the variation in topography and consequent change in flow direction well (Figure 4-6 and Figure 4-8). The model was also able to predict the spread of the landslide front at lower elevations and gentle slopes when stoppage would occur (Figure 4-10). In order to measure performance

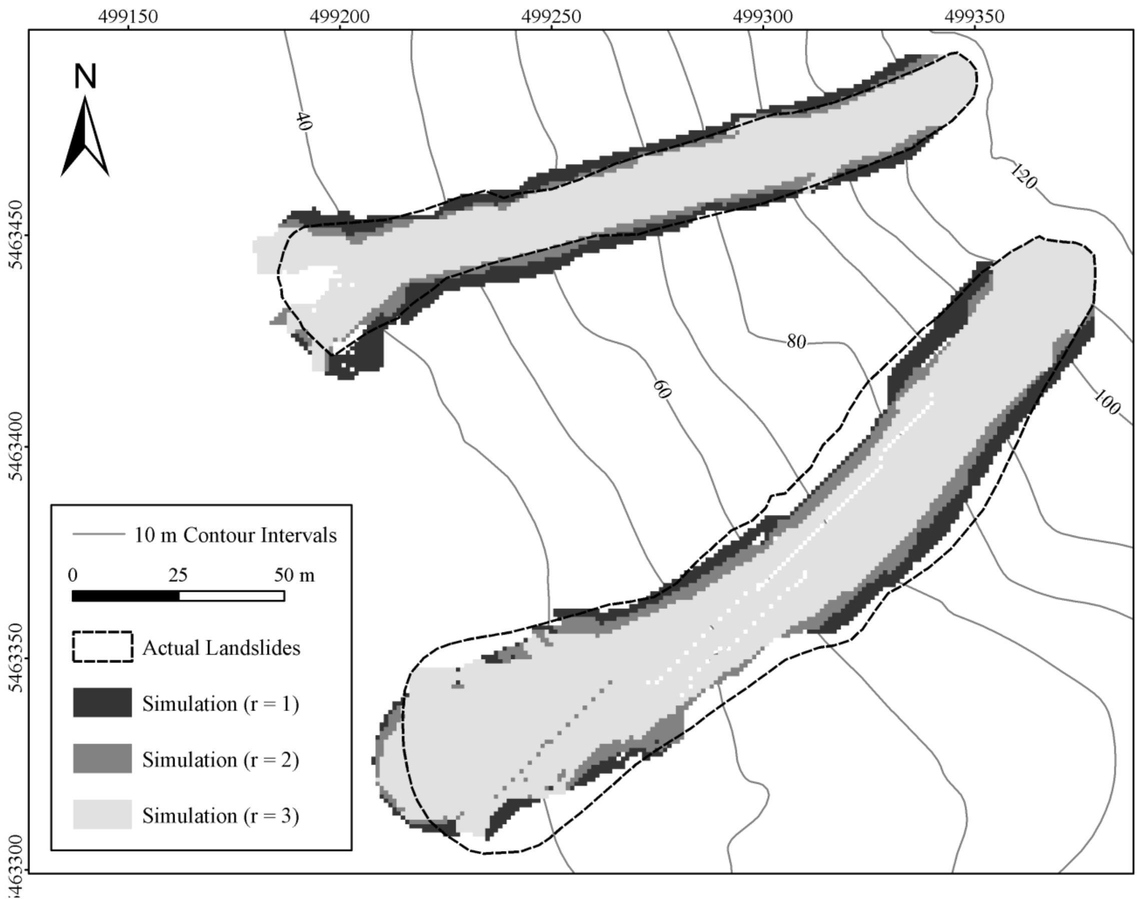

Figure 4-5. Simulation results under changing neighbourhood sizes (radii = 1, 2, 3).

quantitatively, three ratios were calculated (Table 4-3) and they can be described as 1) accurately predicted landslide cells, 2) real landslide cells that were missed, and 3) over-predicted landslide cells each normalized by the real number of landslide cells (D'Ambrosio et al. 2002). It should be noted that error resulting from under predictions were considered more serious than those that were over predicted. The most accurate CA simulation was Landslide 3 (Figure 4-7), registering near 96% accuracy; however, a large proportion (30%) was grossly over-predicted. The average accuracy across all six landslides on the escarpment was 89%, also 11% were missed predictions and 13% were predicted where landslides did not occur. These indices showed that overall, the CA model incorporating MCE-derived transition rules was successful. By utilizing a Moore neighbourhood that spanned in all eight directions, the CA relied solely on flow direction and the susceptibility inputs from the MCE.

The results only represent the final stages of the CA modelling, but each landslide required a unique amount of time steps until the stoppage took place (Table 4-3). The actual duration of each landslide event was not recorded, therefore there is no way of translating time steps to real speeds. The CA changed non-landslide cells at the flow front at a rate of a single cell per time step, thus the landslide front moves at 1 m per time step. The shortest landslide event required 27 time steps, whereas the longest landslide event required 160 time steps. The lack of additional details on historical landslides prevents the back-calculation for velocities and duration of landslide events.

Table 4-3. Simulation accuracy ratios and time steps.

Landslide	**Accurate (%)**	**Missed (%)**	**Over (%)**	**Time Steps**
LS 1 - December 1972	89.0	11.0	15.0	147
LS 2 - December 1979	84.0	16.0	4.3	150
LS 3 - December 1979	95.8	4.2	29.8	160
LS 4 - December 1979	85.8	14.2	11.3	140
LS 5 - January 1999	90.5	9.5	14.9	27
LS 6 - January 2005	88.8	11.2	3.5	118

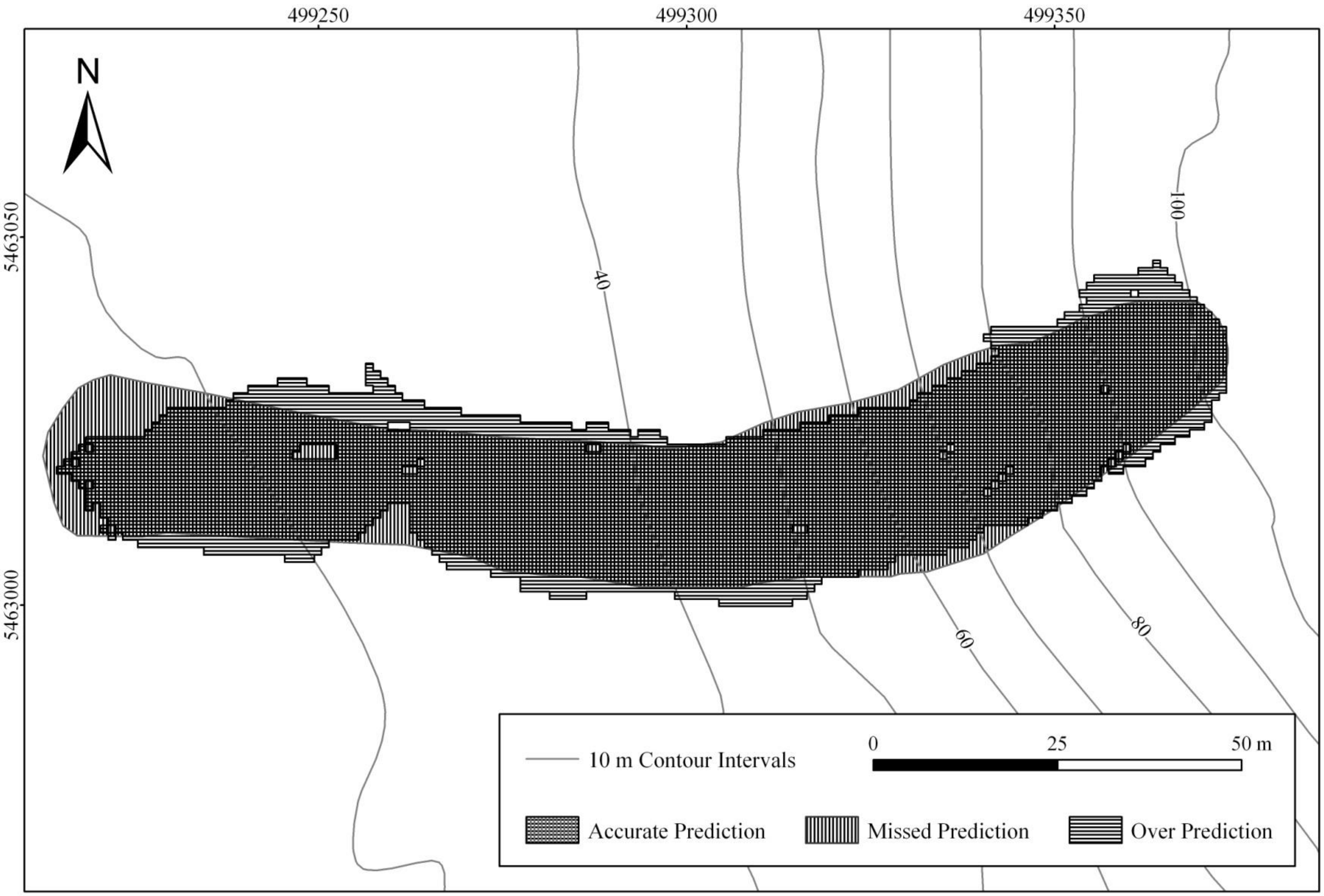

Figure 4-6. Simulation result of Landslide 1 (final step, t = 147).

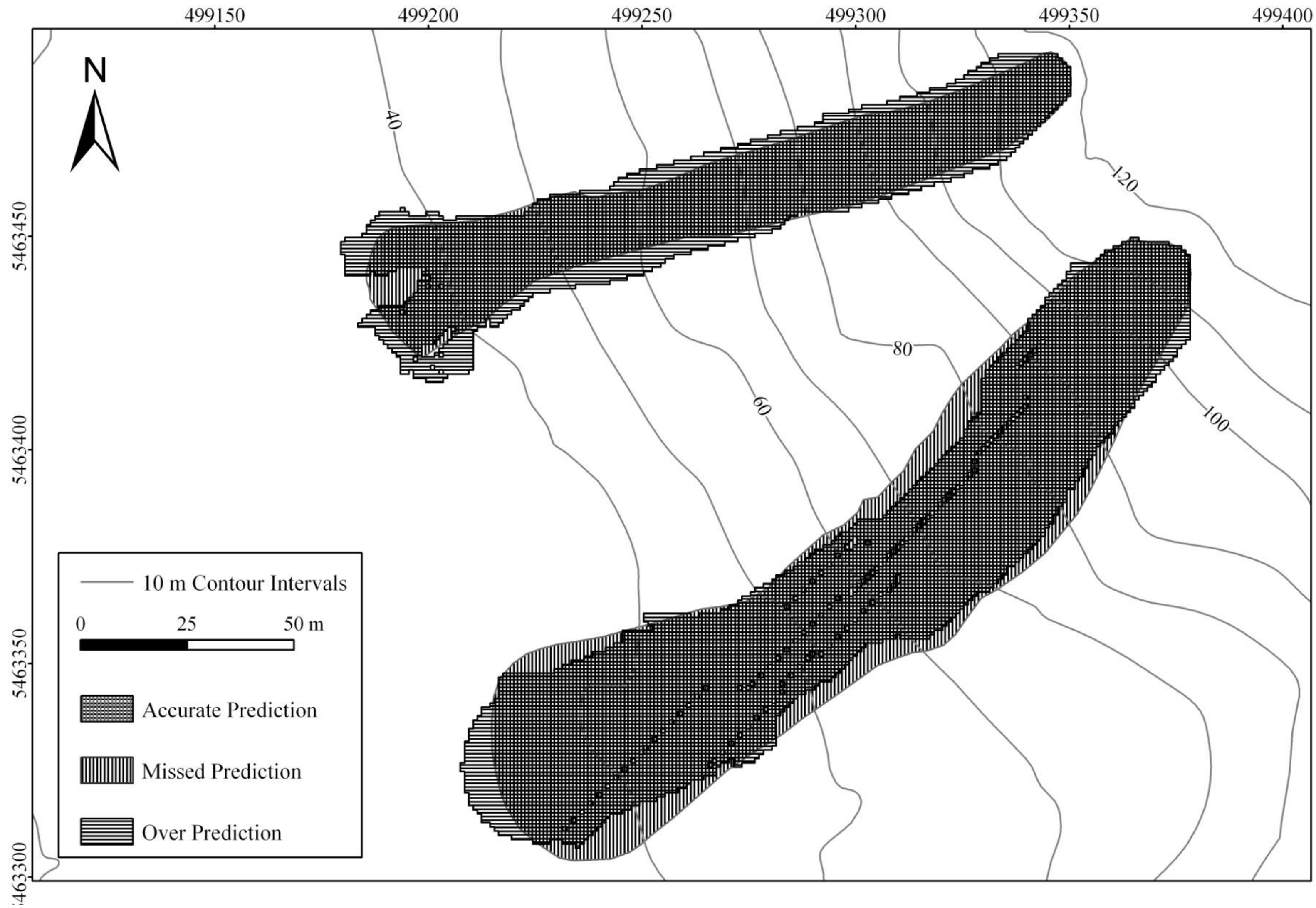

Figure 4-7. Simulation result of Landslide 2 (final step, t = 150) and Landslide 3 (final step, t = 160).

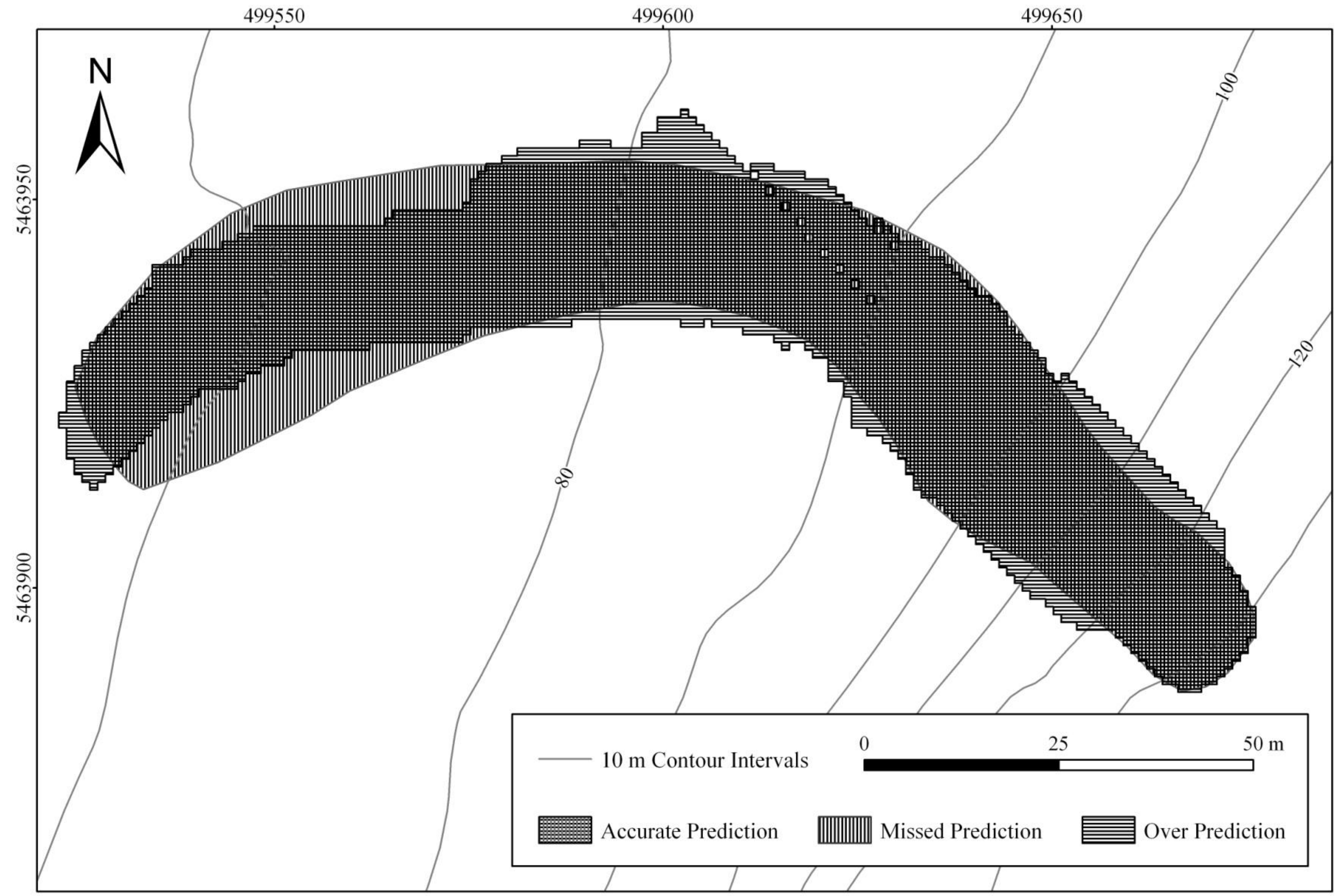

Figure 4-8. Simulation result of Landslide 4 (final step, t = 140).

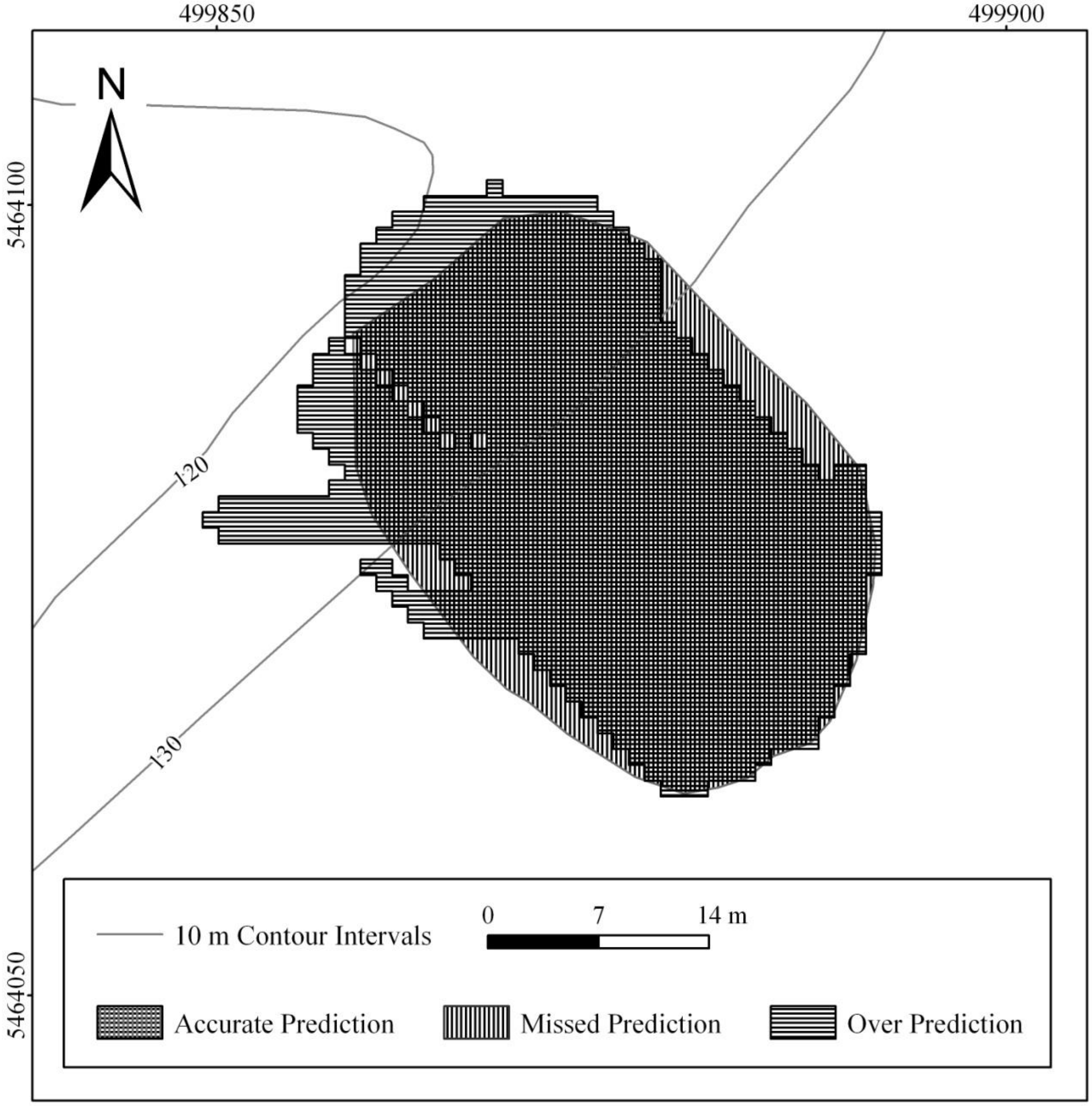

Figure 4-9. Simulation result of Landslide 5 (final step, t = 27).

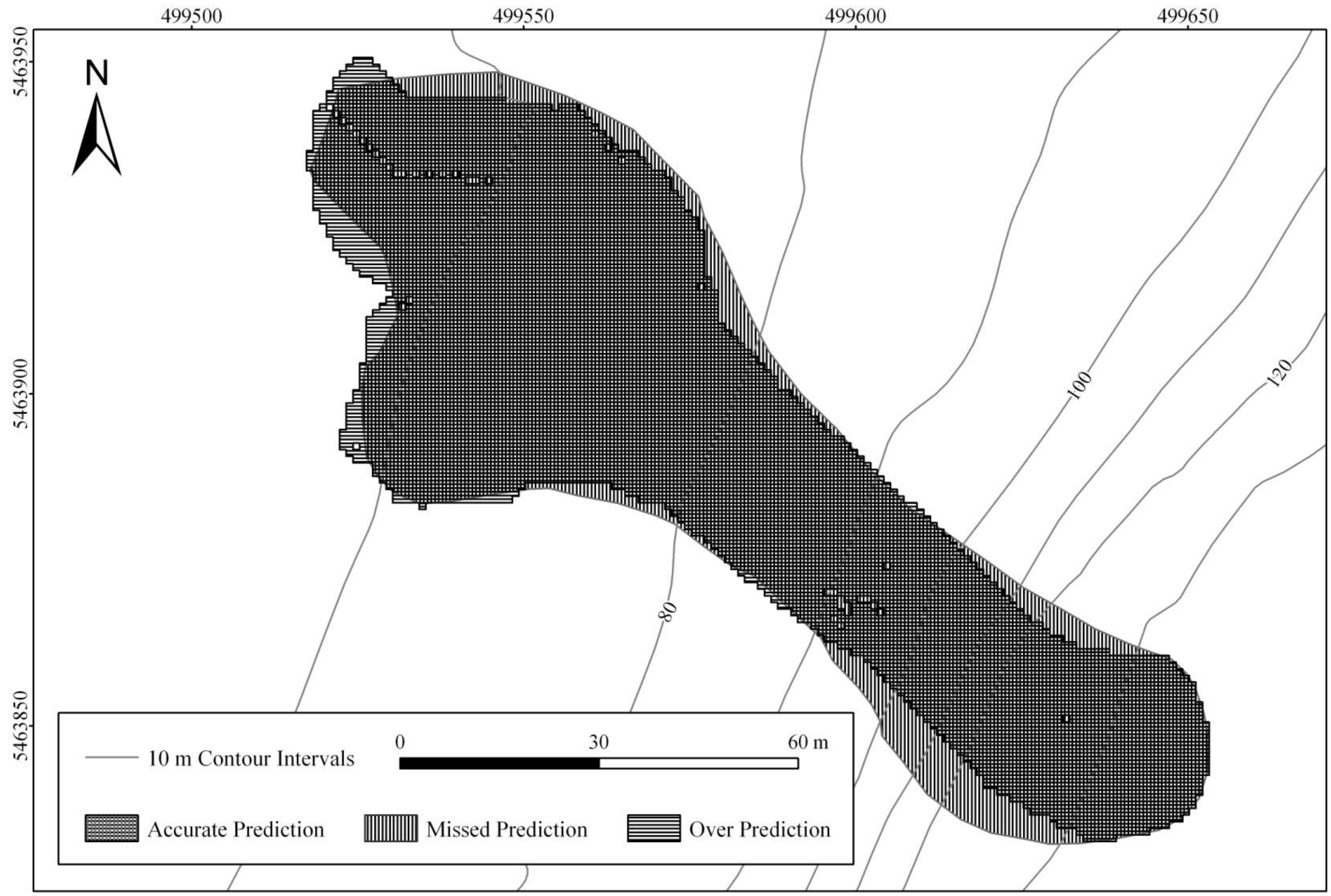

Figure 4-10. Simulation results of Landslide 6 (final step, t = 118).

4.6 Conclusion

A novel approach that couples MCE and CA models for the prediction of landslide flow has been presented. This study further reinforced the notion that CA is a feasible alternative to solving traditional flow equations based on partial differentials. The approach relied on the ease with which parameters were derived from a high resolution DEM and GIS data to produce a susceptibility map, which then provided information for the CA modelling. The success of a CA simulation lies in the elicitation of the transition rules and in this study using a multicriteria decision approach to derive such rules has proven to be effective. Further, the proposed model can determine where landslide fronts would flow given any direction based on the 8-neighbour (Moore) interaction. The choice of CA neighbourhood size was important to derive more accurate simulation outcomes. It was found that missed predictions increased as the radius of the neighbourhood size increased. The proposed MCE-CA landslide simulation approach can be used by urban planners who face landslide hazards and need to make plans for new residential developments. The flexibility of the evaluation in the MCE process tailors the CA model to the specific nature of the study site; however it is a challenge to acquire available high-resolution data sets and additional information on historical landslides in order to properly test the model and therefore provide predictive landslide occurrences based on model simulations at larger municipal scale.

Acknowledgements

The authors are thankful for the full support of the Natural Sciences and Engineering Research Council (NSERC) of the Canada Discovery Grants awarded to the second and third author.

4.7 References

Akgun, A. and N. Turk (2010). "Landslide susceptibility mapping for Ayvalik (Western Turkey) and its vicinity by multicriteria decision analysis." Environmental Earth Sciences **61**(3): 595-611.

Almeida, C. M., J. M. Gleriani, et al. (2008). "Using neural networks and cellular automata for modelling intra-urban land-use dynamics." International Journal of Geographical Information Science **22**(9): 943-963.

Anderson, R. S. and K. L. Bunas (1993). "Grain-size segregation and stratigraphy in aeolian ripples modeled with a cellular-automaton." Nature **365**(6448): 740-743.

Avolio, M. V., S. Di Gregorio, et al. (2000). "Simulation of the 1992 Tessina landslide by a cellular automata model and future hazard scenarios." International Journal of Applied Earth Observation and Geoinformation **2**(1): 41-50.

Barredo, J. I., M. Kasanko, et al. (2003). "Modelling dynamic spatial processes: simulation of urban future scenarios through cellular automata." Landscape and Urban Planning **64**(3): 145-160.

Batty, M. and Y. Xie (1994). "From cells to cities." Environment and Planning B-Planning & Design **21**: 531-538.

BC Stats (2010). Community Facts: North Vancouver District Municipality.

Benda, L. E. and T. W. Cundy (1990). "Predicting deposition of debris flows in mountainous channels." Canadian Geotechnical Journal **27**: 409-417.

Bone, C., S. Dragićević, et al. (2006). "A fuzzy-constrained cellular automata model of forest insect infestations." Ecological Modelling **192**(1-2): 107-125.

Clarke, K. C., S. Hoppen, et al. (1997). "A self-modifying cellular automaton model of historical urbanization in the San Francisco Bay area." Environment and Planning B-Planning & Design **24**(2): 247-261.

Coppola, E., B. Tomassetti, et al. (2007). "Cellular automata algorithms for drainage network extraction and rainfall data assimilation." Hydrological Sciences Journal **52**(3): 579-592.

Crisci, G. M., G. Iovine, et al. (2008). "Lava-flow hazard on the SE flank of Mt. Etna (Southern Italy)." Journal of Volcanology and Geothermal Research **177**(4): 778-796.

D'Ambrosio, D., S. Di Gregorio, et al. (2002). "Simulating the Curti-Sarno debris flow through cellular automata: the model SCIDDICA (release S2)." Physics and Chemistry of the Earth **27**(36): 1577-1585.

D'Ambrosio, D., S. Di Gregorio, et al. (2003). "First simulations of the Sarno debris flows through Cellular Automata modelling." Geomorphology **54**(1-2): 91-117.

Dalponte, D., P. Rinaldi, et al. (2007). "A validated fast algorithm for simulation of flooding events in plains." Hydrological Processes **21**(8): 1115-1124.

Di Gregorio, S., R. Rongo, et al. (1999). "Mount ontake landslide simulation by the cellular automata model SCIDDICA-3." Physics and Chemistry of the Earth Part a-Solid Earth and Geodesy **24**(2): 131-137.

Doeschl-Wilson, A. B. and P. E. Ashmore (2005). "Assessing a numerical cellular braided-stream model with a physical model." Earth Surface Processes and Landforms **30**(5): 519-540.

Eastman, J. R. (2009). IDRISI Taiga. Worcester, MA, Clark University.

Eisbacher, G. H. and J. J. Clague (1981). "Urban landslides in the vicinity of Vancouver, British Columbia, with special reference to the December 1979 rainstorm." Canadian Geotechnical Journal **18**(2): 205-216.

Evans, S. G. and K. W. Savigny (1994). Landslides in the Vancouver-Fraser Valley-Whistler region. Geology and geological hazards of the Vancouver region, southwestern British Columbia. J. W. H. Monger, Geogological Survey of Canada, Bulletin 481**:** 251-286.

Fang, S. F., G. Z. Gertner, et al. (2005). "The impact of interactions in spatial simulation of the dynamics of urban sprawl." Landscape and Urban Planning **73**(4): 294-306.

Gorsevski, P. V., P. Jankowski, et al. (2006). "An heuristic approach for mapping landslide hazard by integrating fuzzy logic with analytic hierarchy process." Control and Cybernetics **35**(1): 121-146.

Guthrie, R. H., P. J. Deadman, et al. (2008). "Exploring the magnitude-frequency distribution: a cellular automata model for landslides." Landslides **5**(1): 151-159.

Iovine, G., S. Di Gregorio, et al. (2003). "Debris-flow susceptibility assessment through cellular automata modeling: an example from 15–16 December 1999 disaster at Cervinara and San Martino Valle Caudina (Campania, southern Italy)." Natural Hazards and Earth System Sciences **3**: 457-468.

Iverson, R. M. (2000). "Landslide triggering by rain infiltration." Water Resources Research **36**(7): 1897-1910.

Jiang, H. and J. R. Eastman (2000). "Application of fuzzy measures in multi-criteria evaluation in GIS." International Journal of Geographical Information Science **14**(2): 173-184.

Karafyllidis, I. (1997). "A model for the prediction of oil slick movement and spreading using cellular automata." Environment International **23**(6): 839-850.

Karafyllidis, I. and A. Thanailakis (1997). "A model for predicting forest fire spreading using cellular automata." Ecological Modelling **99**(1): 87-97.

Kocabas, V. and S. Dragicevic (2007). "Enhancing a GIS Cellular Automata Model of Land Use Change: Bayesian Networks, Influence Diagrams and Causality." Transactions in GIS **11**(5): 681-702.

Kocabas, V. and S. Dragićević (2006). "Assessing cellular automata model behaviour using a sensitivity analysis approach." Computers Environment and Urban Systems **30**(6): 921-953.

Li, X. and A. G. Yeh (2002). "Neural-network-based cellular automata for simulating multiple land use changes using GIS." International Journal of Geographical Information Science **16**(4): 323-343.

Li, X. and A. G. O. Yeh (2001). "Calibration of cellular automata by using neural networks for the simulation of complex urban systems." Environment and Planning A **33**(8): 1445-1462.

Liu, Y. and S. R. Phinn (2003). "Modelling urban development with cellular automata incorporating fuzzy-set approaches." Computers, Environment and Urban Systems **27**(6): 637-658.

Malamud, B. D. and D. L. Turcotte (2000). "Cellular-automata models applied to natural hazards." Computing in Science & Engineering **2**(3): 42-51.

Manson, S. M. (2001). "Simplifying complexity: a review of complexity theory." Geoforum **32**(3): 405-414.

Mehta, A. and G. C. Barker (1994). "The dynamics of sand." Reports on Progress in Physics **57**(4): 383-416.

Ménard, A. and D. J. Marceau (2005). "Exploration of spatial scale sensitivity in geographic cellular automata." Environment and Planning B-Planning & Design **32**(5): 693-714.

Moreno, N., R. Quintero, et al. (2007). "Biocomplexity of deforestation in the Caparo tropical forest reserve in Venezuela: An integrated multi-agent and cellular automata model." Environmental Modelling & Software **22**(5): 664-673.

Nield, J. M. and A. C. W. Baas (2008). "Investigating parabolic and nebkha dune formation using a cellular automaton modelling approach." Earth Surface Processes and Landforms **33**(5): 724-740.

Packard, N. H. and S. Wolfram (1985). "Two-dimensional cellular automata." Journal of Statistical Physics **38**(5-6): 901-946.

Parsons, J. A. and M. A. Fonstad (2007). "A cellular automata model of surface water flow." Hydrological Processes **21**(16): 2189-2195.

Paulin, G. L. and M. Bursik (2009). "Logisnet: A tool for multimethod, multiple soil layers slope stability analysis." Computers & Geosciences **35**(5): 1007-1016.

Rao, M., S. V. C. Sastry, et al. (1991). A weighted index model for urban suitability assessment - A GIS approach. Bombay, India, Bombay Metropolitan Regional Development Authority.

Robinson, V. B. (2003). "A Perspective on the Fundamentals of Fuzzy Sets and their Use in Geographic Information Systems." Transactions in GIS **7**(1): 3-30.

Rongo, R., W. Spataro, et al. (2008). "Lava Flow Hazard Evaluation Through Cellular Automata and Genetic Algorithms: an Application to Mt Etna Volcano." Fundamenta Informaticae **87**: 247-267.

Rundle, J., D. L. Turcotte, et al. (2000). Geocomplexity and the physics of earthquakes, American Geophysical Union.

Saaty, T. L. (1977). "Scaling method for priorities in hierarchical structures." Journal of Mathematical Psychology **15**(3): 234-281.

Saaty, T. L. (1980). The analytical hierarchy process: Planning, priority setting, resource allocation. New York, McGraw-Hill.

Saaty, T. L. (1990). "How to make a decision: The analytic hierarchy process." European Journal of Operational Research **48**(1): 9-26.

Salles, T., S. Lopez, et al. (2007). "Cellular automata model of density currents." Geomorphology **88**(1-2): 1-20.

Santini, M., S. Grimaldi, et al. (2009). "Pre-processing algorithms and landslide modelling on remotely sensed DEMs." Geomorphology **113**(1-2): 110-125.

Shou, K. J. and C. F. Wang (2003). "Analysis of the Chiufengershan landslide triggered by the 1999 Chi-Chi earthquake in Taiwan." Engineering Geology **68**(3-4): 237-250.

Soares, B. S., G. C. Cerqueira, et al. (2002). "DINAMICA - a stochastic cellular automata model designed to simulate the landscape dynamics in an Amazonian colonization frontier." Ecological Modelling **154**(3): 217-235.

Suzen, M. L. and V. Doyuran (2004). "A comparison of the GIS based landslide susceptibility assessment methods: multivariate versus bivariate." Environmental Geology **45**(5): 665-679.

Thomas, R. and A. P. Nicholas (2002). "Simulation of braided river flow using a new cellular routing scheme." Geomorphology **43**(3-4): 179-195.

Toffoli, T. (1984). "Cellular Automata as an alternative to (rather than an approximation of) differential equations in modeling physics." Physica D: Nonlinear Phenomena **10**(1-2): 117-127.

Turcotte, D. L. (2006). "Modeling geocomplexity: A new kind of science." Geological Society of America Special Papers **413**: 39-50.

Van Westen, C. J. and M. T. J. Terlien (1996). "An approach towards deterministic landslide hazard analysis in GIS. A case study from Manizales (Colombia)." Earth Surface Processes and Landforms **21**(9): 853-868.

von Neumann, J. (1966). Theory of self-reproducing automata. Urbana, IL, University of Illinois.

Voogd, H. (1983). Multicriteria evaluation for urban and regional planning. London, Pion.

Wang, G. W., J. P. Chen, et al. (2007). Monitoring desertification using the integrated CA, GIS and RS with AHP-derived weights: A case study of Beijing and its neighboring areas in recent 20 years. Geoinformatics 2007: Geospatial Information Science. J. Chen and Y. Pu. Bellingham, WA, Proceedings of SPIE, Vol. 6753. **6753:** 1-10.

Weatherley, D., S. C. Jaume, et al. (2000). "Evolution of stress deficit and changing rates of seismicity in cellular automaton models of earthquake faults." Pure and Applied Geophysics **157**(11-12): 2183-2207.

White, R. and G. Engelen (2000). "High-resolution integrated modelling of the spatial dynamics of urban and regional systems." Computers, Environment and Urban Systems **24**(5): 383-400.

White, R., G. Engelen, et al. (1997). "The use of constrained cellular automata for high-resolution modelling of urban land-use dynamics." Environment and Planning B-Planning & Design **24**(3): 323-343.

Wilkinson, P. L., M. G. Anderson, et al. (2002). "Landslide hazard and bioengineering: towards providing improved decision support through integrated numerical model development." Environmental Modelling & Software **17**(4): 333-344.

Wolfram, S. (1983). "Statistical mechanics of cellular automata." Reviews of Modern Physics **55**(3): 601-644.

Wu, F. L. (2002). "Calibration of stochastic cellular automata: the application to rural-urban land conversions." International Journal of Geographical Information Science **16**(8): 795-818.

Wu, F. L. and C. J. Webster (1998). "Simulation of land development through the integration of cellular automata and multicriteria evaluation." Environment and Planning B-Planning & Design **25**(1): 103-126.

Wu, W. M. and R. C. Sidle (1995). "A distributed slope stability model for steep forested basins." Water Resources Research **31**(8): 2097-2110.

Yalcin, A. (2008). "GIS-based landslide susceptibility mapping using analytical hierarchy process and bivariate statistics in Ardesen (Turkey): Comparisons of results and confirmations." Catena **72**(1): 1-12.

Yassemi, S., S. Dragićević, et al. (2008). "Design and implementation of an integrated GIS-based cellular automata model to characterize forest fire behaviour." Ecological Modelling **210**(1-2): 71-84.

Yeh, A. G. O. and X. Li (2001). "A constrained CA model for the simulation and planning of sustainable urban forms by using GIS." Environment and Planning B-Planning & Design **28**(5): 733-753.

Zadeh, L. A. (1965). "Fuzzy sets." Information and Control **8**(3): 338-353.

Zhang, Y. A., M. R. Peterman, et al. (2008). "Cellular automata: Simulating alpine tundra vegetation dynamics in response to global warming." Arctic Antarctic and Alpine Research **40**(1): 256-263.

CHAPTER 5 CONCLUSIONS

5.1 General Conclusions

The focus of this research was to develop several mutually complementary and reinforcing GIS-based modelling methods and tools for landslide prediction. This was accomplished firstly by integrating GIS, CA, and logistic regression (LR) techniques to develop a landslide flow model; secondly by implementing a multicriteria evaluation (MCE) for landslide susceptibility at multiple scales; and thirdly by incorporating MCE with a GIS-based CA model to refine the transition rules for landslide flow simulations. Idrisi Taiga, a GIS software developed by Clark Labs, was used for implementing all methods of this research (Eastman 2009).

In the first component of the research, a GIS-based model integrating CA and LR was developed for modelling landslides using a high resolution DEM. The CA modelling approach was used to simulate landslides from the Berkley Escarpment (Patrick Slide and Dawson-Chu Slide) using an initial failure site. The CA propagation across the landscape was based on transition rules derived from the LR analysis of topographic variables. Topographic variables such as slope and curvature were calculated from the DEM and their influence to landslide incidence was measured as fitted to a logit model. The importance of topographic variables in relation to landslides was the basis of determining simple transition rules. The landslide flow results proved successful and robust based on a few simple rules. Performance ratios calculated from various cross tabulations compared favourably to the landslide CA model SCIDDICA (D'Ambrosio et al. 2002).

Landslide movement not only flowed correctly downslope, but also followed the correct curvature within the channel as given by the DEM. This finding showed that a complex phenomenon such as landslide flow can be realistically modelled using only a DEM, which can be useful in data limited areas.

The second component of the research developed a model for understanding how spatial scale and spatial resolution affect landslide susceptibility since data availability typically constricts the type and scale of analyses performed. Both scale and resolution are limiting factors when considering the many landslide-conditioning parameters in the MCE. Some parameters were either included or excluded based on the size of the grid cell. For example, a 50 m by 50 m cell occupied by a road is an incorrect data representation. The MCE approach was based on expert knowledge gathered from a literature review of landslide causing parameters. Multiple evaluation techniques were used at different stages. Determining the reliability of calculated relative importance of factors was measured by the consistency ratio and the evaluation technique used to validate the final susceptibility maps was known as seed cell area index. The measured performance indices indicated that the results were accurate and consistent over multiple scales. Also, it was possible to verify results by overlaying maps of different scales and resolutions to demonstrate that calculated susceptibilities were comparable in common areas. The main purpose of assessing landslide susceptibility at multiple scales was to examine the differences and whether results were accurate, but the MCE procedure was a precursor to the third and final component of the research.

The third component of the research developed an integrated approach where the MCE results were used to derive transition rules for use in a CA model to simulate landslide flow. Specifically, the susceptibility map produced for the local scale Berkley Escarpment were implemented into the CA modelling as a basis of transition rules for landslide propagation. The model was tested on six historical landslides on the escarpment, which accurately predicted an average of 89% of the landslide area. The performance of this model even surpasses the first component of this research that integrated CA and LR approaches. This accuracy measure indicated that using MCE to derive CA transition rules was successful. The success of this model relied on the ease at which landslide parameters were calculated from a high resolution DEM to produce a MCE susceptibility map, which then fed information for CA modelling. Also, by using a multicriteria decision approach to derive transition rules, the MCE process can be tailored to model landslides specific to a study area.

5.2 Contributions

The method and results derived from this research contributes to the fields of GIScience, particularly to spatio-temporal modelling, as well as physical geography and landslide science by providing effective solutions to three limitations of current landslides research. The difficulty in applying GIS-based CA modelling lies in characterizing the transition rules that dictate the evolution of the phenomena. In Chapter 2, simple transition rules were based on LR analyses of landslide-conditioning parameters to model landslide flow. Chapter 3 investigated landslide susceptibility at multiple spatial scales and resolutions. The result from the fine scale susceptibility map provided the input for MCE-CA model in Chapter 4. Chapter 4 sought to improve the transition rule elicitation process by incorporating a decision making approach by incorporating information provided by the landslide susceptibility. With regards to determining transition rules for CA modelling, using MCE results within the CA framework for landslide flow was tested with much success. These limitations are predicting landslide occurrence at different spatial scales, incorporating a temporal component to the modelling, and overcoming limited data availability. The developed solutions are summarized below.

The results produced from the landslide CA models demonstrates that it is possible to use CA as an alternative to calculating partial differential equations for a realistic representation of landslide flow movement. Modelling shallow landslides using complex systems theory by describing the interactions between each cell and its neighbours essentially replaces the differential equations normally required (Toffoli 1984). It was also shown that it is feasible to model a complex physical geography phenomenon with limited data available since this research was carried out with DEMs and road and stream network files derived from maps.

5.3 Future Directions

This research was successful in accomplishing its goals of developing GIS-based models that incorporated multiple methods at multiple scales for landslide prediction. A similar landslide CA model operated on both a square and hexagonal grid space for comparison and it was found that the hexagonal mesh yields more realistic results because the distances between neighbouring centre points of cells were of equal distance (D'Ambrosio et al. 2007). However, the model proposed in this thesis follows a traditional CA framework that is relatively limited due to the use of common raster GIS. Specfically, Idrisi limited the grid space for both CA models in this research to a regular square grid, but a hexagonal tessellation may be preferred phenomena such as landslides.

In addition, a landslide event is an inherently spatial dynamic process that has been addressed by an integration of GIS and a two dimensional CA framework; however, a landslide is governed by the force of gravity acting on slope. This implies elevation and employing a three dimensional spatial structure for CA to represent the landscape and flow of a landslide would be an important improvement but challenging to accomplish. Model testing and computational issues arise as complications when adding the third spatial dimension, but such a four dimensional landslide model may produce additional results (i.e. volume and time).

While the current GIS-based MCE-CA integrated approaches proved adequate for modelling landslide flow while relying on limited data sources, the introduction of additional data could enhance the final product. Since urban landslides in Metro Vancouver are typically rainstorm-triggered, a real-time spatially distributed precipitation data feed to the model could transform the existing model to a hazard warning system (Yu et al. 2007).

The models can also be extended to operate on the Internet. For instance, the CA-MCE model for the Berkley Escarpment could be translated to a browser extension or applet that would allow planners to assess online where landslide flows may extend to given hypothetical events. A user would click and point to a hypothetical failure location along the escarpment and the simulated model results would also be viewed from the browser.

In closing, the methods presented in this research demonstrate that the lack of geospatial data do not necessarily restrict the type of applications that can be used in the field of modelling landslide susceptibilities and dynamics. This research also presents a foundation with which the next stage of landslide modelling should be developing capable of handling three spatial dimensions, a temporal dimension, and a multitude of various spatial tessellations, all within a GIS environment.

5.4 References

D'Ambrosio, D., S. Di Gregorio, et al. (2002). "Simulating the Curti-Sarno debris flow through cellular automata: the model SCIDDICA (release S2)." Physics and Chemistry of the Earth **27**(36): 1577-1585.

D'Ambrosio, D., G. Lovine, et al. (2007). "A macroscopic collisional model for debris-flows simulation." Environmental Modelling & Software **22**(10): 1417-1436.

Eastman, J. R. (2009). IDRISI Taiga. Worcester, MA, Clark University.

Toffoli, T. (1984). "Cellular Automata as an alternative to (rather than an approximation of) differential equations in modeling physics." Physica D: Nonlinear Phenomena **10**(1-2): 117-127.

Yu, F. C., C. Y. Chen, et al. (2007). "A web-based decision support system for slopeland hazard warning." Environmental Monitoring and Assessment **127**(1-3): 419-428.

APPENDICES

Appendix A: Co-authorship Statement

Chapter 2

Title: Development of an urban landslide cellular automata model: A case study of North Vancouver, Canada

Co-Author: Suzana Dragićević

Role of Co-author: Manuscript preparation

Chapter 3

Title: GIS-based fuzzy multicriteria evaluation and multiscale analysis to characterize landslide susceptibility

Co-Author: Suzana Dragićević, Shivanand Balram

Role of Co-author: Manuscript preparation

Chapter 4

Title: Integration of multicriteria evaluation and cellular automata methods for landslide simulation modelling

Co-Author: Suzana Dragićević, Margaret Schmidt

Role of Co-author: Manuscript preparation

Appendix B: Copyright Clearance from Springer

SPRINGER LICENSE
TERMS AND CONDITIONS

Aug 26, 2011

This is a License Agreement between Terence Lai ("You") and Springer ("Springer") provided by Copyright Clearance Center ("CCC"). The license consists of your order details, the terms and conditions provided by Springer, and the payment terms and conditions.

All payments must be made in full to CCC. For payment instructions, please see information listed at the bottom of this form.

License Number	2736230441558
License date	Aug 25, 2011
Licensed content publisher	Springer
Licensed content publication	Earth Science Informatics
Licensed content title	Development of an urban landslide cellular automata model: a case study of North Vancouver, Canada
Licensed content author	Terence Lai
Licensed content date	Jan 1, 2011
Volume number	4
Issue number	2
Type of Use	Thesis/Dissertation
Portion	Full text
Number of copies	5
Author of this Springer article	Yes and you are a contributor of the new work
Order reference number	
Title of your thesis / dissertation	Modelling Spatial Dynamics of Landslides: Integration of GIS-Based Cellular Automata and Multicriteria Evaluation Methods
Expected completion date	Aug 2011
Estimated size(pages)	140
Total	0.00 USD
Terms and Conditions	

Introduction
The publisher for this copyrighted material is Springer Science + Business Media. By clicking "accept" in connection with completing this licensing transaction, you agree that the following terms and conditions apply to this transaction (along with the Billing and Payment terms and conditions established by Copyright Clearance Center, Inc. ("CCC"), at the time that you opened your Rightslink account and that are available at any time at http://myaccount.copyright.com).

Limited License

With reference to your request to reprint in your thesis material on which Springer Science and Business Media control the copyright, permission is granted, free of charge, for the use indicated in your enquiry. Licenses are for one-time use only with a maximum distribution equal to the number that you identified in the licensing process.

This License includes use in an electronic form, provided it is password protected or on the university's intranet, destined to microfilming by UMI and University repository. For any other electronic use, please contact Springer at (permissions.dordrecht@springer.com or permissions.heidelberg@springer.com)

The material can only be used for the purpose of defending your thesis, and with a maximum of 100 extra copies in paper.

Although Springer holds copyright to the material and is entitled to negotiate on rights, this license is only valid, provided permission is also obtained from the (co) author (address is given with the article/chapter) and provided it concerns original material which does not carry references to other sources (if material in question appears with credit to another source, authorization from that source is required as well). Permission free of charge on this occasion does not prejudice any rights we might have to charge for reproduction of our copyrighted material in the future.

Altering/Modifying Material: Not Permitted
However figures and illustrations may be altered minimally to serve your work. Any other abbreviations, additions, deletions and/or any other alterations shall be made only with prior written authorization of the author(s) and/or Springer Science + Business Media. (Please contact Springer at permissions.dordrecht@springer.com or permissions.heidelberg@springer.com)

Reservation of Rights
Springer Science + Business Media reserves all rights not specifically granted in the combination of (i) the license details provided by you and accepted in the course of this licensing transaction, (ii) these terms and conditions and (iii) CCC's Billing and Payment terms and conditions.

Copyright Notice:
Please include the following copyright citation referencing the publication in which the material was originally published. Where wording is within brackets, please include verbatim.
"With kind permission from Springer Science+Business Media: <book/journal title, chapter/article title, volume, year of publication, page, name(s) of author(s), figure number(s), and any original (first) copyright notice displayed with material>."

Warranties: Springer Science + Business Media makes no representations or warranties with respect to the licensed material.

Indemnity
You hereby indemnify and agree to hold harmless Springer Science + Business Media and CCC, and their respective officers, directors, employees and agents, from and against any and all claims arising out of your use of the licensed material other than as specifically

authorized pursuant to this license.

No Transfer of License
This license is personal to you and may not be sublicensed, assigned, or transferred by you to any other person without Springer Science + Business Media's written permission.

No Amendment Except in Writing
This license may not be amended except in a writing signed by both parties (or, in the case of Springer Science + Business Media, by CCC on Springer Science + Business Media's behalf).

Objection to Contrary Terms
Springer Science + Business Media hereby objects to any terms contained in any purchase order, acknowledgment, check endorsement or other writing prepared by you, which terms are inconsistent with these terms and conditions or CCC's Billing and Payment terms and conditions. These terms and conditions, together with CCC's Billing and Payment terms and conditions (which are incorporated herein), comprise the entire agreement between you and Springer Science + Business Media (and CCC) concerning this licensing transaction. In the event of any conflict between your obligations established by these terms and conditions and those established by CCC's Billing and Payment terms and conditions, these terms and conditions shall control.

Jurisdiction
All disputes that may arise in connection with this present License, or the breach thereof, shall be settled exclusively by the country's law in which the work was originally published.

Other terms and conditions:

v1.2

Gratis licenses (referencing $0 in the Total field) are free. Please retain this printable license for your reference. No payment is required.

If you would like to pay for this license now, please remit this license along with your payment made payable to "COPYRIGHT CLEARANCE CENTER" otherwise you will be invoiced within 48 hours of the license date. Payment should be in the form of a check or money order referencing your account number and this invoice number RLNK11044653.
Once you receive your invoice for this order, you may pay your invoice by credit card. Please follow instructions provided at that time.

Make Payment To:
Copyright Clearance Center
Dept 001
P.O. Box 843006
Boston, MA 02284-3006

For suggestions or comments regarding this order, contact Rightslink Customer Support: customercare@copyright.com or +1-877-622-5543 (toll free in the US) or +1-978-646-2777.